

***Fluorine-Promoted Intramolecular Aryl-Aryl Coupling.
Toward the Isomer-Specific Fullerene Synthesis***

Von der Fakultät Chemie der Universität Stuttgart

zur Erlangung der Würde eines

Doktors der Naturwissenschaften (Dr. rer. nat.) genehmigte Abhandlung

Vorgelegt von

Mikhail Kabdulov

aus Luga
Russland

Hauptberichter: Prof. Dr. Dr. h. c. M. Jansen

Mitberichter: Prof. Dr. F. Effenberger

Prüfungsvorsitzender: Prof. Dr. B. Plietker

Tag der Einreichung der Arbeit: 17.09.2012

Tag der mündlichen Prüfung: 12.02.2013

Max Planck Institut für Festkörperforschung

2013

Table of contents

Abstract of the Dissertation	v
1. Literature overview	1
1.1. Carbon and carbon based structures.....	3
1.1.1. Introduction.....	3
1.1.2. Allotropes of carbon	3
1.1.2.1. sp^3 -carbon based allotropes.....	5
1.1.2.2. sp^2 -carbon based allotropes.....	6
1.1.2.3. sp -carbon based allotropes.....	8
1.1.2.4. Hybrid carbon allotropes	10
1.1.3. Discovery of fullerenes, structure and isomerism	13
1.1.3.1. Classical methods of fullerene production	14
1.1.3.2. Combustion synthesis of fullerenes	15
1.1.3.3. Pyrolysis of hydrocarbons.....	15
1.1.3.4. Higher fullerenes and fullerene isomerism	15
1.2. Polycyclic aromatic hydrocarbons	20
1.2.1. Introduction.....	20
1.2.2. Nomenclature.....	20
1.2.3. Bay, cove and fjord regions ^[69]	24
1.2.4. Alternant and non-alternant PAHs.....	24
1.2.5. Kata- and peri-condensed PAHs	25
1.2.6. PAHs containing five-membered rings	27
1.2.7. Non-planar PAHs.....	29
1.2.8. Properties of PAHs	30
1.2.9. Analysis and characterization of large PAHs.....	32
1.3. Rational fullerene synthesis	34
1.3.1. Introduction.....	34
1.3.2. Total synthesis of corannulene	34

1.3.3. Flash vacuum pyrolysis.....	35
1.3.3.1. Buckybowl synthesis	39
1.3.3.2. Attempts of rational fullerene synthesis	41
1.3.3.3. Advantages and limitation of FVP	42
1.3.4 Alternative Aryl-Aryl coupling techniques	42
1.3.4.1. Photocyclization.....	42
1.3.4.2. Oxidative Aryl-Aryl coupling.....	44
1.3.4.3. Palladium catalyzed Aryl-Aryl coupling	46
1.3.4.4. Condensation on the metal surfaces.....	47
1.4. References	49
2. Direct Fullerene synthesis.....	59
2.1. FVP approach	61
2.1.1. Introduction.....	61
2.1.2. Alternative radical promoters for efficient intramolecular condensation	62
2.1.3. HF - homoelimination	76
2.1.4. Synthesis of fullerene precursors containing fluorine in key positions	84
2.1.4.1. Synthesis on the base of truxene	84
2.1.4.2. Synthesis on the base of aldol trimerization of cyclic ketones.....	88
2.1.5. Condensation of fluorinated C ₆₀ precursor to C ₆₀ fullerene	98
2.1.6. Condensation under FVP conditions	98
2.1.7. Condensation under LDI-MS conditions	99
2.2. Non-pyrolytical approach.....	101
2.2.1. Introduction.....	101
2.2.2. Al ₂ O ₃ mediated Cove-Region-Closure via HF elimination	102
2.2.3. Synthesis of extended buckybowl.....	105
2.2.4. Perspectives of Al ₂ O ₃ media for synthesis of fullerenes, nanotubes and other carbon based structure	111
2.3. References	112
3. Experimental Part	117
3.1. Measurements	119

3.2. General procedures.....	120
3.2.1. Synthesis of bromomethylarenes.....	120
3.2.2. Synthesis of phosphonium salts	120
3.2.3. Synthesis of diarylethenes	121
3.2.4. Photocyclization.....	122
3.2.5. Flash vacuum pyrolysis (FVP)	122
3.2.6. Cove-Region-Closure via Al ₂ O ₃ mediated HF Elimination.....	123
3.3. Synthesis	125
3.4. References	163
Zusammenfassung	165
Abbreviations	171
Publications and poster contributions	173
Acknowledgements	175
Eidesstattliche Erklärung	176

Abstract of the Dissertation

Direct synthesis of fullerenes is of considerable interest as a method to access new fullerenes which cannot be obtained in the uncontrolled process of graphite evaporation or form in low yields as a “hard-to-isolate” mixture. The general strategy of the direct approach to fullerenes is based on the synthesis of polycyclic aromatic hydrocarbons (PAH) that already contain the required carbon framework. Such “unrolled” molecules can be “rolled up” to form fullerenes through intramolecular Aryl-Aryl condensation under flash vacuum pyrolysis (FVP) conditions. The presence of chlorine or bromine in the initial precursor is essential for effective Aryl-Aryl condensation via free radical mechanism. On the other hand the use of chlorine and bromine functionalizations reaches its limits in the case of large molecules such as fullerene precursors. Availability of alternative promoters which do not have these disadvantages is a key prerequisite for successful direct fullerene synthesis.

In this work various functional groups have been tested as alternative promoters of Aryl-Aryl intramolecular condensation under FVP conditions. Methyl and fluorine functionalization has been found to be promising approaches. Unexpected high selectivity in cyclization was observed for fluorine derivatives. It was found that HF elimination is a synchronous process leading directly to the target molecule without any intermediates, thus producing no side products. The small size and low molecular weight of fluorine as well as high thermostability of the C-F bond, makes fluorine a “perfect” activating group for rational fullerene synthesis. Since fluorine can promote the desired ring closure only if hydrogen is placed neighboring in space in the precursor structure, full control in the direction of the condensation can be achieved. It was shown that the use of fluorine, as an activating group, solves the problem of selectivity in FVP and provides an effective conversion of the respective PAH precursors.

Several fullerene precursors containing fluorine atoms in key positions have been synthesized and investigated as a precursor for direct fullerene synthesis. Furthermore optimization has led to the discovery of a highly effective alternative solid-state strategy for intramolecular Aryl-Aryl coupling via HF elimination. The efficiency of the approach has been demonstrated by quantitative transformation of the precursor molecules to the desired PAHs and buckyowl structures.

The quantitative conversion to the extended C_{46} buckyowl, representing more than 75% of the C_{60} fullerene connectivity, demonstrates the high potential of the technique for construction of extended non-planar carbon based nanostructures, including higher fullerenes, giant buckybowls and nanotubes. The results obtained point the way to the fabrication fullerenes as well as other carbon based nanostructures such as single walled nanotubes and nanoribbons in a fully controllable manner.

1. Literature overview

1.1. Carbon and carbon based structures

1.1.1. Introduction

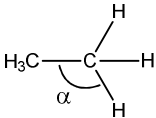
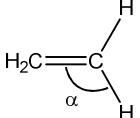
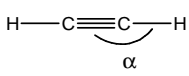
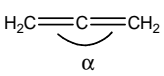
Carbon is a unique element compared to all others of the periodic system. Due to its moderate electronegativity carbon can form stable covalent bonds with itself and other more electronegative and electropositive elements. This leads to an incredible variety of possible carbon based molecular structures. Even elemental carbon can exist in numerous modifications or allotropes - the property of elements to exist in two or more different forms. Here carbon takes a leading place among all elements. The richness of carbon allotropes is a direct consequence of the possibility to form strong single, double and triple carbon-carbon bonds. In nature, elemental carbon was found in two allotropic modifications – diamond and graphite which are known since antiquity. During the last decades many new carbon allotropes such as graphene,^[1,2] nanotubes,^[3-7] and fullerenes^[8,9] were discovered and well characterized. The latest were also found in nature on Earth (mineral Shungit),^[10] and recently in interstellar space.^[11] Importantly, the physical and chemical properties of all carbon allotropes strongly depend on the type of carbon atom hybridization and the connectivity.

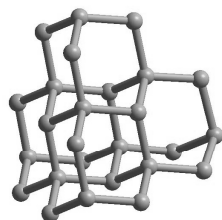
1.1.2. Allotropes of carbon

Carbon has the peculiarity to exist in three different stable states of hybridization sp^3 , sp^2 and sp which strongly influence the bond length, bond strength and the molecular geometry, thus determining many related properties of corresponding carbon-based materials (Table 1.1). The sp^3 -carbon based structures are typical isolators due to the lack of electron mobility. In contrast free electrons of sp - and sp^2 -hybridized carbon atoms can give rise to delocalization and corresponding structures usually conduct electrical current very effectively. Thus for example, the current density in carbon nanotubes may be a thousand times higher than that at which copper wires explode.^[12] The high stability of the carbon-carbon bonds is

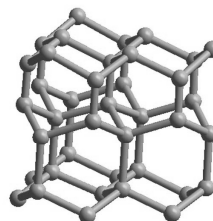
responsible for the specific mechanical properties of many carbon based materials, some of which are predicted to be the strongest materials. For example, the Young's modulus of nanotubes is much higher than that of diamond.^[13] Importantly that many physical properties can be precisely tuned by the structure, which makes carbon based materials very prospective for many applications from medicine and mechanics to molecular electronics.

Table 1.1. Typical C-C bond energies (bond-dissociation energies) and C-C bond lengths for differently hybridized carbon atoms.^[14]

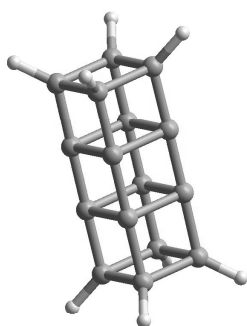
	Hybridization			
	sp^3	sp^2	sp	sp
Example structure				
C-C bond type	single	double	triple	double
Bond energy [kcal/mol]	83.8	148	202	
C-C bond length [pm]	154	133	120	131.5
Ideal bond angles α [°]	109.5	120.0	180.0	180.0



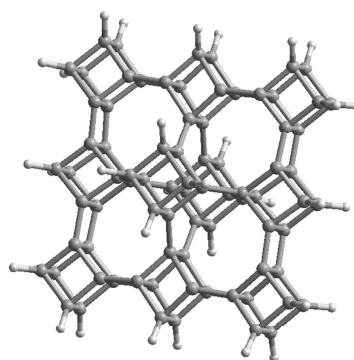
Diamond



Lonsdaleite



Poly[4]prismane



Prismane C8

Figure 1.1. sp^3 -carbon based allotropes. Fragments of diamond and lonsdaleite structures (top). Polyprismane structures - a theoretically predicted metastable form of sp^3 -hybridized carbon (bottom).

1.1.2.1. sp^3 -carbon based allotropes

Diamond is the modification based on pure sp^3 -hybridized carbon in which carbon atoms form four covalent bonds with neighboring atoms resulting in a tetrahedral coordination. These corner linked tetrahedra form the three-dimensional crystal structure. Due to its three-dimensional covalent network, diamond is one of the hardest known solids (10 on the Mohs scale) and has extremely high thermal

conductivity of more than 2000 W/(mK).^[15] It is transparent to light in the visible range and has a high refractive index. Due to many useful properties diamond is widely used in jewelry, as abrasive, in cutting tools and heat traps. **Lonsdaleite**,^[16,17] which is also known as hexagonal diamond, has a hexagonal unit cell, related to the diamond unit cell in the same way that the hexagonal and cubic close packed crystal systems are related. Another interesting example of carbon allotropes composed of sp^3 -carbon exclusively are **Prismanes** - theoretically-predicted metastable modifications (Figure 1.1).^[18]

1.1.2.2. sp^2 -carbon based allotropes

Graphite is a well-known modification of sp^2 -hybridized carbon representing the most stable carbon form under standard conditions. In graphite each carbon atom is covalently bonded to three neighboring ones producing planar hexagonal rings (carbon atoms are formally packed in a honeycomb crystal lattice). These six-membered rings form flat layers which are arranged one above the other with an interlayer spacing of around 3.4 Å.^[19] Since one electron remains “free” a high degree of delocalization takes place and graphite conducts electrons along the layers effectively. The individual graphite layer represents another well-known allotrope of sp^2 -carbon - **graphene** which has many fascinating properties, such as mechanical stiffness, very high electrical conductivity and high thermal conductivity. Due to these unique properties, graphene is considered to be a very promising material for many nanotechnological applications.^[20] Formally graphene can be considered as a starting "material" from which many other forms of sp^2 -hybridized carbon can be derived (Figure 1.2). Thus **single walled carbon nanotubes (SWCNTs)** can be thought of as a graphene layer rolled-up into a tube. **Fullerenes** and **buckybowl** molecules formally can be imagined as a defect graphene where introduction of pentagons (defects) results in the formation of bowl-shaped molecules (buckybowl) or closed cage-structures (fullerenes). Both fullerenes and

nanotubes are characterized by rich structural variations. Thus differently "rolled up" graphene sheets will produce different types of carbon nanotubes. Depending on the orientation of the hexagonal lattice with respect to the tube's axis, the resulting nanotubes can be classified as zigzag, armchair or chiral (Figure 1.3). Importantly, the electronic structure of nanotubes is fully defined by the chirality.^[21-24] Thus, armchair nanotubes are metallic whereas zigzag and chiral nanotubes can be either metallic or semiconducting.^[24] The number of possible fullerene structures is virtually unlimited and each fullerene cage formally represents a new allotropic form of carbon with its related properties. The possible structural variations and isomerism of fullerene cages will be discussed in more detail in chapter 1.1.3.4.

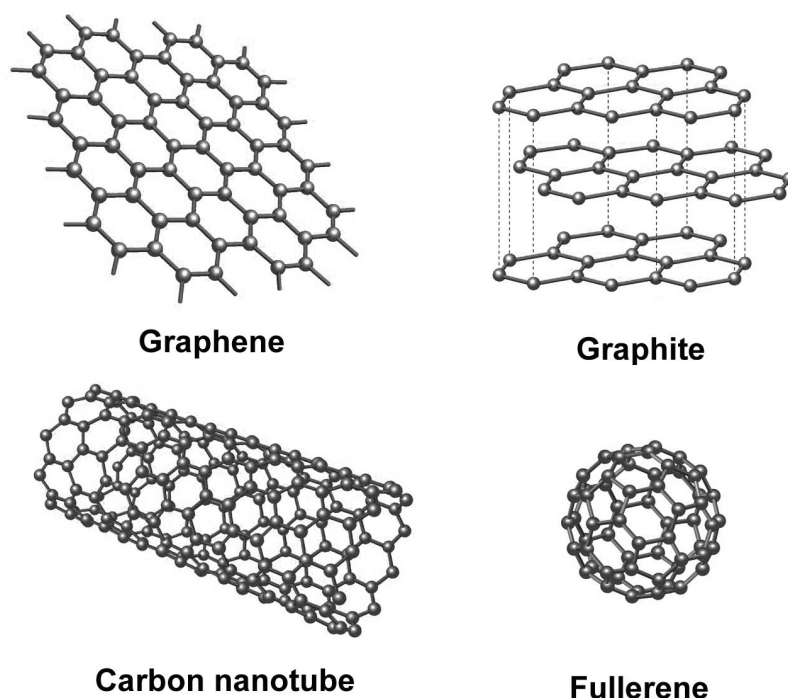


Figure 1.2. sp^2 -carbon allotropes: graphite, graphene, nanotubes and fullerenes.

Obviously the number of possible sp^2 -carbon based structures is not limited by these derived from the honeycomb graphene lattice. It is easy to imagine that the

combination of differently membered rings can give many alternative 2D carbon based allotropes which can be considered as isomeric forms of graphene. Consequently many other 0D, 1D and 3D structures can be derived in analogy to graphene. Thus the polyphenylene structure (Figure 1.4) can be viewed as a starting point for construction of polyphenylene-like nanotubes and fullerenes. Although polyphenylene-like graphene still exists on paper only, small polyphenylene blocks have been already synthesized and have been found to be stable.^[25]

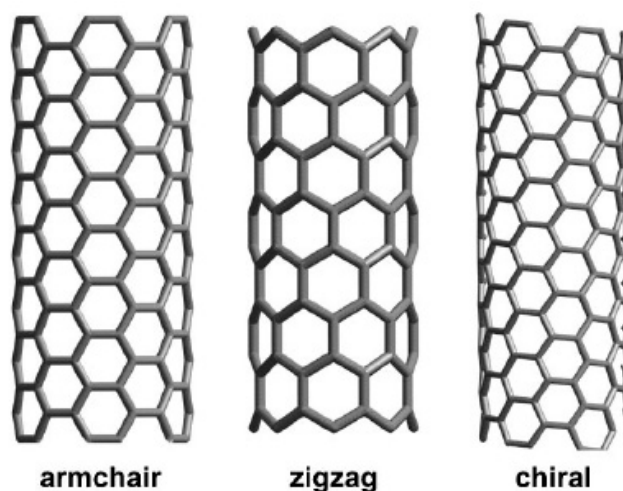


Figure 1.3. Examples of different types of single-walled carbon nanotubes: armchair, zigzag and chiral.

1.1.2.3. *sp*-carbon based allotropes

Carbyne is a linear polymer, in which *sp*-hybridized carbon atoms are connected in a chain of alternating single and triple-bonds (α -carbyne), or exclusively double bonds (β -carbyne or polycumulene structure) as presented on the Figure 1.5. According to some researchers, unambiguous and rigorous proof of identity and structure of carbyne has not yet been provided.^[26-29] On the contrary, other authors believe that such evidence is available.^[30] Although the existence of linear polyynes is still not settled, cyclic polyynes have been synthesized and well studied.^[31] As in the case of

fullerenes differently membered polyene rings represent an individual allotrope of carbon with related particular properties.

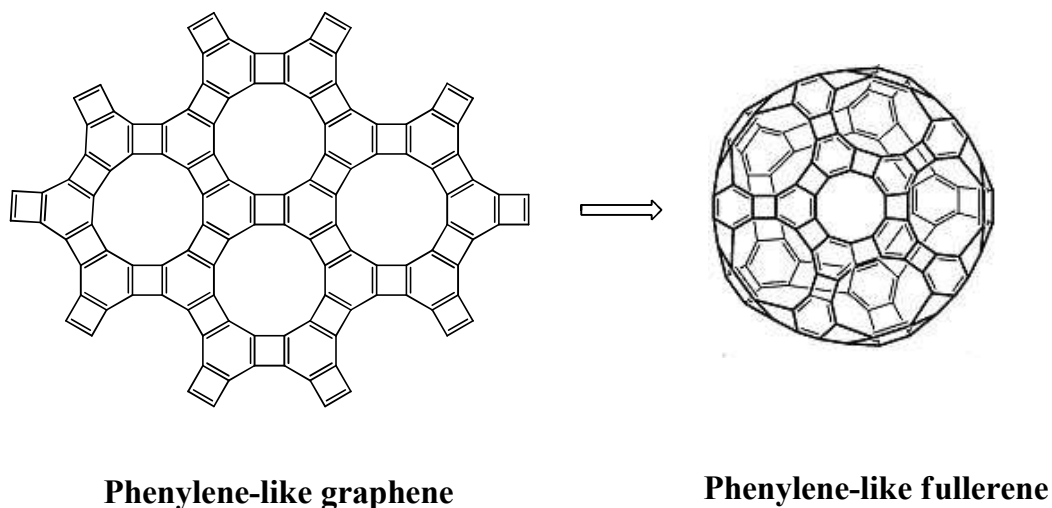


Figure 1.4. The structure of polyphenylene based 2D carbon allotrope and an example of the derived polyphenylene based "fullerene" molecule (both structures are theoretically predicted).

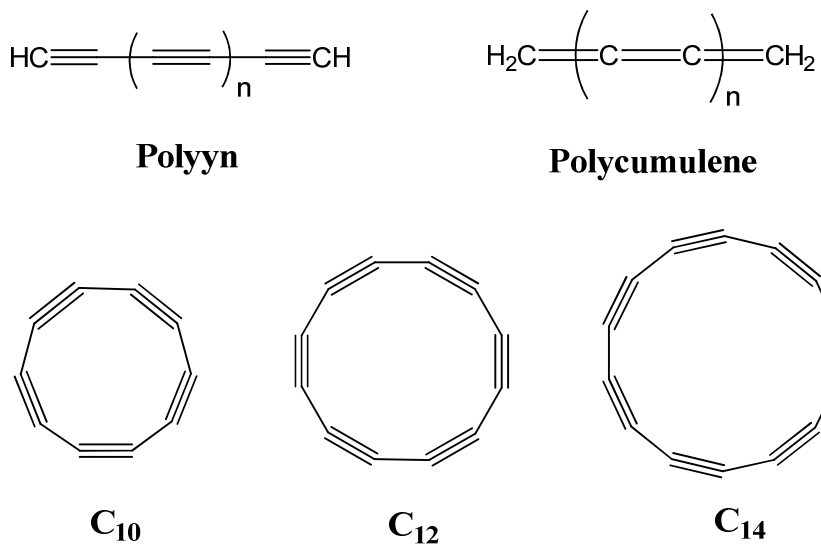


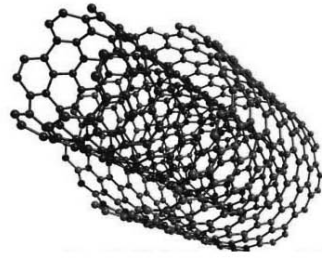
Figure 1.5. The structures of sp-carbon based allotropes: polyyn (α -carbyne); polycumulene (β -carbyne) and three cyclic polyyn structures.

1.1.2.4. Hybrid carbon allotropes

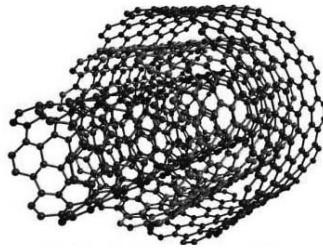
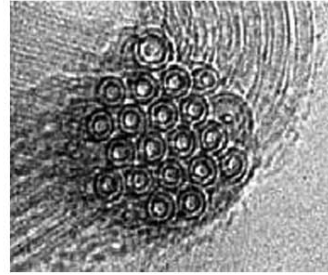
The chemistry of pure carbon is so rich that it is impossible to describe even small part of all possible structures which can be obtained by combination of different types of carbon allotropes. In this part only several interesting examples of experimentally observed allotropes will be briefly considered aiming to demonstrate the virtually unlimited structural variations. Many new structures can be obtained by simple combination of known allotropes. Thus, the so-called **double-walled-** and **multi-walled- nanotubes** (DWCNT and MWCNT) are a good example. In both cases individual single-wall-nanotubes are placed inside each other and are held together by Van-der-Waals forces. Both DWCNTs and MWCNTs are experimentally observed species. Alternatively carbon nanotubes can be bonded covalently, like logs in the construction of buildings or “bunch in Forest” (Figure 1.6).^[32,33,34]

In analogy to nanotubes, fullerene molecules can also be placed each in other or linked together covalently. The first type are the well known **carbon onions** which form as a byproduct under conventional synthesis of carbon nanotubes.^[35] The covalently linked fullerene-based allotropes have been observed in C₆₀ crystals after exposure to high pressure (Figure 1.7).^[36]

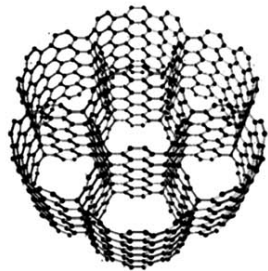
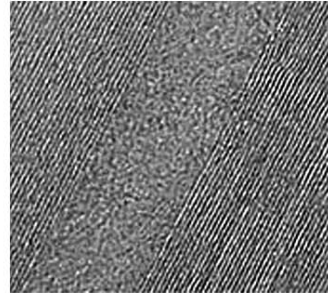
Experimentally observed carbon **nanobuds** represent a combination of nanotubes and fullerenes. In these materials the fullerene fragments are covalently bonded to the walls of the nanotube as presented on the Figure 1.8.^[37] Carbon **peapods** are another example of a hybrid allotrope in which fullerene molecules are trapped inside a nanotube.^[38] Recently observed graphenated carbon nanotubes, a combination of graphene and nanotubes,^[39,40,41] once again underline the uniqueness of carbon and the unlimited number of carbon based nanostructures which can be obtained (Figure 1.9).



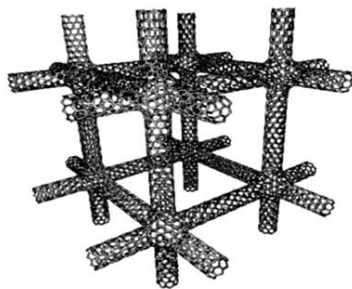
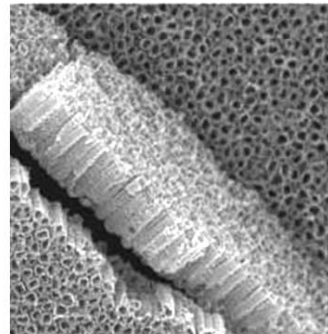
**Double-walled
carbon nanotubes
(DWCNT)**



**Multi-walled
carbon nanotubes
(MWCNT)**



Nanotubes “bunch”



Nanotube network



Figure 1.6. Several experimentally observed (right, TEM images) CNT-based carbon allotrope structures obtained by nanotube joining.

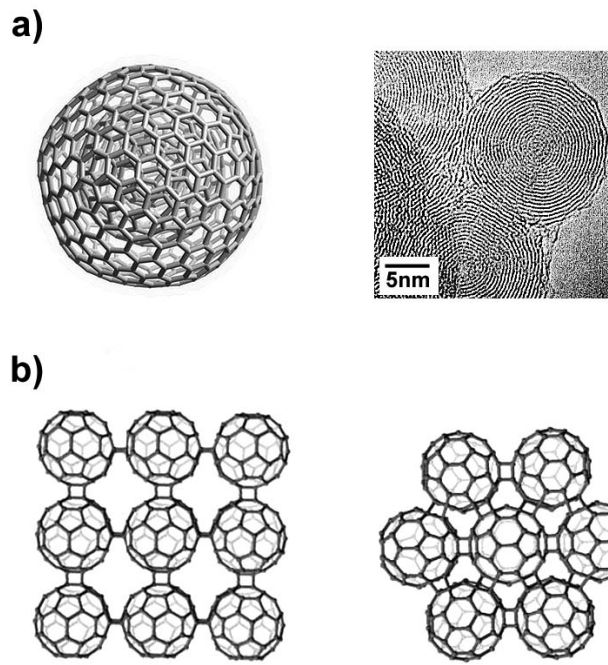


Figure 1.7. Several experimentally observed fullerene-based carbon allotropes. a) molecular structure (left) and TEM image of the carbon onions.^[35] b) the most probable structures of covalently linked C_{60} fullerenes.^[36]

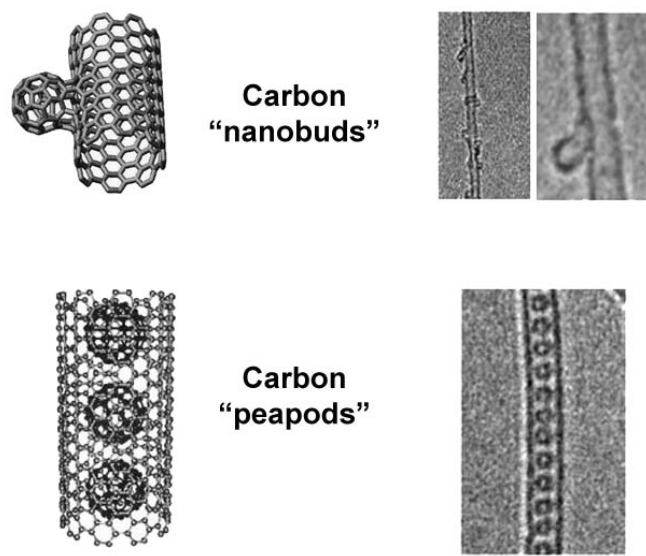


Figure 1.8. Experimentally observed hybrid carbon based nanostructures: nanobuds and peapods.

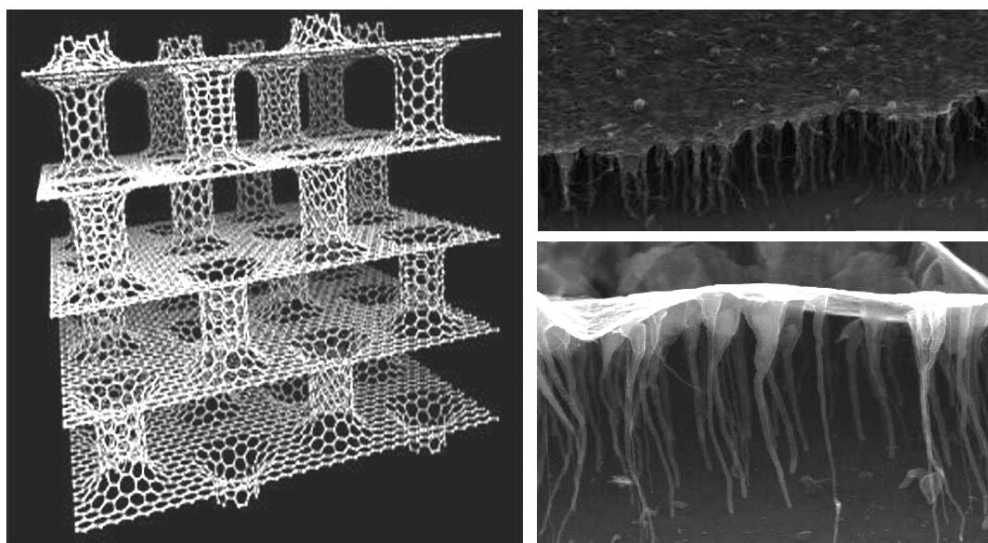


Figure 1.9. Experimentally observed graphenated carbon nanotubes.^[41]

1.1.3. Discovery of fullerenes, structure and isomerism

The first reliable experimental evidence for the existence of fullerene was obtained in 1985,^[8] but only in 1991 a method for C_{60} fullerene production in macroscopic amounts has been developed.^[9] In the first experiments, carbon was vaporized from the surface of a graphite disc under helium atmosphere using a focused pulsed laser. The resulting carbon clusters were detected by time-of-flight mass spectrometry (TOF-MS). It was immediately found that under certain clustering conditions the peak corresponding to C_{60} has a remarkably higher intensity in comparison to signals of other clusters (Figure 1.10).

The structure of the C_{60} cluster was proposed to have the geometry of a truncated icosahedron (polyhedron composed from 12 pentagons and 20 hexagons) and was given the name “buckminsterfullerene” in honor of the famous architect Buckminster Fuller.^[43] As soon as C_{60} had become available in a bulk, its structure was unambiguously confirmed by several spectroscopic and crystallographic methods.^[44]

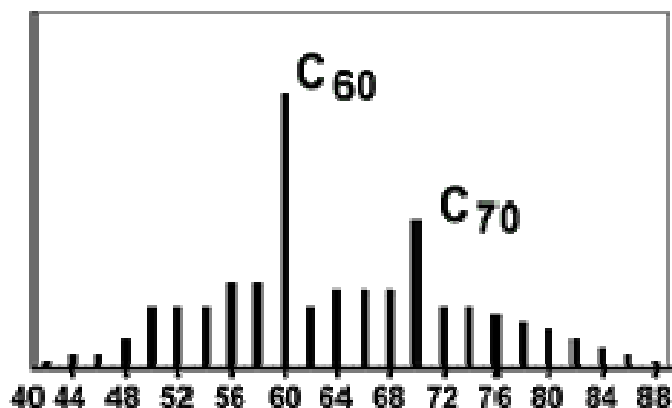


Figure 1.10. TOF-MS spectrum of carbon clusters obtained by laser vaporization of graphite.^[42]

1.1.3.1. Classical methods of fullerene production

Soon after the discovery of buckminsterfullerene several alternative methods were developed for fullerene synthesis, including vaporization of graphite,^[45] synthesis in sooting flames^[46-48] and pyrolysis of hydrocarbons.^[49-51] The first preparative method, which Krätschmer has used for the production of fullerenes, is based on the **resistive heating of graphite** electrodes. Upon applying a voltage, the electric current passing through the electrodes causes heating at the narrow region of contact. This leads to a bright glow in this area associated with the vaporization of carbon. The **arc-discharge** technique is an alternative approach to resistive heating.^[52] In this set-up, the sharpened graphite electrodes are kept in close proximity, but not in direct contact; thus, the electrical power is dissipated in an arc but not in resistive heating. In the **solar generator** method, a solar furnace is used for heating of graphite.^[53] A parabolic mirror collects sunlight and focuses it onto a graphite sample. In comparison to other techniques, the efficiency of the solar generator method is rather low. Fullerenes can also be produced using inductive

heating of a carbon body.^[54,55] In this case more control over the synthesis parameters can be achieved.

1.1.3.2. Combustion synthesis of fullerenes

It has been found that the fullerene formation takes place in optimized sooting flames.^[46,47] Here, premixed laminar benzene-oxygen-argon flames have been found to be effective.^[48] The main disadvantage of this route is the formation of many polycyclic aromatic hydrocarbons which complicate further purification. The amount of fullerenes produced is of around 0.1 - 5 % of the soot mass. Despite the relatively low yield, this process can be easily scaled up. Later a combustion system allowing to produce fullerenes at the ton scale has been developed.^[56]

1.1.3.3. Pyrolysis of hydrocarbons

Fullerene formation has been also detected during the pyrolysis of several PAHs, such as naphthalene,^[49] corannulene and benzofluoranthene,^[50] and perchlorofulvalene.^[51] The yields of C₆₀ in these cases were found to be around 0.5 % or less. Although this approach can't be used for fullerene productions it is rather interesting from the theoretical point of view and sheds some light on the fullerene formation mechanism. This approach represents a first attempt to rationalize the fullerene formation process. Its further improvement has led to the development of the direct synthesis approach which will be discussed in detail in chapter 2.

1.1.3.4. Higher fullerenes and fullerene isomerism

All methods of fullerene production discussed above are based on spontaneous carbon cage assembly, and as a result of the spontaneous nature of formation, a complex mixture of several fullerenes forms. The soot obtained contains typically about 5-15% of fullerenes depending on the technique used for the production. The soluble fullerenes can be extracted using an organic solvent whereas the non-soluble remainder can be separated from the amorphous carbon and graphite by

subsequent sublimation under vacuum. Among the insoluble fullerene species, only the most abundant C_{74} fullerene has been separated and recently unambiguously characterized.^[58]

The C_{60} fullerene is the most abundant soluble fullerene which can be easily isolated by means of high performance liquid chromatography (HPLC) in bulk amounts. The next fullerene which can also be isolated on a preparative scale is C_{70} (Figure 1.11). Besides C_{60} and C_{70} the fullerene soot extract contains around 2-3% of soluble higher fullerenes. These species still remain poorly investigated because of difficulties related to their separation. In contrast to C_{60} and C_{70} all higher fullerenes (starting from C_{76}) have several structural isomers which obey the IPR rule, stating that all pentagons must be surrounded by hexagons in order to form a stable cage.^[59,60] The number of possible IPR isomers increases exponentially with increasing carbon cage size (number of carbon atoms) (Table 1.2). Thus, for example, while C_{78} has only five IPR cages, C_{84} has 24 IPR isomers (Figure 1.12), C_{100} has already 450 stable isomers. Because of the big number of isomeric structures which often display similar chromatographic behavior and their small share in the fullerene extract, the separation of isomerically pure higher fullerenes is frequently difficult. Despite the rather intense research in the field of fullerenes during the last decades, only few higher fullerenes have been successfully isolated and characterized.^[58,61-66]

It is important to emphasize, that despite the structural similarity each individual fullerene has its unique spectrum of magnetic, electrical, optical and chemical properties, thus representing very interesting objects for many applications. On the other hand, since none of the existing techniques can provide access to the higher fullerenes, their applications remain highly elusive. It is obvious, that in order to access these unique molecules in bulk and in isomerically pure form, an alternative synthetic method, which is able to address all disadvantages of the conventional production routes, has to be developed.

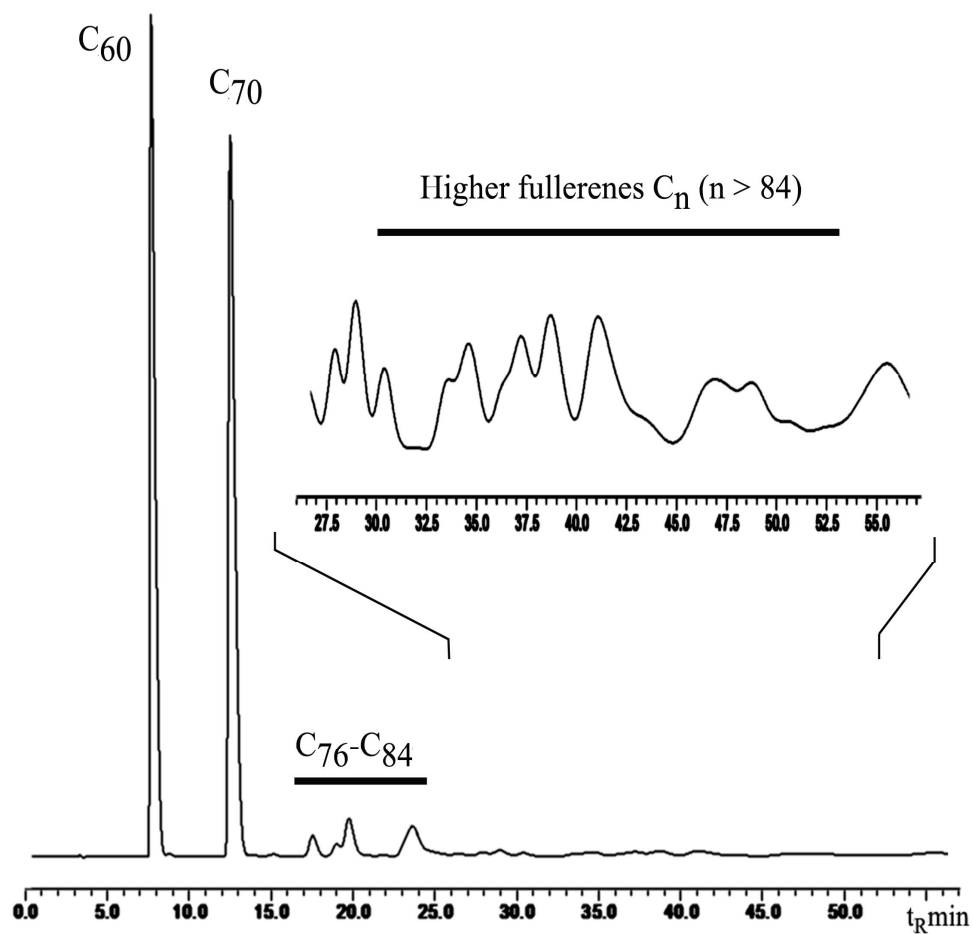


Figure 1.11. Typical HPLC profile of fullerene extract. Two intense signals correspond to C_{60} and C_{70} fullerenes which can be rather easily isolated in pure form by single step HPLC separation. Several abundant higher fullerenes $C_{76}-C_{84}$ can be separated by multi stage HPLC procedure. The big number of overlapping peaks corresponds to other higher fullerenes (insert - shows the 100x zooming of the corresponding region).

Table 1.2. The number of theoretically possible isomers and the number of possible IPR cages for C_{60} - C_{102} fullerenes.^[67]

Number of carbon atoms in the cage	Number of possible fullerene isomers	Number of possible IPR isomers
60	1 812	1
62	2 385	0
64	3 465	0
66	4 478	0
68	6 332	0
70	8 149	1
72	11 190	1
74	14 246	1
76	19 151	2
78	24 109	5
80	31 924	7
82	39 718	9
84	51 592	24
86	63 761	19
88	81 738	35
90	99 918	46
92	126 409	86
94	153 493	134
96	191 839	187
98	231 017	259
100	285 914	450
102	341 658	616

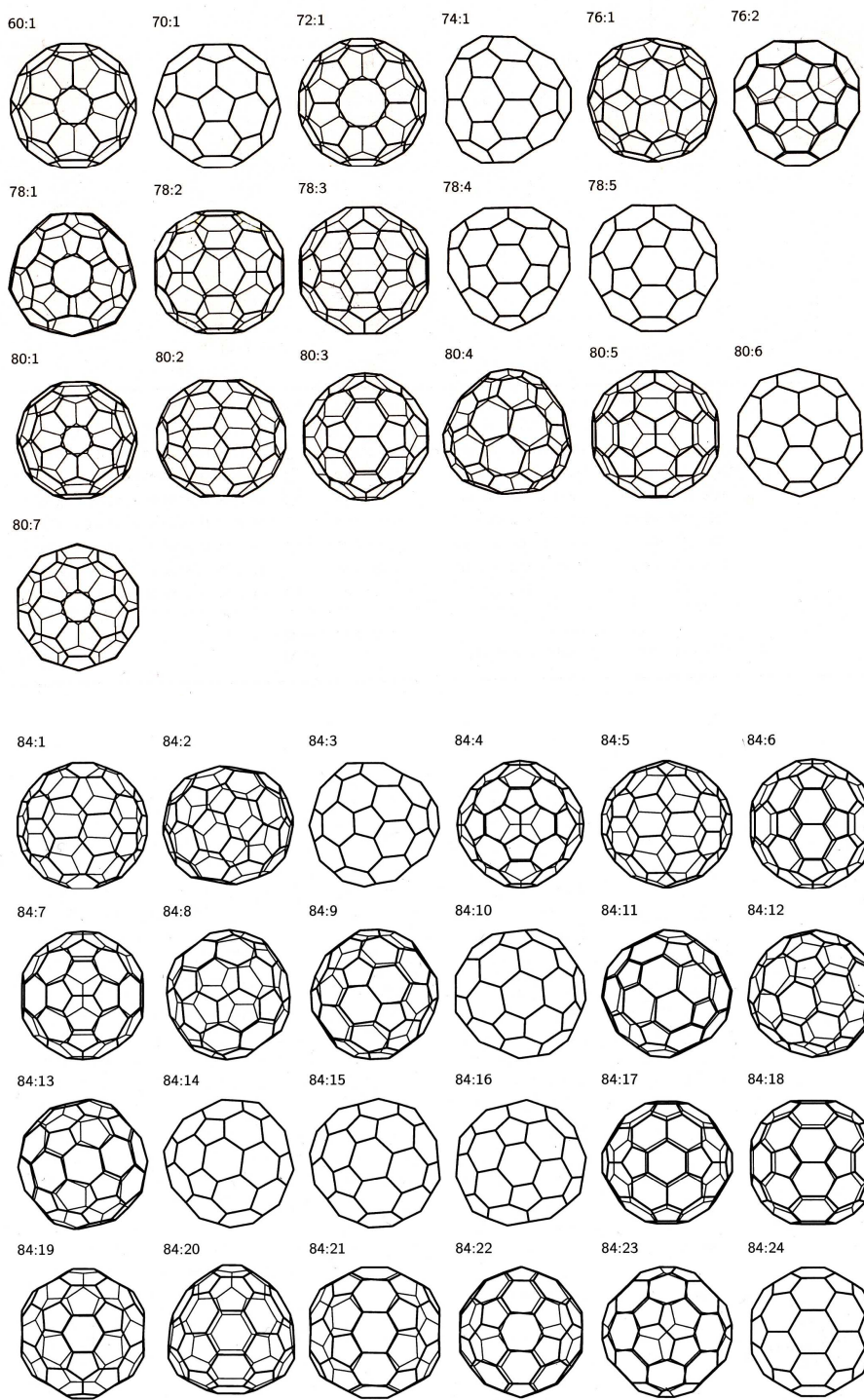


Figure 1.12. Possible IPR of C_{60} - C_{80} fullerenes (top) and all IPR isomers of C_{84} (bottom).
 Reproduced from reference.^[67]

1.2. Polycyclic aromatic hydrocarbons

1.2.1. Introduction

Polycyclic aromatic hydrocarbons (PAHs) are compounds consisting of only carbon and hydrogen with two or more fused aromatic rings. The PAH molecules can be considered as building blocks of carbon based nanostructures such as graphene, nanotubes and fullerenes. Since the general strategy used in this work is based on the synthesis of PAH precursor molecules, a brief description of several PAH types and their nomenclature will be given.

1.2.2. Nomenclature

Since the IUPAC nomenclature has been adopted for PAHs only in 1979, the names encountered in the earlier literature are usually uniform and often confusing. Here, only a short description of IUPAC nomenclature necessary for further discussion will be given. The detailed IUPAC rules can be found in the original literature.^[68, 70]

The simplest member of PAH is naphthalene which contains only two condensed aromatic rings. In contrast, the biphenyl molecule which also has two benzenoid rings, formally does not belong to the PAH family, since the two aromatic rings are not fused (Figure 1.13). Nevertheless this type of compound is often called a non-condensed PAHs in the literature.

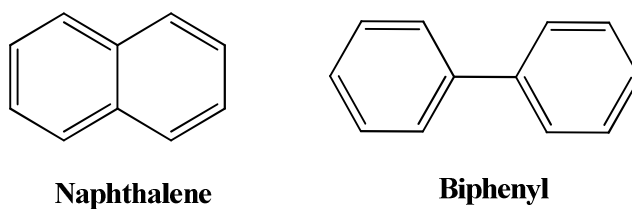


Figure 1.13. Naphthalene, the simplest member of PAHs (left). Biphenyl, no PAH (right).

The number of possible PAH isomers strongly increases with the increase of the number of fused rings. Only one isomer is possible for the two-benzenoid ring

system, two isomers for the three-ring system and six isomers for the four-ring system. A PAH containing ten fused hexagons has already several thousand isomers. All small PAH molecules have a trivial name. The most important members are listed in Figure 1.14.

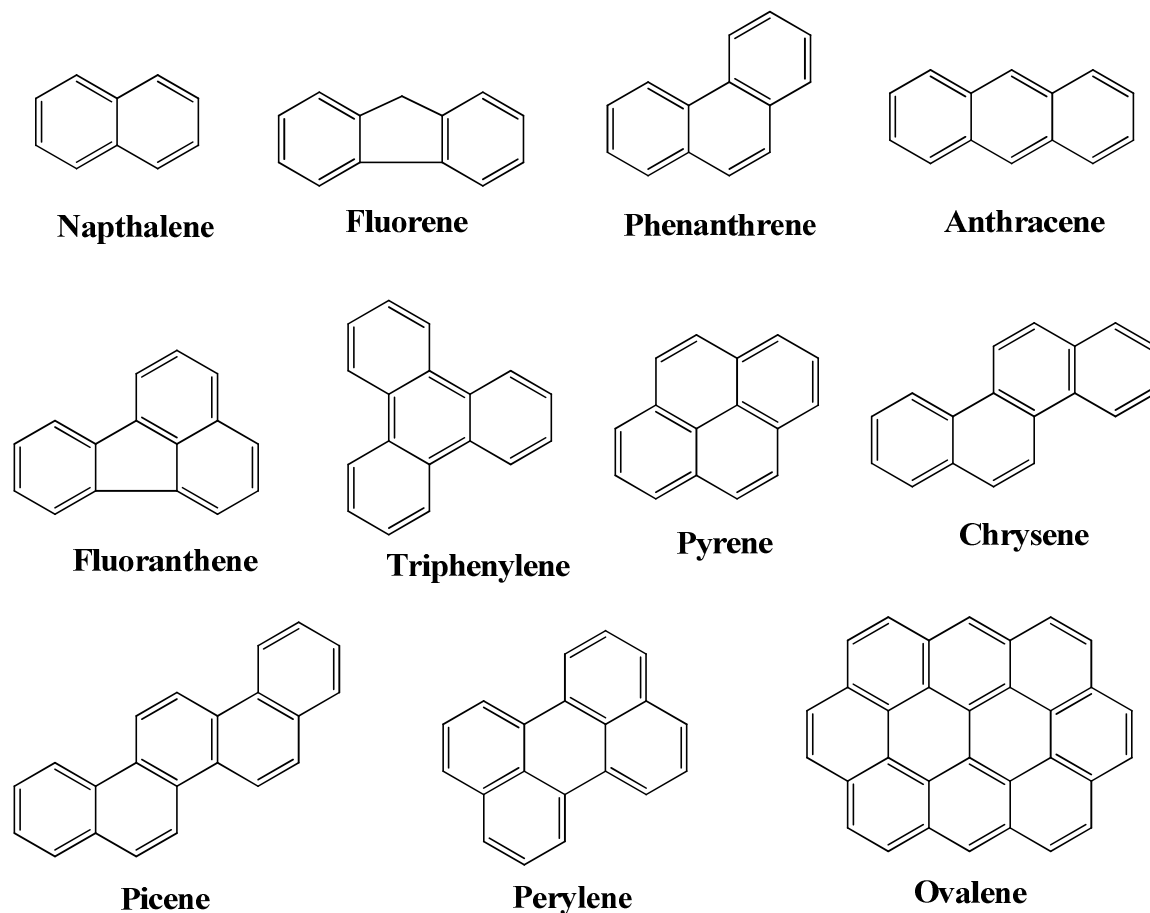


Figure 1.14. IUPAC names of several common PAHs.

For practical use, each carbon atom has to be numbered. Before numbering, the molecule has to be placed in such a way, that the maximum number of rings will be oriented in a horizontal line. If two or more orientations meet these requirements, the one having the greatest number of the remaining rings in the upper right

quadrant and as few rings as possible in the lower left quadrant should be chosen (Figure 1.15).

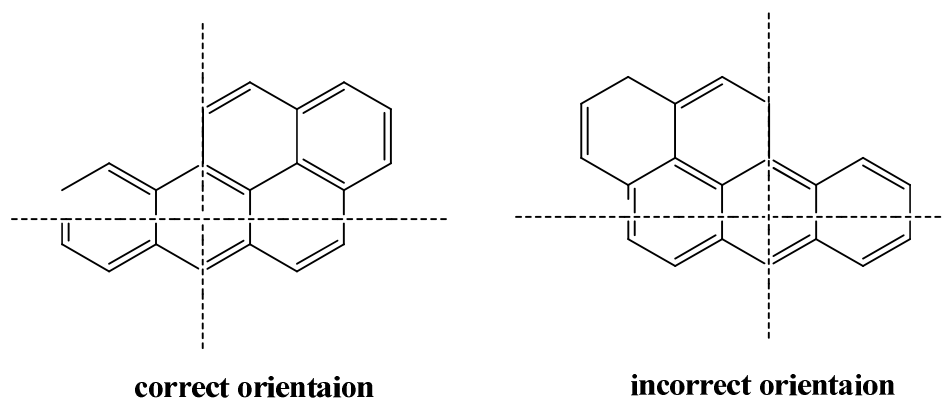


Figure 1.15. Correct orientation and an example of incorrect orientation of PAH molecule for numbering.

Numbering begins (in clockwise manner) from the ring located on the right in the top starting with the carbon atom that is not part of two rings. Meanwhile, only carbon atoms connecting to hydrogen should be numbered. Analogously, all “external” bonds of the PAH molecule are lettered in alphabetic order as presented in Figure 1.16. Anthracene and phenanthrene are exceptions of these rules, their numberings are given additionally in Figure 1.16.

The attached components should be as simple as possible. For example, the addition of a benzo-fragment to the position *e* in the pyrene molecule and the addition of a benzo fragment to the position *def* in triphenylene will result in the same compound (Figure 1.17). The base component in the resulting structure is pyrene, because it comes later than triphenylene in Figure 1.14. Thus, the correct name is benzo[*e*]pyrene, but not benzo[*def*]triphenylene. Another example is dibenzo[*a,k*]chrysene. Naphtho[*c*]chrysene is not correct name, because “benzo” is simpler than “naphtho”, even if there are two benzo-additional components and only one naphtha-additional component (Figure 1.17). Since the IUPAC names of

more complex PAHs are too complicated for practical use, many trivial names are offered for large PAHs in the literature.

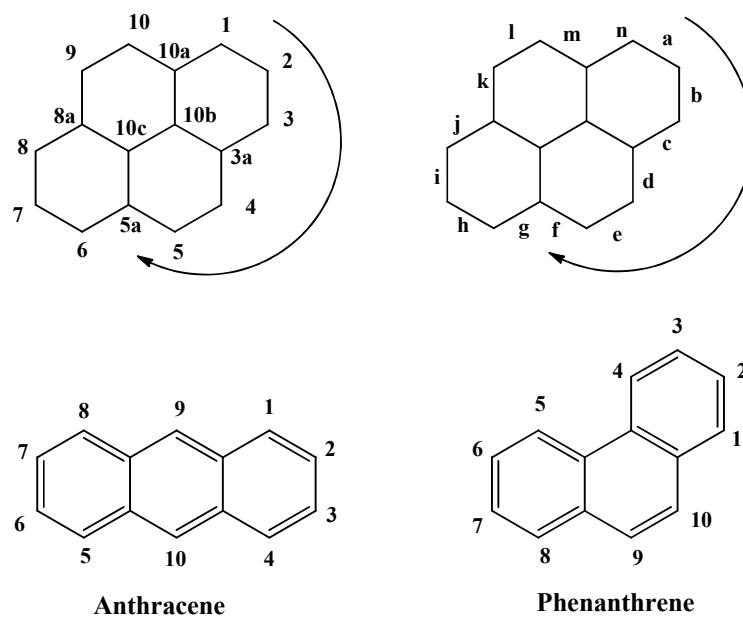


Figure 1.16. IUPAC numbering and lettering of PAHs. (bottom) Numbering of anthracene and phenanthrene (exceptions of the rule).

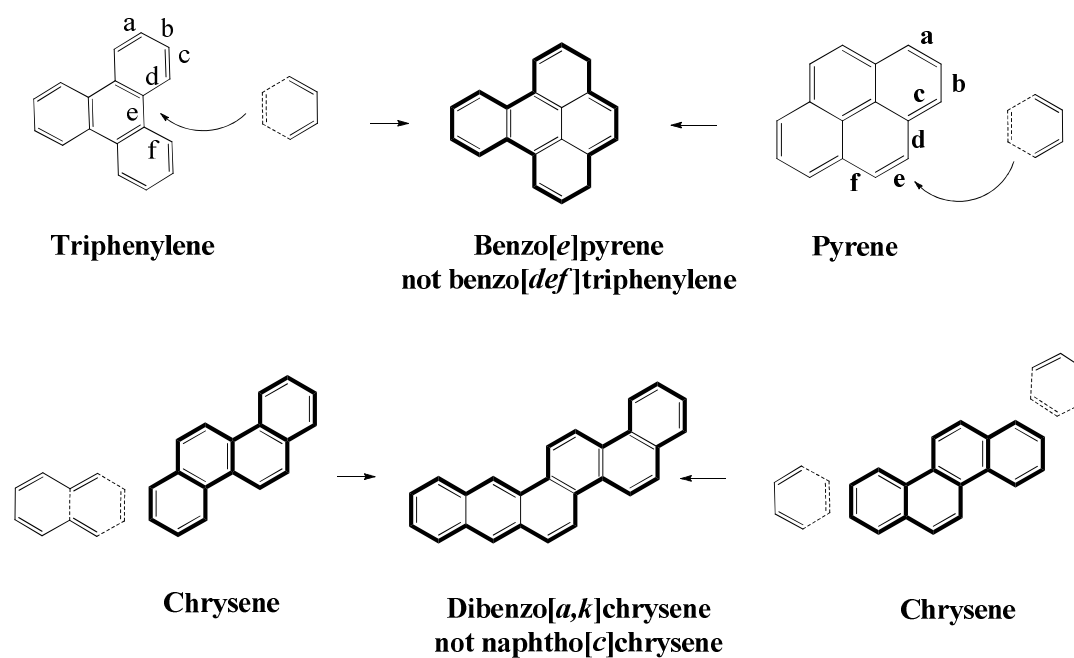


Figure 1.17. Two examples of naming of complex fused ring systems.

1.2.3. Bay, cove and fjord regions^[69]

PAHs have engendered a specialized terminology outside the formal rules. Thus the terms “bay”, “cove” and “fjord” regions coming from landscapes and bodies of water, are widely used for the description of the PAH geometry (periphery). A bay region refers to a molecular region between two angularly fused aromatic rings (like 4,5-positions in phenanthrene). Two following fusions with hexagons in angular manner result in cove and fjord regions, respectively, as it presented in Figure 1.17.

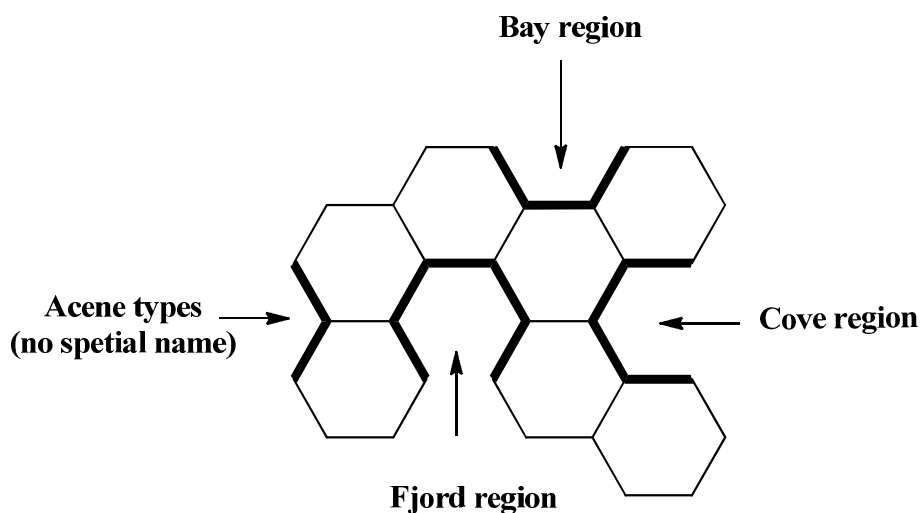


Figure 1.18. Different molecular regions in PAH molecule.

1.2.4. Alternant and non-alternant PAHs

All PAHs can be classified as alternant or non-alternant.^[70] In alternant PAHs all carbon atoms can be labeled alternately in such a way that no adjacent carbon atoms marked with an asterisk will appear and the number of labeled and non-labeled carbon atoms has to be equal (Figure 1.19).

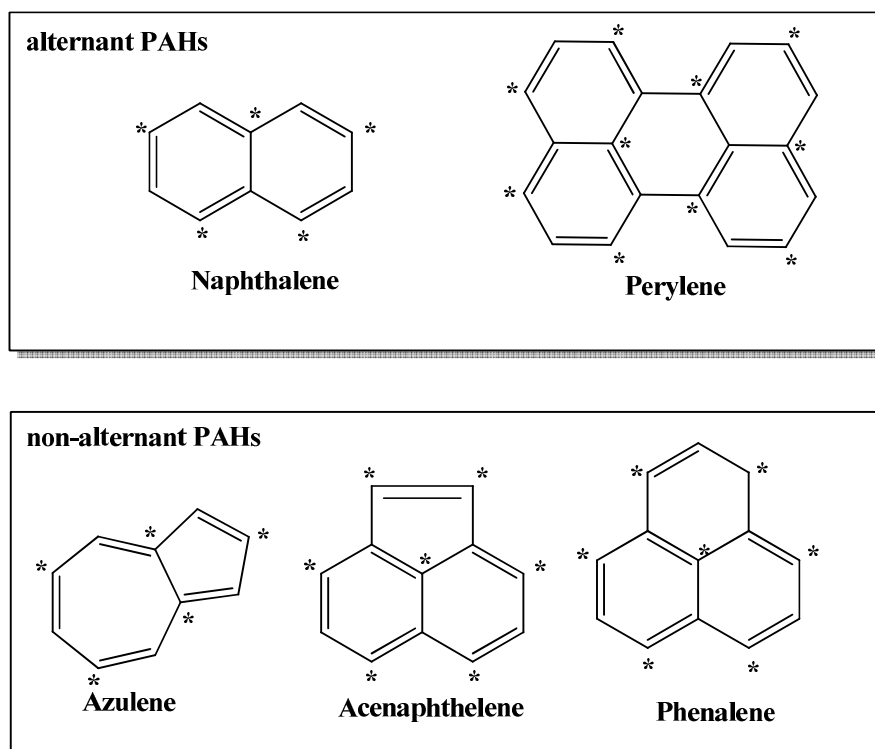


Figure 1.19. Typical examples of alternant and non-alternant PAHs.

1.2.5. Kata- and peri-condensed PAHs

All alternant PAHs can be further classified depending on the type of ring connectivity, as kata- or peri-condensed.^[70] Acenes and phenes are typically kata-condensed PAHs, in which carbon belongs maximally to two rings. Acenes have benzenoid rings fused in a linear arrangement. Examples are anthracene, tetracene, pentacene and hexacene. In contrast, phenes (phenanthrene, tetraphene, pentaphene, hexaphene) consist of benzenoid rings fused in an angular arrangement. Another class of kata-condensed PAHs are helicenes, containing the benzenoid rings arranged in a helical manner (Figure 1.20).

In peri-condensed structures, at least one carbon atom belongs to three rings. Pyrene and perylene are typical peri-condensed PAHs (Figure 1.14).

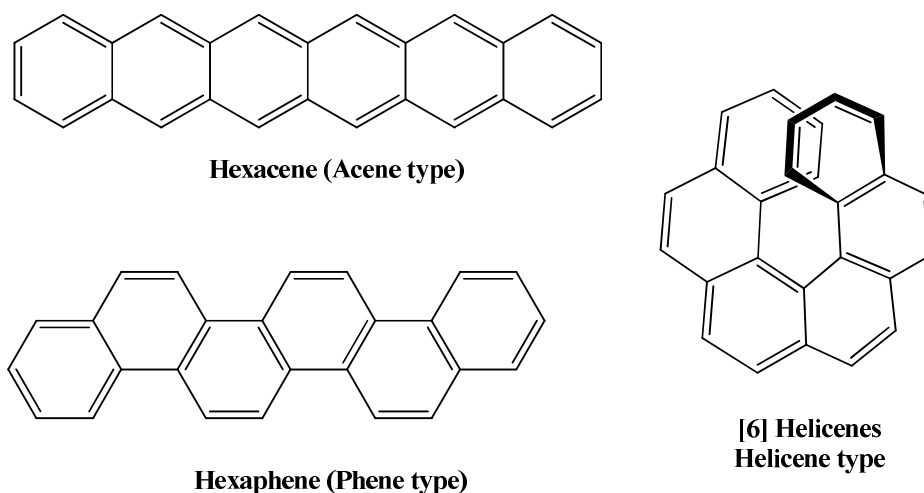


Figure 1.20. Typical members of kata-condensed PAHs.

Kata- and peri-condensed PAHs are different not only in the structural organization, but also show remarkably different properties. Independently their kata- or peri-condensed nature, the so-called fully benzoid structures^[69] (Clar's hydrocarbons) represent an important subclass of alternant PAHs. These PAHs are formally constructed only from benzene rings that are connected together by (formally) single C-C bonds. Benzene itself is the smallest representative of this group. All fully benzoid PAHs are characterized by an exceptionally high stability comparable to benzene. Several important members of this class are given in Figure 1.21.

All other polyarenes, which can not be "separated" in individual "benzol" fragments, are more reactive than fully benzoid PAHs, because of the partially localized double bond which gives an olephinic character (Figure 1.22). According to the Clar's rule the resonance structure containing the maximal number of "separated" sextets contributes mainly to the stability and determines the chemical properties of the corresponding PAH molecule.

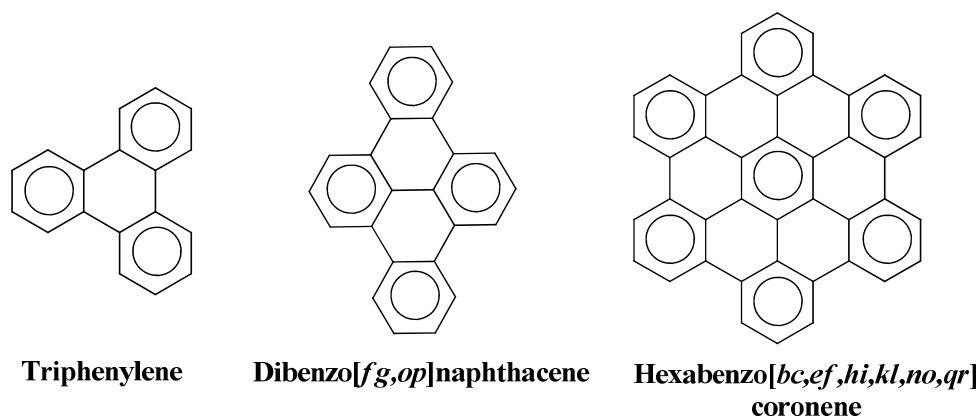


Figure 1.21. Examples of fully benzenoid PAHs. Each circles correspond to an aromatic sextet (a group of six delocalized electrons, benzene-like moieties).

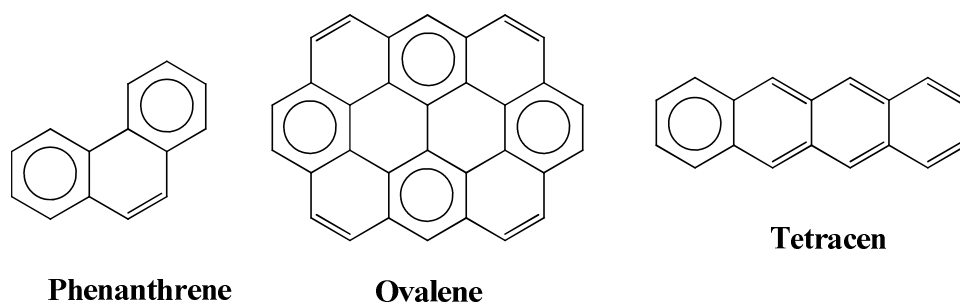
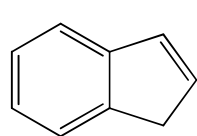


Figure 1.22. The resonance structures of several non fully benzenoid PAHs having maximal number of sextets. The presence of localized double bond is responsible for partial olefinic character in these compounds.

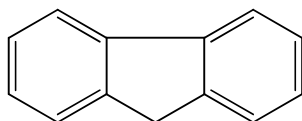
1.2.6. PAHs containing five-membered rings

In principle, aromatic hydrocarbons may have not only hexagonal rings in the structure, but also four-, five-, seven- or eight- membered rings. PAHs containing five-membered rings are of greater interest for us, since they are fragments of buckybowls, fullerene precursors, and fullerenes. All PAHs containing pentagons are non-alternant and can be divided into several subtypes depending on how the rings

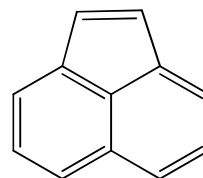
are connected. Thus, compounds where the pentagon is fused only with one hexagon belong to indene type. The PAHs where the pentagon is fused with two hexagons can be divided into fluorene and acenaphthylene types. Three hexagon rings can surround a pentagon ring in two different ways, which yield fluoranthrene and phenanthrene types. Four hexagon rings can surround a pentagon ring only in one way producing benzo[ghi]fluoranthrene. The simplest PAH in which the pentagon is completely surrounded by hexagons is corannulene. Corannulene is of particular interest because of its non-planar geometry, which will be discussed in the next chapter.



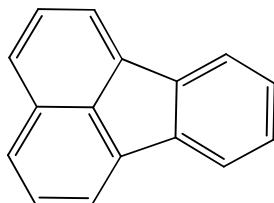
Indene



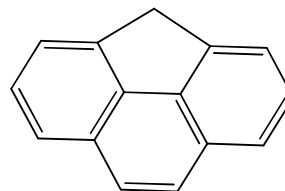
Fluorene



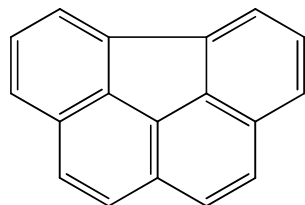
Acenaphthylene



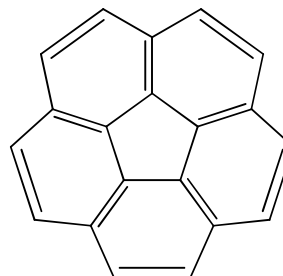
Fluoranthene



4H-Cyclopenta[def]phenanthrene



Benzo[ghi]fluoranthrene



Corannulene

Figure 1.22. Different types of pentagon-containing PAHs.

1.2.7. Non-planar PAHs

The steric congestion of the hydrogen atoms frequently gives rise to a non-planar geometry of PAH molecules. Thus, the strain in the cove regions of hexabenzocoronene causes remarkable deviations from planarity. Helicenes represent an extreme example of such kind of strain. Cyclophanes are another major class of non-planar PAHs, where the inherently planar PAH molecules is typically connected by chains in such a way that aromatic part adopts bent geometry. The carbon nanotubes formally belong to this class of non-planar PAHs. The introduction of five-membered rings in PAHs as well introduce remarkable strain in the system. Thus, corannulene where the five-membered ring is completely surrounded by hexagons, displays deviations from planar since the circumference is too small to yield a flat molecule. The force which retains the typical C-C bond distances turns the system out of the plane and the molecule adopts a bowl shape. Such compounds (containing pentagons surrounded by hexagons) form a big family of the so-called geodesic polyarenes or buckybowls (Figure 1.23). Fullerenes can be classified in this term as “closed geodesic polyarenes” which represent an ultimate extension of buckybowls, forming a sphere of solely carbon atoms.

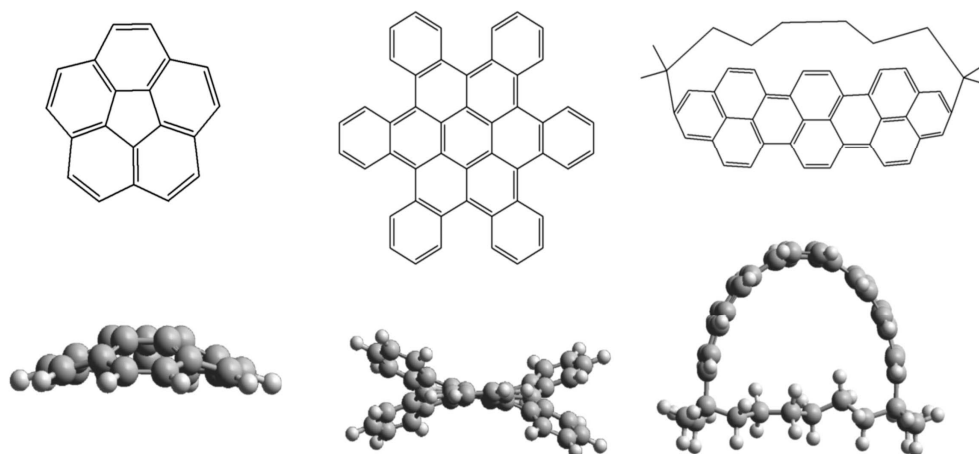


Figure 1.23. Examples of non planar PAHs: Corannulene (buckybowls, fullerenes), hexabenzocoronene and 1,1,8,8-tetramethyl[8](2,11)-teropyrenophane (cyclophanes, nanotubes).

1.2.8. Properties of PAHs

The solubility, reactivity and stability of PAH molecules are very important aspects which have to be taken into account before planning the synthesis of new PAH molecules, especially in the case of large PAHs such as fullerene precursors.

In general the solubility of organic molecules is dependent upon numerous factors. Although as a rule the solubility tends to diminish with increasing molecular size the molecular weight is not a major factor. The most important of these are related to the crystal formation energy and the ability of molecules to fit closely together in a crystal lattice.^[70] The factors include molecular symmetry, planarity, and the presence of substituents. Highly symmetrical and planar alternant polyarenes without any functional groups are usually able to pack in a crystal lattice very effectively, so that the energy required for solubilization is rather high. Conversely, polyarenes that lack symmetry, deviate from planarity, and/or possess bulky substituents are often reasonably soluble in organic media. Low solubility may often be countered by substitution in appropriate molecular sites. Methyl substitution tends to markedly enhance the solubility of most PAHs, probably by steric interference with the close association of planar fused aromatic ring systems in the crystal lattice. As a rule an introduction of polar functionality tends to enhance the solubility of PAH molecules in polar organic media.

Chemical properties and reactivity are also directly dependent on the molecular structure of PAHs. Some PAHs display exceptionally high chemical stability due to effectively delocalized π -systems, whereas some PAHs are very reactive and unstable molecules. As was mentioned before, the fully benzenoid structures possess the highest stability among all PAH classes. Phenenes and helicenes are also relatively stable, but more reactive than fully benzenoid structures due to partially localized double bonds. Thus phenanthrenes, for instance, easily undergo a bromine addition typical for alkenes instead of an electrophilic substitution typical for aromatic compounds. Acenes show the highest reactivity among all PAHs, which is enhanced with increasing numbers of rings, leading to a decrease of the energy

HOMO-LUMO gap and therefore to a higher chemical reactivity. For example, anthracene is a rather stable compound, hexacene must be handled under an inert atmosphere, whereas heptacene has never been obtained in pure state.

The reactivity of extra large PAHs can be easily distinguished by an analysis of their periphery which correlates with the resonance energy.^[69] The best stabilization is observed for arm-chair periphery. In contrast, a zig-zag periphery typical for acenes, leads to low stabilization and consequently to higher reactivity (Figure 1.24).^[69]

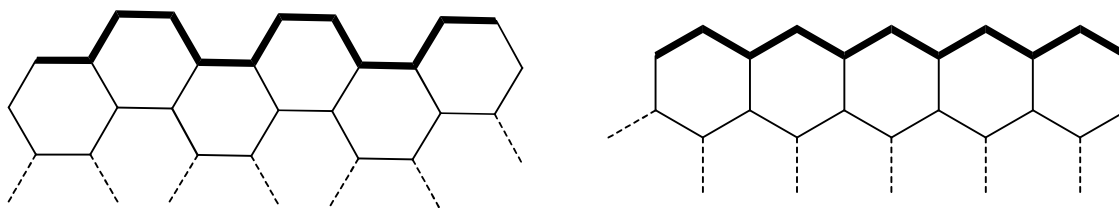
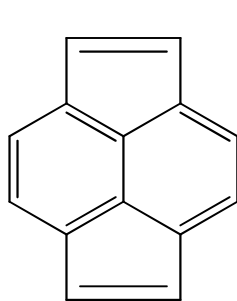


Figure 1.24. Stable arm-chair and reactive zig-zag periphery determined the reactivity/stability of large PAHs.

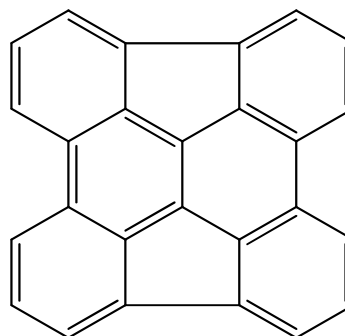
In contrast to the alternant polyarenes, the chemical stability of non-alternant PAHs can't be predicted so easily. Frequently non-alternant PAHs demonstrate surprisingly high differences in their stability. Thus for example, Diindeno[1,2,3,4-defg:1',2',3',4'-mnop]chrysene can be distilled at 550 °C, whereas pyracylene decomposes already at room temperature (Figure 1.25).^[70]

Deviation from planarity also influences the reactivity, and non-planar PAHs typically display enhanced reactivity in comparison to planar homologues. The reason for the higher reactivity is local strain and imperfect overlap of adjacent p-orbitals which reduce the stabilization in the molecule. Such a scenario leads to the partial localization of double bonds and more pronounced olefinic character in these molecules. Nevertheless the C₆₀ fullerene which possess huge strain energy

(of around 609 kcal/mol) is found to be extremely stable and can survive up to 500 °C in bulk and more than 1500 °C in the gas phase.



Pyracylene



Diindeno[1,2,3,4-defg:1',2',3',4'-mnop]chrysene

Figure 1.25. Non-alternant PAHs: stable diindeno[1,2,3,4-defg:1',2',3',4'-mnop]chrysene and highly reactive pyracylene.

1.2.9. Analysis and characterization of large PAHs

Several of the classic tools that are generally used for structure determination are frequently not well suited for the study of large PAHs (PAH). For example, infra-red, ^1H - and ^{13}C -NMR spectroscopy are generally not very useful for isomer differentiation. Infra-red spectra show only carbon ring motions, and motions of the peripheral protons. Since all large PAHs contain these fragments, little information is gained by this analysis. However, infra-red spectroscopy can be used in order to find which types of ring fusions exist in the molecule. In the case of NMR analysis, besides the solubility problem, the spectra need to be collected on extremely high-field instruments in order to resolve the hyperfine couplings. Nevertheless, in some cases ^1H -NMR is rather useful for structural analysis. Thus, sterically crowded bay region protons which show characteristic downfield shifts (8.5-8.8 ppm), the protons in cove regions which exhibit even greater downfield shifts (8.6-9.2 ppm) and protons in the fjord regions exhibiting usually broad shifts (7.5-8.2 ppm) can be easily recognized. Gas chromatography is usually not suitable for the analysis and

separation of large PAHs because the peaks are often not fully resolved. In contrast, HPLC is rather effective in separation of these molecules. Mass spectrometry is often used for analysis since stable PAH molecules can be easily ionized without decompositions using different types of ionization. Even completely insoluble extra large molecules with molecular weight up to 20000 can be analyzed using MALDI-TOF techniques.^[71] Typically each PAH shows a rather characteristic UV-absorbance spectrum. These often possess many absorbance bands and are unique for each ring structure. Thus, for a set of isomers, each isomer has a different UV-absorbance spectrum than the others. This is particularly useful in the identification of PAHs. Functional groups such as methyl, bromine, etc, give predictable bathochromic shifts. Many of the PAHs show intense fluorescence, emitting characteristic wavelengths of light when they are excited. The properties of nitromethane to quench selectively fluorescence emission of alternant PAHs can be very useful in order to distinguish between alternant and non-alternant PAHs (emission intensities of non-alternant PAHs are usually unaffected).^[72]

1.3. Rational fullerene synthesis

1.3.1. Introduction

Numerous attempts to optimize the graphite vaporization process clearly demonstrate that selective formation of isomerically pure fullerenes can not be achieved by this technique. The next step in this direction is a rational chemical synthesis which is based on the controlled construction of the desired fullerene cage. The method is of practical interest not only as method for synthesis of higher fullerenes in pure form, but also as a prospective method for synthesis of various carbon based nanostructures which cannot be obtained by the uncontrolled process of graphite evaporation. The construction of the fullerene cage is not a trivial task because of several reasons. First of all, even in the case of the smallest stable C₆₀ fullerene, it is necessary to connect 32 rings. Moreover, since the non-planar nature of the fullerene π -system results in enormous strain energy such an assembly is very challenging.

1.3.2. Total synthesis of corannulene

The first attempts to synthesize compounds with non-planar π -system were made in 1971 (14 years before the discovery of fullerenes).^[73] Barth and Lawton have successfully synthesized corannulene (the smallest member of geodesic polyarenes) by a 18 step synthesis (Figure 1.26). The total synthesis approach based on step-by-step construction turned out to be so complicated that it has been reproduced only once during the next 41 years. Obviously, that such an approach cannot be applied to the synthesis of more complex structures such as fullerenes. It is also clear that the creation of large and highly strained systems such as fullerenes requires alternative synthetic approaches.

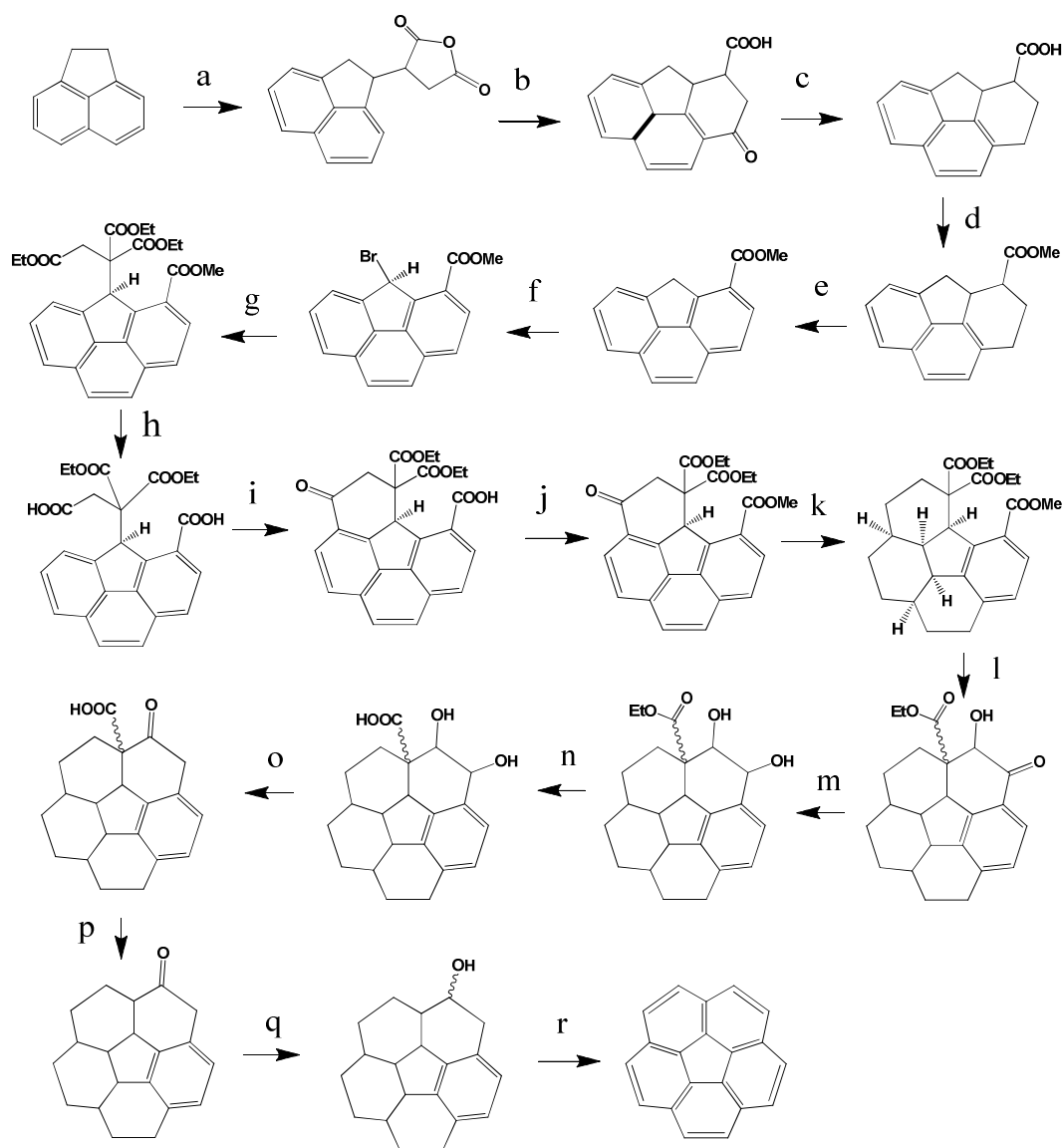


Figure 1.26. The first synthesis of corannulene by Barth and Lawton.^[73] a) maleic anhydride, 210-240 °C; b) eutectic melt of AlCl₃ - NaCl; c) N₂H₄, KOH; d) Mg, Et₂O, CdCl₂; e) Pd/C, p-cymene; f) *N*-bromosuccinimide, CCl₄; g) triethyl-1,1,2-ethanetricarboxylate, *t*BuOK; h) KOH; i) H₃PO₄; j) MeOH, H₂SO₄, 1,2-dichloehane; k) H₂, Pd/C, AcOH; l) Et₂O, NH₃ Na; m) 1) CH₂N₂ 2) Na/NH₃; n) 1) NaBH₄ 2) KOH, n-PrOH; o, p, q) heat; r) 1) NaBH₄ 2) Pd/C

1.3.3. Flash vacuum pyrolysis

In 1974 Roger Brown presented an effective method for generating carbene species from acetylene derivatives under high temperatures shock conditions.^[75] Nowadays, this method is well known as a flash vacuum pyrolysis (FVP). FVP consists in the heating of molecules in the gas phase to very high temperatures for a very short

time. The typical FVP set up is presented in Figure 1.27. Typically the sample is sublimed at reduced pressure under inert atmosphere and the vapors pass through a quartz tube heated by an electric furnace. A gentle stream of carrier gas (argon or nitrogen) is commonly used to facilitate the flight of large molecules. The “heating time” is short, around 10^{-6} sec, which is enough to introduce a large amount of energy into the molecules, but not enough for their decomposition. The pyrolysis products are collected in a cold trap.

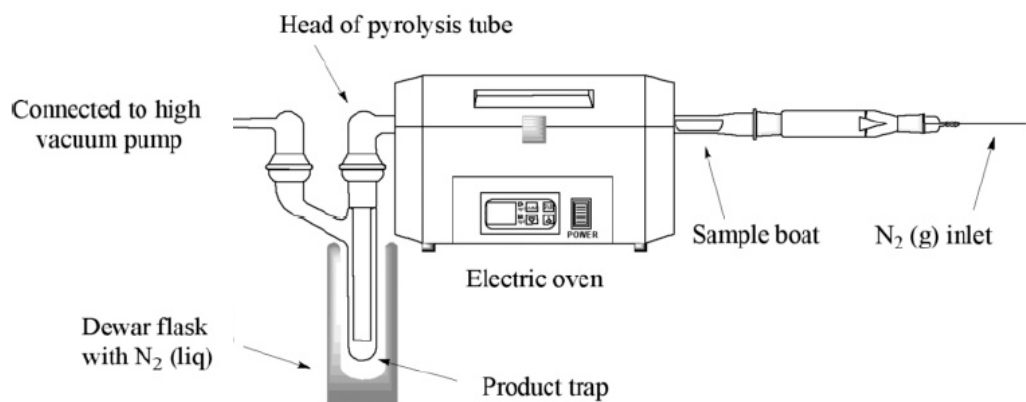


Figure 1.27. Typical FVP set up. Reproduced from reference.^[74]

In the first experiments, Brown has shown that in the case of biphenylacetylene pyrolysis, the reactive carbene formed attacks the neighboring carbon atom, resulting in C-C bond formation. Such an intramolecular condensation leads to phenanthrene, as it presented in Figure 1.28.^[75]

In 1992 this approach has been successfully applied for the "second" synthesis of corannulene by Scott et al. using a 7,10-diethynylfluoranthene (Figure 1.29).^[76] The corannulene yield was found to be low, because of partial polymerization and destruction of the precursor during sublimation. After this discovery a variety of possible precursors with optimized structures (bearing masked acetylene groups) were investigated.^[77,78]

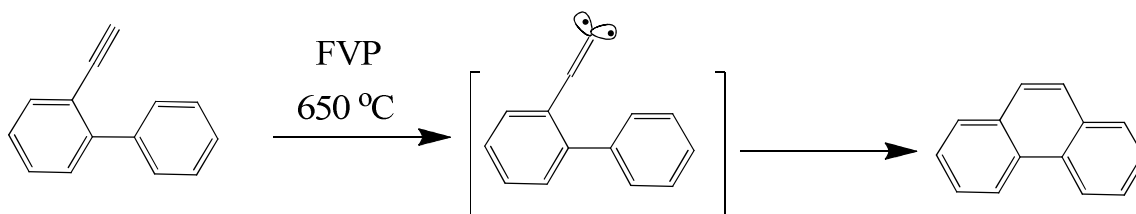


Figure 1.28. The mechanism of efficient intramolecular condensation in binaphthylacetylene under FVP conditions.

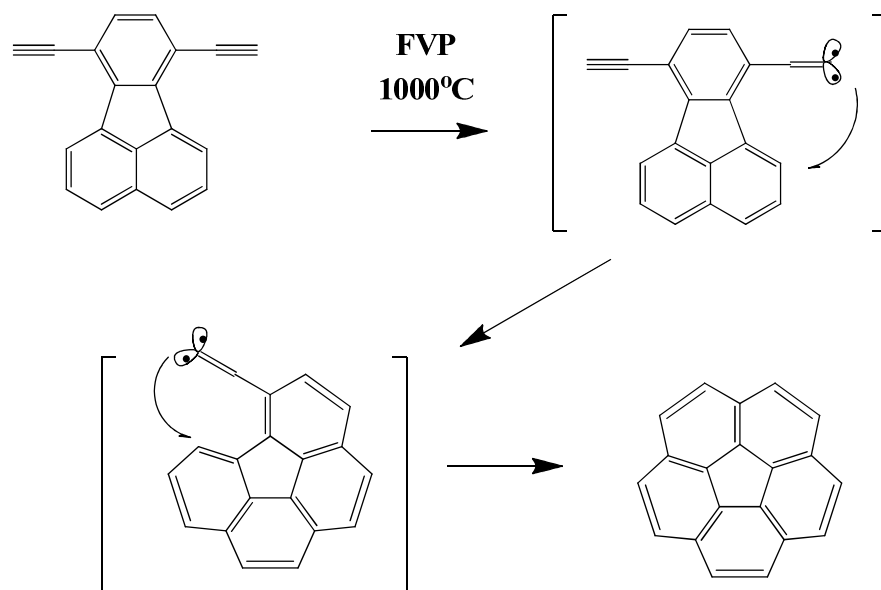


Figure 1.29. Second synthesis of corannulene using FVP approach.

As a result of this work the best precursor found is dichlorodivinylfluoranthene^[79] (Figure 1.30 compound B), pyrolysis of which gave corannulene with 40 % yield.

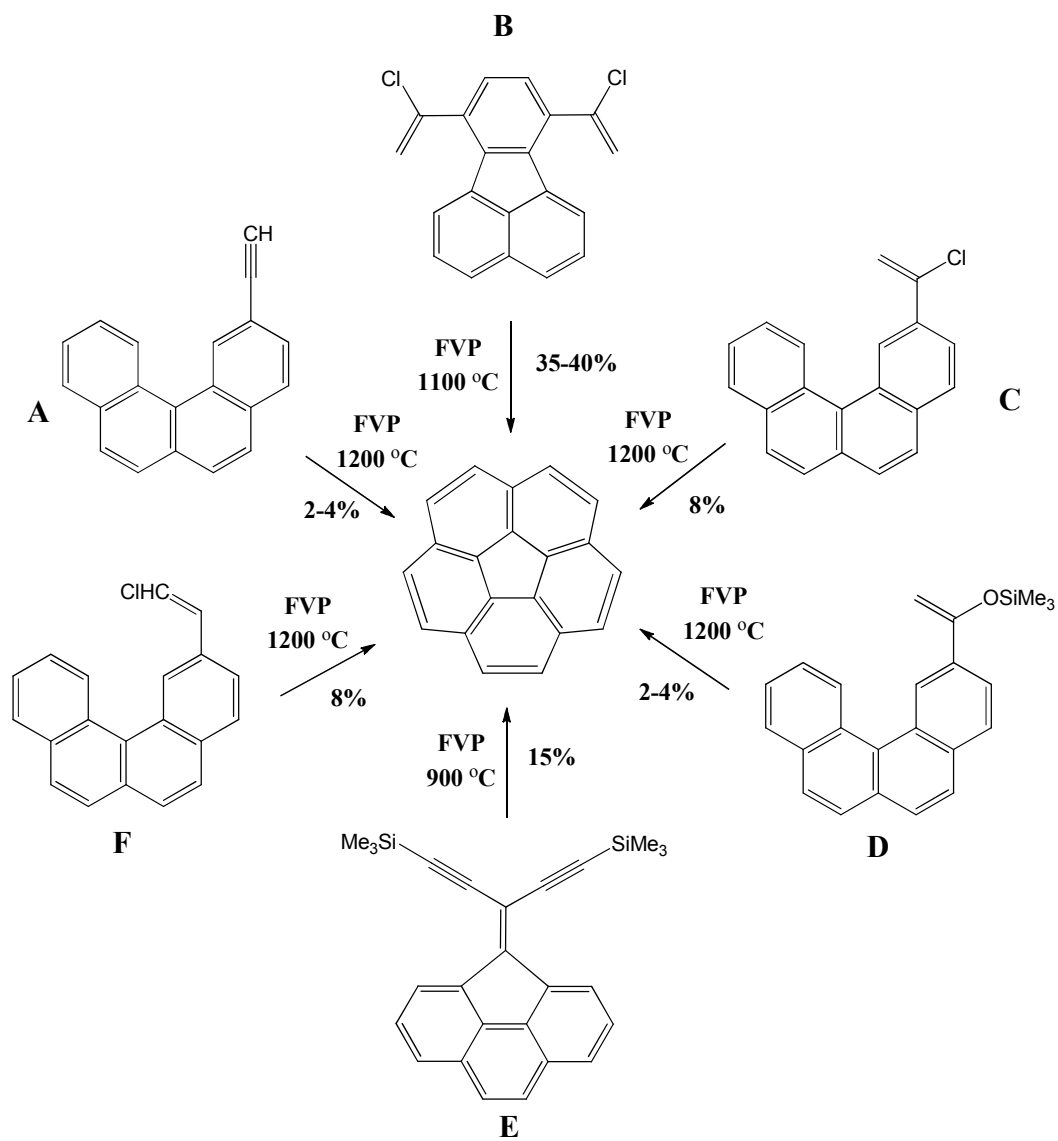


Figure 1.30. FVP precursors of corannulene.

Later, it has been found that not only acetylene derivatives can be used for synthesis of geodesic PAH via intramolecular condensation. Namely, it was discovered that radical species possess enough energy for such cyclization as well (Figure 1.31).

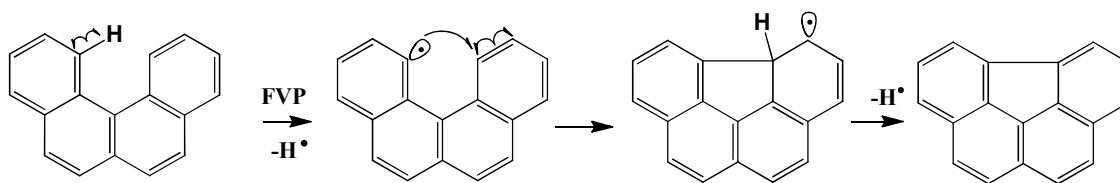


Figure 1.31. The mechanism of intramolecular condensation via radical mechanism under FVP on the example of condensation in the cove region of benzo[*c*]phenanthrene.

1.3.3.1. Buckybowl synthesis

Soon after, based on this strategy many geodesic polyarenes were obtained by intramolecular Aryl-Aryl coupling in polycyclic aromatic precursor molecules with the required location of all carbon atoms in the structure. It has also been found that the introduction of a halogen atom in the initial precursor, to carbon atoms where a new bond is desired, significantly increases the yield of the product.^[80-82] Such effect is the result of effective radical generation. The carbon-halogen bond breaks homolytically more easily during pyrolysis than the C-H bond and the radical formed attacks the neighbouring carbon atom with formation of required carbon-carbon bond. Two examples of such activation are given on Figure 1.32.

Later, it was found that the introduction of halogen atoms in the α -position to carbon atoms where a new bond is desired, also provokes cyclization quite effectively (Figure 1.33).^[84-86] This discovery is very important from a practical point of view, since the introduction of a halogen atom in the cove and/or fjord regions is usually difficult or practically impossible because of sterical hindrance.

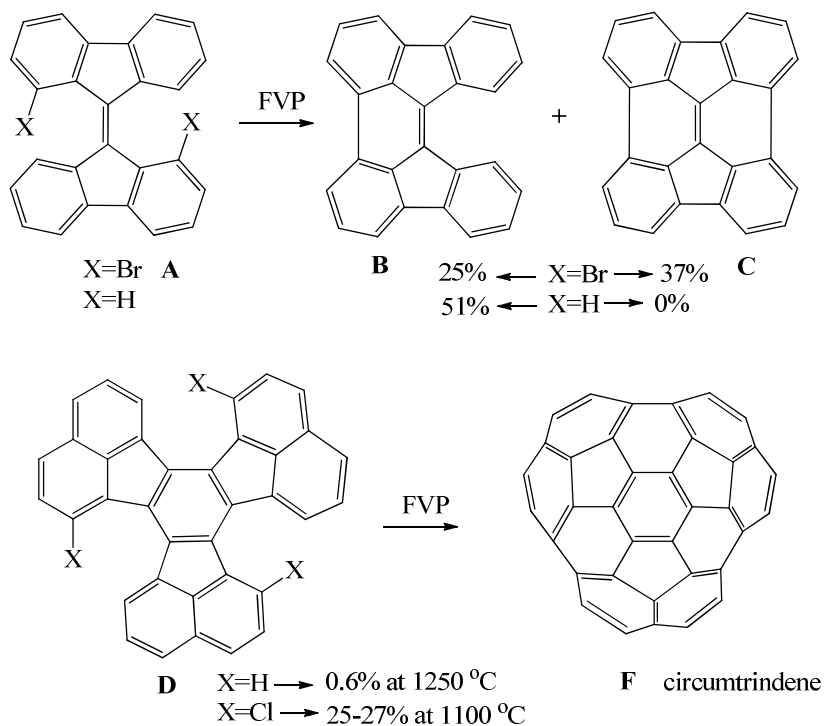


Figure 1.32. Effective ring closure under FVP conditions using activation by chlorine functionality.^[83]

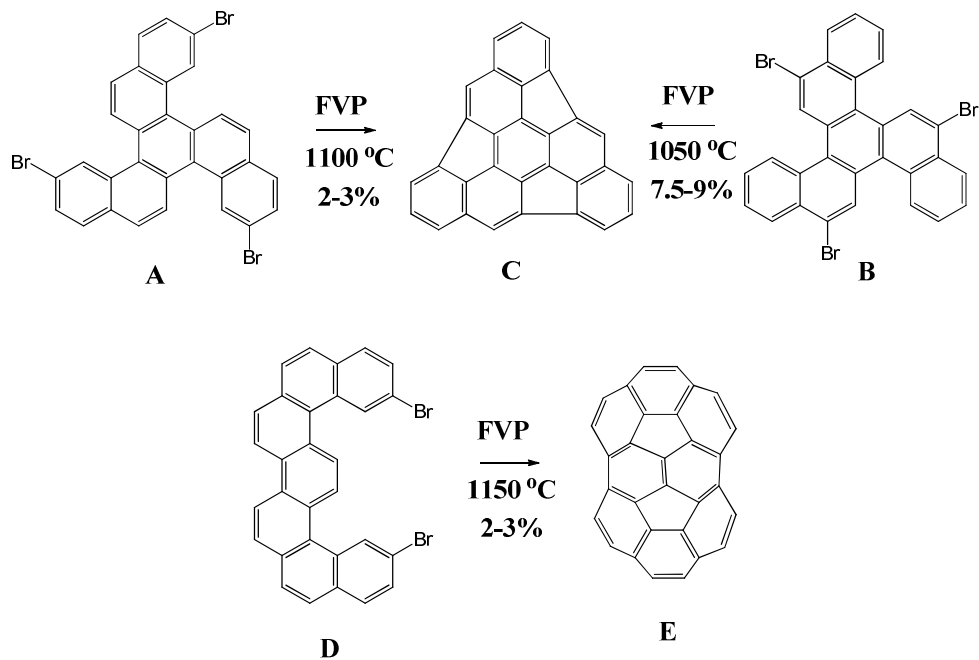


Figure 1.33. Examples of an effective condensation under FVP conditions of precursor molecules containing halogen atoms in α -positions.

1.3.3.2. Attempts of rational fullerene synthesis

The same strategy has been used in the first rational synthesis of C₆₀ by the Scott group.^[87] The C₆₀ precursor, containing all 60 carbon atoms at the for fullerene formation required positions and three chlorine atoms for radical generation has been obtained through an 11-step synthesis. After the FVP of this precursor at 1100 °C, the C₆₀ fullerene has been obtained with 0.1 to 1 % yield (Figure 1.34).

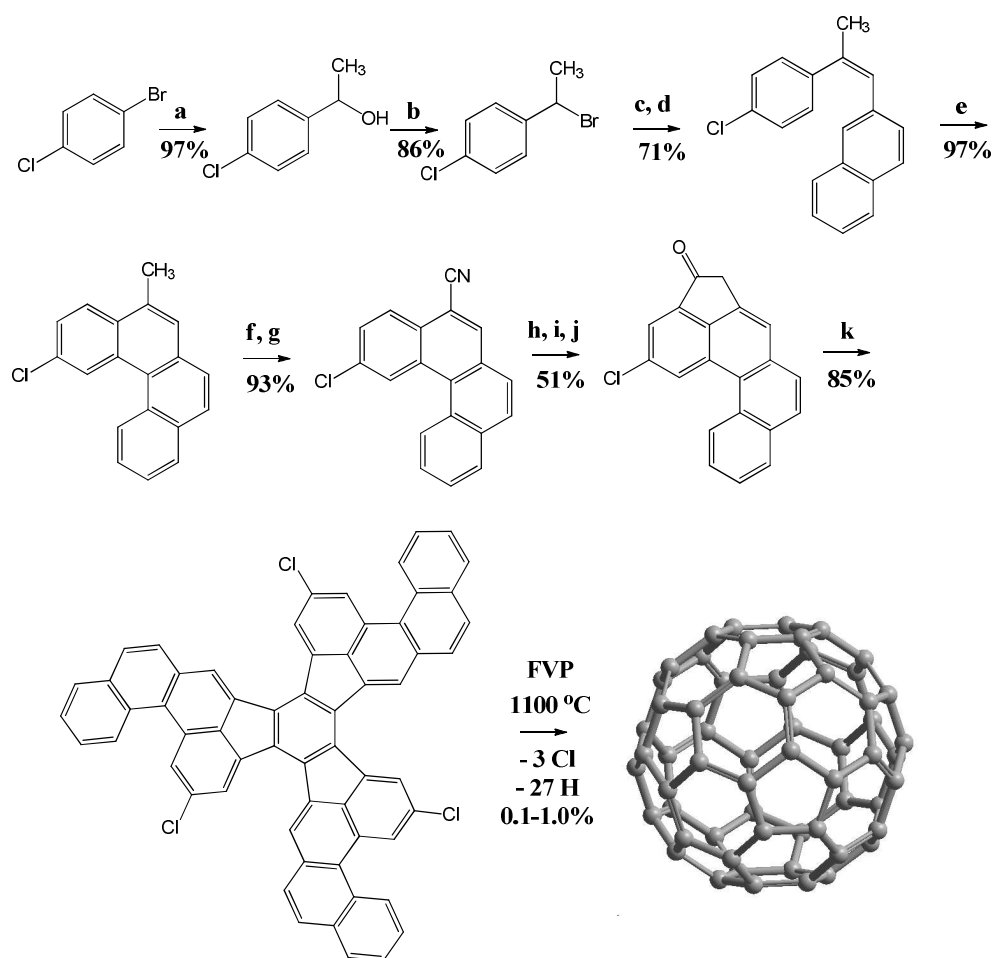


Figure 1.34. The first direct synthesis of C₆₀ fullerene.^[87] a) Mg, Et₂O, CH₃CHO; b) PBr₃, benzene; c) PPh₃, toluene; d) LiOCH₂CH₃, 2-naphthaldehyde, ethanol/dichloromethane; e) *hν*, I₂, propylene oxide, cyclohexane; f) *N*-bromosuccinimide, dibenzoylperoxide, CCl₄; g) KCN, tetrabutylammonium hydrogensulfate, water/dichloromethane; h) KOH, ethylene glycol; i) SOCl₂; j) AlCl₃, dichloromethane; k) TiCl₄, *o*-dichlorobenzene, 140 °C.

1.3.3.3. Advantages and limitation of FVP

From one side Scott's work on C₆₀ synthesis has demonstrated the possibility of selective rational synthesis of fullerenes (no other fullerenes were detected), on the other hand this experiment clearly demonstrates the limitation of the FVP approach for synthesis of big molecules such as fullerenes as can be seen from the disappointing low yield. The main problem is the activation of the Aryl-Aryl coupling process. The fullerene formation requires fifteen tandem Aryl-Aryl condensations, but only three chlorine atoms are involved in the structure. Introduction of a bigger number of halogens will significantly increase the molecular weight and such molecules cannot be transferred in the gas phase without decomposition. Moreover in the example above, the chlorine atoms are not placed in the key position which also affects the efficiency of condensation. The introduction of chlorine atoms in sterically hampered cove or fjord regions is a difficult task. Recently, the possibility of higher fullerene synthesis by FVP has also been demonstrated, although because of the above mentioned reasons the yield remains disappointingly low.^[88,89]

1.3.4. Alternative Aryl-Aryl coupling techniques

The "classical" methods for Aryl-Aryl coupling such as Scholl,^[90,91] Pschorr^[92-94] reactions or Wurtz^[95] and Ullmann^[96] couplings tend to involve harsh reaction conditions and as a consequence the selectivity and yields are usually low. In this chapter only mild methods for Aryl-Aryl coupling, which proceed with high selectivity and provide high yields, will be briefly discussed.

1.3.4.1. Photocyclization

Stilbenes and many related structures frequently undergo intramolecular cyclization under UV irradiation in the presence of an oxidant such as oxygen or iodine.^[97] Mallory photocyclization methods were found to be very effective for the synthesis of various phenes and helicenes, and rather widely applied for the synthesis of large PAHs. For example benzo[c]phenanthrene, picene, hexabenzocoronene have been obtained by this route with good to excellent yields (Figure 1.35).^[98-100]

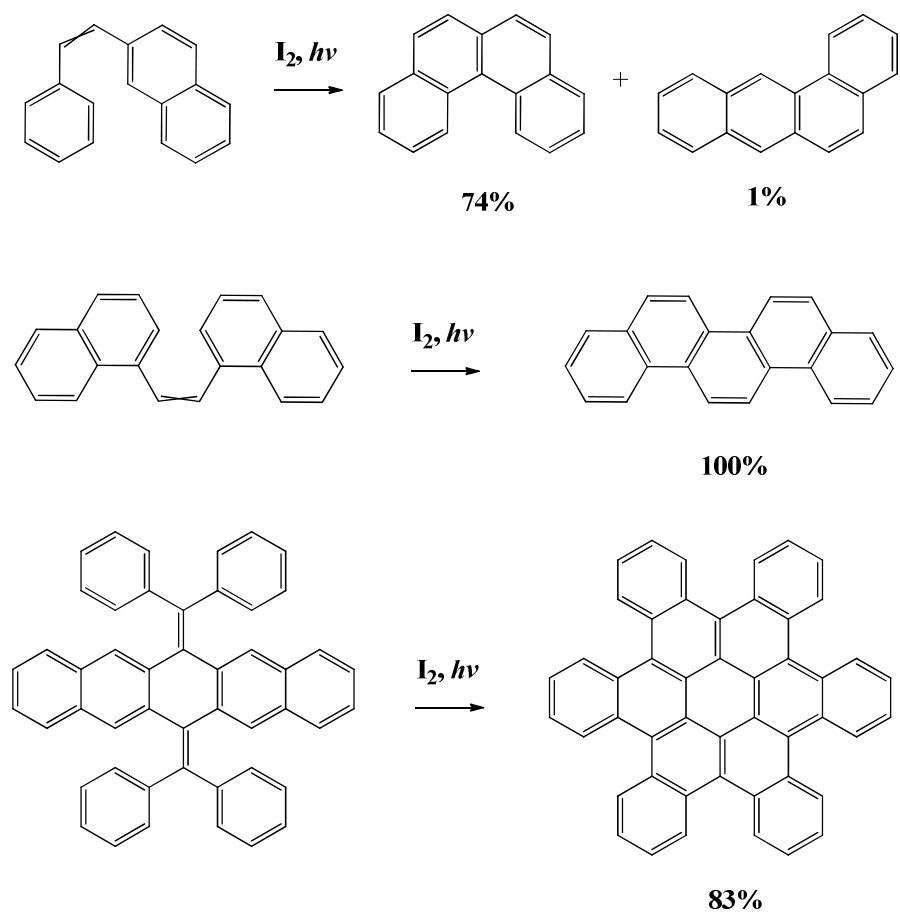


Figure 1.35. Several examples of successful Mallory photocyclization.

The big advantage of this method is a high tolerance to many functionalities and no need to introduce any functional groups to provoke C-C bond formation. On the other hand the reactions are very capricious and the yields frequently vary from quantitative to virtually zero percent. Thus as an example, for two rather similar condensations in tetraphenylethylene, only one C-C bond forms under UV irradiation (Figure 1.36). The high inertness of 1,1'-binaphthyl under photocyclization is another good example demonstrating limitation of this route. Although the photocyclization technique was found to be very effective for the formation of strained PAHs such as helicenes, no examples of buckybowls synthesis

by this approach are known. As a rule the introduction of pentagons in the structure completely prevents further cyclodehydrogenation (Figure 1.36.).^[98]

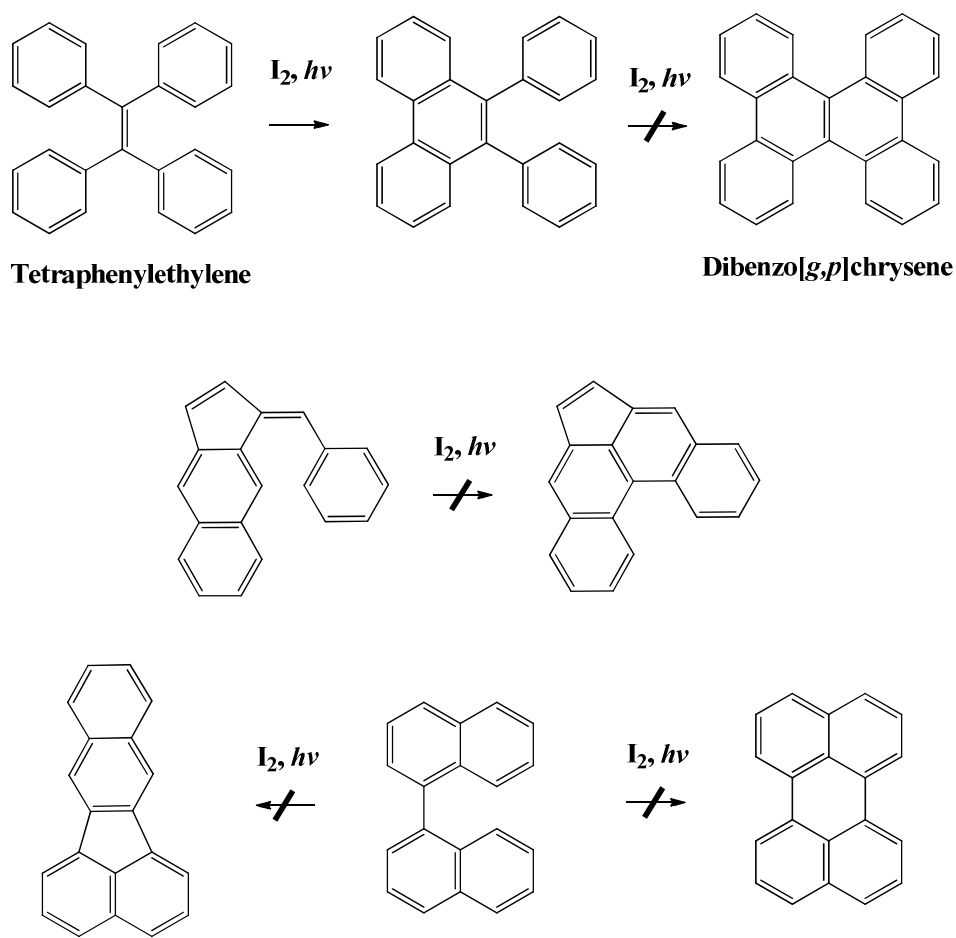


Figure 1.36. Several examples of failed cyclodehydrogenation under UV irradiation.

1.3.4.2. Oxidative Aryl-Aryl coupling

Many polyphenylene based systems readily undergo intramolecular dehydrogenation in the presence of strong acids (as well as Lewis acids) and an oxidizing agent.^[101] Although the oxidative Aryl-Aryl coupling is known more than 50 years (Scholl reaction), for a long time its use has been limited to synthesis of substituted triphenylenes and only recently this approach has become of practical interest.^[102,103] The main drawback of this method is bad control over the reaction

because of the radical-cation nature of the condensation. The process is often complicated by various side reactions and polymerization, and the outcome is frequently unpredictable. Oxidations and partial chlorination during the reactions are other disadvantages of the method. Nevertheless in several cases the successful multifold cyclization has been realized with good to excellent yield even in the case of extra-large PAHs (Figure 1.37). On the other hand this method works very well only in the case of formation of planar graphene-like structure and especially good in the case of full-benzoid PAHs.^[104]

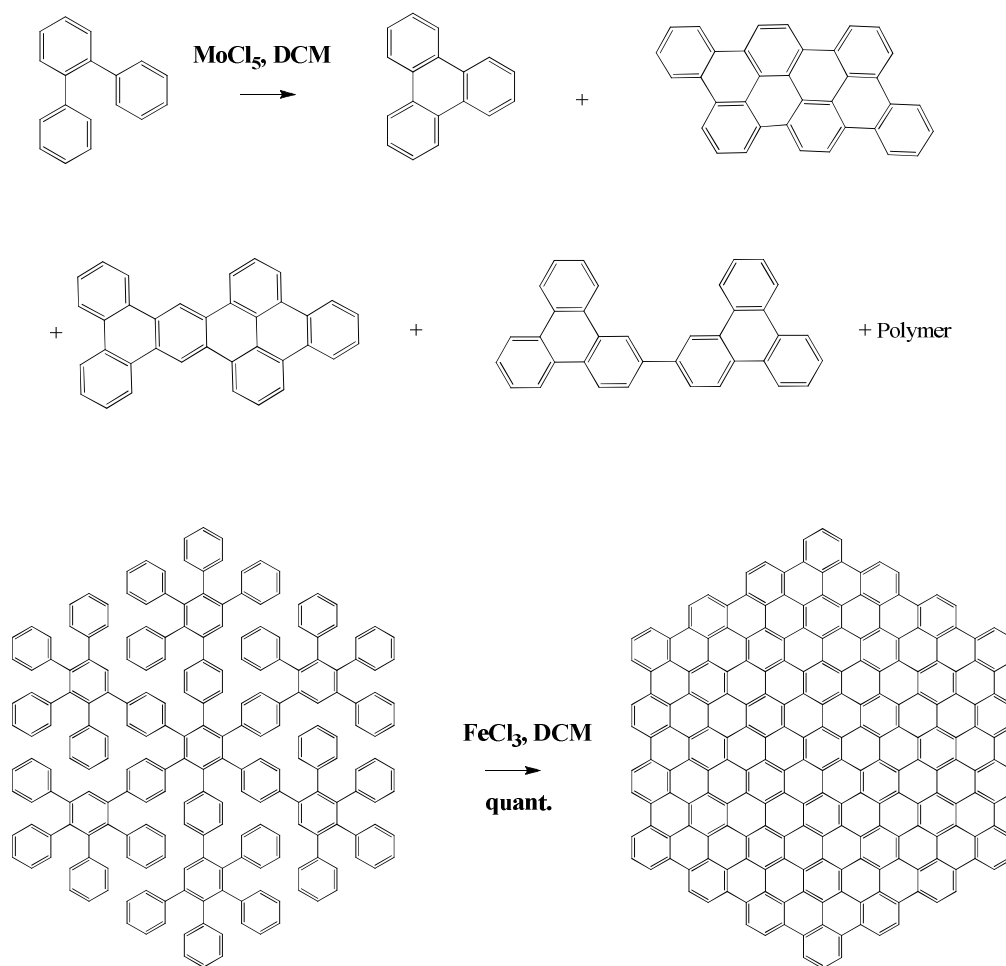


Figure 1.37. Examples of large PAHs synthesis by oxidative Aryl-Aryl coupling.

1.3.4.3. Palladium catalyzed Aryl-Aryl coupling

The Pd catalyzed Aryl-Aryl coupling is a powerful method for the construction of complex PAH molecules. It has been shown that effective Aryl-Aryl coupling can be achieved in many cases.^[105] The method was found to be effective for the fabrication of large planar or close to planar PAHs. Moreover the technique works rather good in the case of intermolecular and intramolecular condensations and allows construction of both hexagons and pentagons. The palladium(0)-catalyzed direct arylation utilizing bromo and chloro derivatives or aryl triflates has been found to be effective for the synthesis of small buckybowls and related structures.^[106-108] The effective cove-region closure by palladium-catalyzed intramolecular coupling has been demonstrated on the synthesis of benzo[ghi]fluoroanthenes which has been obtained with 85% yield (Figure 1.38, reaction A).

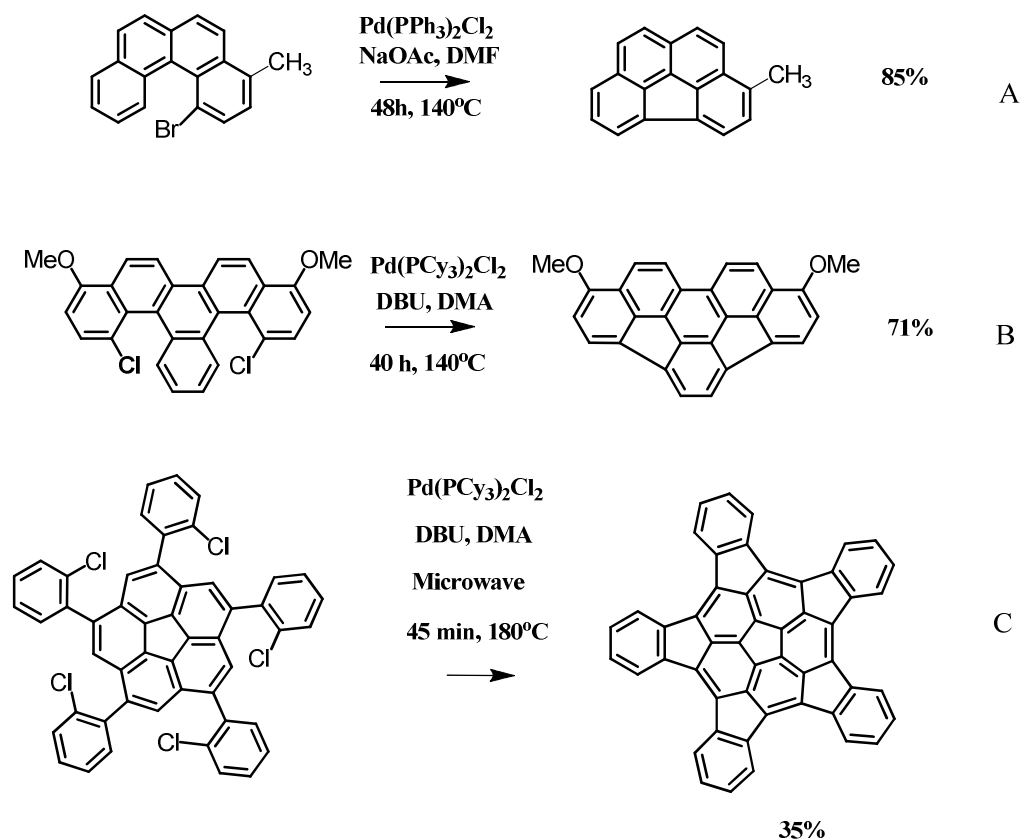


Figure 1.38. Buckybowl synthesis via palladium mediated Aryl-Aryl coupling.

Later the possibility to synthesize non-planar PAHs has been demonstrated. Thus an effective double palladium-mediated cyclization in dichlorobenzopencene was achieved in the presence of the strong organic base (DBU) with more than 70% yield (Figure 1.38, reaction B). Later Scott and co-workers have reported an elegant synthesis of pentabenzocorannulene by means of microwave-assisted palladium-mediated intramolecular coupling (Figure 1.38, reaction C).^[109] Although the method is very powerful for the synthesis of large planar molecules, the yield usually drops significantly in the case of non-planar PAHs. Concerning direct fullerene synthesis, the main drawback are aggressive reaction conditions with respect to the fullerene species.^[110]

1.3.4.4. Condensation on the metal surfaces

Although the rather effective cove region closure in bezo[c]phenanthrene on the Pd/C has been reported more than 50 years ago, only recently this technique has been applied for synthesis of geodesic PAHs. The first step towards synthesis of buckybowls on a surface was made in 2007 where an effective formation of a C₄₆ bowl from a PAH precursor has been demonstrated utilizing a Ruthenium surface.^[111] Soon after, the efficiency of this method has been demonstrated on the synthesis of C₆₀ fullerene on a Platinum surface with quantitative yield.^[112] Recently the high selectivity of this process has been confirmed experimentally and the first example of rational synthesis of higher fullerenes has been also demonstrated (Figure 1.39).^[113] Although the surface-catalyzed cyclization was found to be highly selective, it is limited to only picomole amount production. On the other hand these results demonstrate the principal possibility of specially designed precursors to condense very effectively to the desired fullerene molecules.

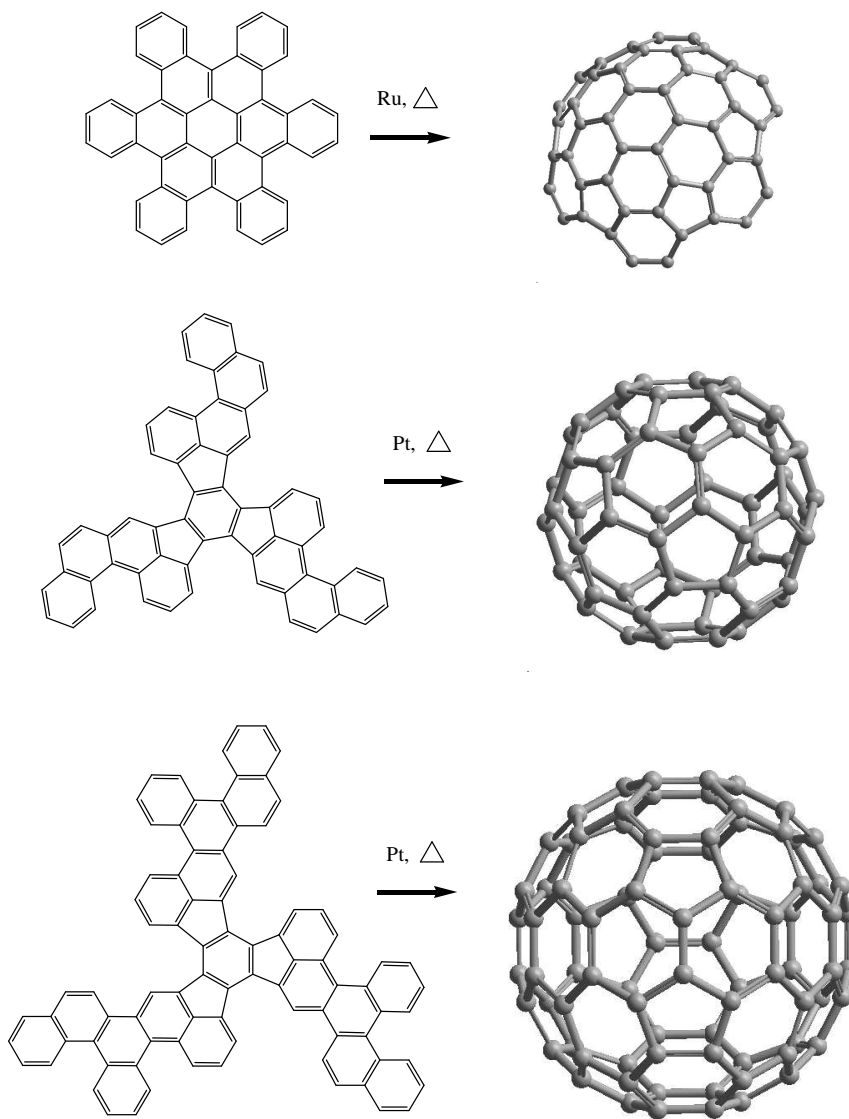


Figure 1.39. Synthesis of C₄₈ buckybowl, C₆₀ and C₈₄ fullerene via metal catalyzed cyclodehydrogenation.

1.4. References

1. H. P. Boehm; A. Clauss; G. O. Fischer; U. Hofmann, Dünnsche Kohlenstoff-Folien, *Z. Naturforsch.* **1962**, 17 b, 150.
2. K. S. Novoselov; A. K. Geim; S. V. Morozov; D. Jiang; M. I. Katsnelson; I. V. Grigorieva; S. V. Dubonos; A. A. Firsov, Two-dimensional gas of massless Dirac fermions in Graphene", *Nature* **2005**, 438, 197.
3. L. V. Radushkevich; V. M. Lukyanovich, O strukture ugleroda, obrazujucesja pri termiceskom razlozenii okisi ugleroda na zeleznom kontakte, *Zurn. Fisic. Chim.* **1952**, 26, 88.
4. H. P. Boehm, Carbon from Carbon Monoxide Disproportionation on Nickel and Iron Catalysts: Morphological Studies and Possible Growth Mechanism, *Carbon* **1973**, 11, 583.
5. A. Oberlin; M. Endo, Filamentous Growth of Carbon Through Benzene Decomposition, *J. Cryst. Growth* **1976**, 32, 335.
6. M. Reibold; P. Paufler; A. A. Levin; W. Kochmann; N. Pätzke; D. C. Meyer, Carbon nanotubes in an ancient Damascus saber, *Nature* **2006**, 444, 286.
7. S. Iijima, Helical microtubules of graphite carbon, *Nature* **1991**, 354, 56.
8. H.W. Kroto; J.R. Heath; S.C. O'Brien; R.F. Curl and R.E. Smalley, C₆₀: Buckminsterfullerene, *Nature* **1985**, 318, 162.
9. W. Krätschmer; L.D. Lamb; K. Fostiropoulos and D.R. Huffman, Solid C₆₀: a New Form of Carbon, *Nature* **1990**, 347, 354.
10. P.R. Buseck; S.J. Tsipursky; R. Hettich, Fullerenes from the Geological Environment, *Science* **1992**, 257 (5067), 215–217.
11. P. Ehrenfreund and B. H. Foing., Fullerenes and Cosmic Carbon, *Science* **2010**, 329, 1159.
12. S. Hong; S. Myung, Nanotube Electronics: A flexible approach to mobility. *Nature Nanotechnology* **2007**, 2 (4), 207–208.
13. K. T. Lau; M. Chipara; H. Y. Ling; et al., On the effective elastic moduli of carbon nanotubes for nanocomposite structures, *Composites Part B: Engineering* **2004**, 35, 95–101.
14. H. O. Pierson, Handbook of Carbon, Graphite, Diamond and Fullerenes, Noyes Publications, New Jersey, USA, **1993**.

15. P. G. Read, *Gemmology*. Butterworth-Heinemann, **2005**, 49–50.
16. C. Frondel; U.B. Marvin, Lonsdaleite, a new hexagonal polymorph of diamond, *Nature* **1967**, 214 (5088), 587–589.
17. C. Frondel; U.B. Marvin, Lonsdaleite, a hexagonal polymorph of diamond, *Am.Min.* **1967**, 52.
18. L. A. Openov; V. F. Elesin, Prismane C8: A new form of carbon?, *JETP Letters* **1998**, 68 (9), 726.
19. P. Delhaes. *Graphite and Precursors*, **2001**.
20. C. N. R. Rao; A. K. Sood; K. S. Subrahmanyam; A. Govindaraj; Graphene, The New Two-Dimensional Nanomaterial, *Angew. Chem. Int. Ed.* **2009**, 48, 7752.
21. Z.K. Tang; et al., Superconductivity in 4 Angstrom Single-Walled Carbon Nanotubes, *Science* **2001**, 292 (5526), 2462.
22. J. Haruyama; et al., Superconductivity in Entirely End-Bonded Multiwalled Carbon Nanotubes, *Physical Review Letters* **2006**, 96 (5).
23. M. Bockrath, Carbon nanotubes: The weakest link, *Nature Physics* **2006**, 2, 155.
24. X. Lu; Z. Chen, Curved Pi-Conjugation, Aromaticity, and the Related Chemistry of Small Fullerenes (C₆₀) and Single-Walled Carbon Nanotubes, *Chemical Reviews* **2005**, 105 (10), 3643–3696.
25. D. Bruns; H. Miura; K. P. C. Vollhardt; A. Stanger, On Route to Archimedene: Total Synthesis of C_{3h}-Symmetric [7]Phenylene, *Org. Lett.* **2003**, 5, 549.
26. H. Kroto, Carbyne and other myths about carbon, *Chemistry World* **2010**.
27. A. E. Goresy; G. Donnay, A New Allotropic Form of Carbon from the Ries Crater, *Science* **1968**, 161, 363.
28. A. G. Whittaker, Carbon: A New View of Its High-Temperature Behavior, *Science* **1978**, 200, 763.
29. P. P. K. Smith; P. R. Buseck, Carbyne Forms of Carbon: Do They Exist?, *Science* **1982**, 216, 984.
30. R. H. Baughman, Dangerously Seeking Linear Carbon, *Science* **2006**, 312, 1009–1110.
31. W. A. Chalifoux; R. R. Tykwinsk, Synthesis of extended polyynes: Toward carbyne, *Comptes Rendus Chimie* **2009**, 12 (3), 341–358

32. www.nanonewsnet.ru/blog/nikst/uglerodnye-nanotrubki-eto-chudo-prirody (accessed the 05.06.2012)
33. *NanotechJapan Bulletin* **2011**, 4(5), Green Nanotechnology: Special Topic 9. Challenges In Developing Carbon Nanotube Technology And Exploring Its Applications - Toward Solving Environmental.
34. www3.imperial.ac.uk/materials/facilities/em/2010 (accessed the 05.06.2012)
35. T. Cabioc'h; A. Kharbach; A. Le Roy; et al., Fourier transform infra-red characterization of carbon onions produced by carbon-ion implantation, *Chemical Physics Letters* **1998**, 285, 3-4, 216-220.
36. a) A. M. Rao; P. C. Eklund and et al., Infrared and Raman studies of pressure-polymerized C60, *Phys. Rev. B* **1997**, 55, 4766–4773.
b) A. M. Rao; P. C. Eklund and et al., Properties of C-60 polymerized under high pressure and temperature, *Applied Physics A: Materials Science & Processing* **1996**, 64, 3, 231-2239.
37. <http://phys.org/news94478341.html> (accessed the 05.06.2012)
38. <http://www.nanocenter.umd.edu/labs/NISP/> (accessed the 05.06.2012)
39. <http://news.softpedia.com/news/Graphene-Nanosheets-Can-Now-Be-Mass-Produced-261218.shtml> (accessed the 05.06.2012)
40. F. D. Novaes; R. Rurali and P. Ordejón, Electronic Transport between Graphene Layers Covalently Connected by Carbon Nanotubes, *Acs Nano* **2010**, 4 (12), 7596-7602.
41. V. Jousseume; J. Cuzzocrea; N. Bernier and V. T. Renard, Few graphene layers/carbon nanotube composites grown at complementary-metal-oxide-semiconductor compatible temperature, *Appl. Phys. Lett.* **2011**, 98, 123103.
42. <http://www.chemistry.wustl.edu/~edudev/Fullerene/discovery.html> (accessed the 05.06.2012)
43. R.B. Fuller, editor. *Synergetics: Explorations in the Geometry of Thinking*. Macmillan, New York, **1975**
44. W. Krätschmer; K. Fostiropoulos and D.R. Huffman, The Infrared and Ultraviolet absorption Spectra of Laboratory-produced Carbon Dust: Evidence for the Presence of the C60 Molecule, *Chemical Physics Letters* **1990**, 170, 167.
45. A. Hirsch and M. Brettreich. *Fullerene Production. In Fullerenes: Chemistry and reactions*, p. 6–19. Wiley-VCH, Weinheim, **2005**.

46. P.Gerhardt; S. Löffler and K.H. Homann, Polyhedral Carbon-Ions in Hydrocarbon Flames, *Chemical Physics Letters* **1987**, 137, 306.
47. P.Gerhardt; K.H. Homann, Ions and Charged Soot Particles in Hydrocarbon Flames, *J. Phys. Chem.* **1990**, 94, 5381.
48. J.B. Howard; J.T. McKinnon; Y. Makarovsky; A.I. Lafleur and M.E. Johnson, Fullerenes C₆₀ and C₇₀ in Flames, *Nature* **1991**, 352, 139.
49. R. Taylor; G.J. Langley; H.W. Kroto and D.R.M. Walton, Formation of C₆₀ by Pyrolysis of Naphtalene, *Nature* **1993**, 366, 728.
50. C. Crowley; H.W. Kroto; R. Taylor; D.R.M. Walton; M.S. Bratcher; C. Pei-Chao; L.T. Scott, Formation of [60]Fullerene by Pyrolysis of Corannulene, 7,10-bis(2,2'-Dibromovinyl)fluoranthene, and 11,12-Benzofluoranthene, *Tetrahedron Letters* **1995**, 36, 50, 9215-9218.
51. K.Yu. Amsharov and M. Jansen, Formation of Fullerenes by Pyrolysis of Perchlorofulvalene and its Derivatives. *Carbon* **2007**, 45, 117.
52. R. E. Haufler; J. Conceicao; L. P. F. Chibante; Y. Chai; N. E. Byrne; et. al., Efficient production of C₆₀ (Buckminsterfullerene), C₆₀H₃₆, and the Solvated Buckide Ion. *J. Phys. Chem.* **1990**, 94, 8634.
53. L.P.F. Chibante; A. Thess; J.M. Alford; M.D. Diener and R.E. Smalley, Solar Generation of the Fullerenes. *J. Phys. Chem.* **1993**, 97, 8696.
54. M. Jansen; G. Peters and N. Wagner, Zur Bildung von Fullerenen und endohedralen Metallofullerenen: Darstellung im Hochfrequenzofen, *Z. Anorg. Allg. Chem.* **1995**, 621, 689.
55. G. Peters and M. Jansen, A New Fullerene Synthesis, *Angew. Chem. Int. Ed. Engl.* **1992**, 31, 223.
56. H. Takehara; M. Fujiwara; M.Arikawa; M.D. Diener and J.M. Alford, Experimental Study of Industrial Scale Fullerene Production by Combustion Synthesis, *Carbon* **2005**, 43, 311.
57. K.Yu. Amsharov and M. Jansen, Formation of Fullerenes by Pyrolysis of Perchlorofulvalene and its Derivatives. *Carbon* **2007**, 45, 117.
58. N.B. Shustova; B.S. Newell; S.M. Miller; et. al., Discovering and Verifying Elusive Fullerene Cage Isomers: Structures of C₂-p¹¹-(C₇₄-D_{3h})(CF₃)₁₂ and C₂-p¹¹-(C₇₈-D_{3h}(5))(CF₃)₁₂, *Angew. Chem. Int. Ed.* **2007**, 119, 4189-4192.
59. T.G. Schmalz; W.A. Seitz; D.J. Klein and G.E. Hite, C₆₀ Carbon Cages, *Chemical Physics Letters*, **1986**, 130, 203.

60. H.W. Kroto, The Stability of the Fullerenes C_n, with n = 24, 28, 32, 36, 50, 60 and 70, *Nature* **1987**, 329, 529.
61. a) R. Ettl; I. Chao; F. Diederich; R. L. Whetten, Isolation of C₇₆, a chiral (D₂) allotrope of carbon, *Nature* **1991**, 353, 149–153.
b) K. S. Simeonov; K. Yu. Amsharov; M. Jansen, Connectivity of the Chiral D₂-Symmetric Isomer of C₇₆ through a Crystal-Structure Determination of C₇₆Cl₁₈ · TiCl₄, *Angew. Chem. Int. Ed.* **2007**, 46, 8419-8421
62. a) F. Diederich; R. L. Whetten; C. Thilgen; R. Ettl; I. Chao; M. M. Alvarez, Fullerene Isomerism - Isolation Of C₂-Nu-C₇₈ and D₃-C₇₈, *Science* **1991**, 254, (5039), 1768-1770.
b) T. Wakabayashi; K. Kikuchi; S. Suzuki; H. Shiromaru; Y. Achiba, Pressure-Controlled Selective Isomer Formation of Fullerene C₇₈, *J. Phys. Chem.* **1994**, 98 (12), 3090–3091.
c) K. S. Simeonov; K. Yu. Amsharov; M. Jansen, Chlorinated Derivatives of C₇₈-Fullerene Isomers with Unusually Short Intermolecular Halogen-Halogen Contacts, *Chem. Eur. J.* **2008**, 14, 9585.
d) K. S. Simeonov; K. Yu. Amsharov; E. Krokos; M. Jansen, An epilogue on the C(78)-fullerene family: The discovery and characterization of an elusive isomer, *Angew. Chem. Int. Ed.* **2008**, 47, 6283-6285.
63. a) F. R. Hennrich; R. H. Michel; A. Fischer; S. Richard-Schneider; S. Gilb; M. M. Kappes; D. Fuchs; M. Burk; K. Kobayashi; S. Nagase, Isolation and Characterization of C-80, *Angew. Chem. Int. Ed.* **1996**, 35, 1732.
b) C.-R. Wang; T. Sugai; T. Kai; T. Tomiyama; H. Shinohara, Production and Isolation of an Ellipsoidal C-80 Fullerene, *Chem. Comm.* **2000**, 557.
c) K. S. Simeonov; K. Yu. Amsharov; M. Jansen, C₈₀Cl₁₂: A Chlorine Derivative of the Chiral D-2-C-80 Isomer-Empirical Rationale of Halogen-Atom Addition Pattern, *Chem. Eur. J.* **2009**, 15 (8) 1812-1815.
64. a) M. Zalibera; A. A. Popov; M. Kalbac; P. Rapta; L. Dunsch, The Extended View on the Empty C-2(3)-C(82)Fullerene: Isolation, Spectroscopic, Electrochemical, and Spectroelectrochemical Characterization and DFT Calculations, *Chem. Eur. J.* **2008**, 32 (14) 9960.
b) K. Ziegler; K. Yu. Amsharov; I. Halasz; M. Jansen, Facile Separation and Crystal Structure Determination of C₂-C₈₂(3) Fullerene, *ZAAC* **2011**, 637 (11), 1463-1466.
c) S. I. Troyanov; N. B. Tamm, Crystal and molecular structures of trifluoromethyl derivatives of C-82 fullerene: C-82(CF₃)(12) and C-82(CF₃)(18), *Crystallography Reports*, **2010**, 55, 432- 435.
65. a) K. Kikuchi; N. Nakahara; T. Wakabayashi; et. al., NMR Characterization of Isomers of C-78, C-82 and C-84 Fullerenes, *Nature* **1992**, 357, 142.
d) T. J. S. Dennis; T. Kai; T. Tomiyama; H. Shinohara, Isolation and characterisation of the two major isomers of [84]fullerene (C-84), *Chem. Comm.* **1998**, 619.

- c) L. Epple; K. Amsharov; K. Simeonov; I. Dix; M. Jansen, Crystallographic characterization and identification of a minor isomer of C(84) fullerene, *Chem Comm.* **2008**, 5610.
- d) I.E. Kareev; I.V. Kuvychko; N.B. Shustova; S.F. Lebedkin; V.P. Bubnov; O. P. Anderson; A. A. Popov; O.V. Boltalina; S.H. Strauss, C-1-(C-84-C-2(11))(CF3)(12): Trifluoromethylation Yields Structural Proof of a Minor C-84 Cage and Reveals a Principle of Higher Fullerene Reactivity, *Angew. Chem. Int. Ed.* **2008**, 47, 33, 6204.
66. a) N. B. Shustova; I. V. Kuvychko; R. D. Bolskar; K. Seppelt; S. H. Strauss; A. A. Popov; O. V. Boltalina, Trifluoromethyl Derivatives of Insoluble Small-HOMO-LUMO-Gap Hollow Higher Fullerenes. NMR and DFT Structure Elucidation of C-2-(C-74-D-3h)(CF3)(12), C-s-(C-76-T-d(2))(CF3)(12), C-2-(C-78-D-3h(5))(CF3)(12), C-s-(C-80-C-2v(5))(CF3)(12), and C-2-(C-82-C-2(5))(CF3)(12), *J. Am. Chem. Soc.* **2006**, 128 (49), 15793.
- b) I. E. Kareev; A. A. Popov; I. V. Kuvychko; N. B. Shustova; et. al., Synthesis and X-ray or NMR/DFT Structure Elucidation of Twenty One New Trifluoromethyl Derivatives of Soluble Cage Isomers of C-76, C-78, C-84, and C-90, *J. Am. Chem. Soc.* **2008**, 130, 13471.
- c) N. B. Tamm; L. N. Sidorov; E. Kemnitz; S. I. Troyanov, Isolation and Structural X-ray Investigation of Perfluoroalkyl Derivatives of Six Cage Isomers of C-84, *Chem. Eur. J.* **2009**, 15, 10486.
- d) N. B. Tamm; S. I. Troyanov, Cage connectivities of C-88 (33) and C-92 (82) fullerenes captured as trifluoromethyl derivatives, C-88(CF3)(18) and C-92(CF3)(16), *Chem. Comm.* **2009**, 6035.
- e) N. B. Shustova; B. S. Newell; et. al., Discovering and Verifying Elusive Fullerene Cage Isomers: Structures of C-2-p(11)-(C-74-D-3h)(CF3)(12) and C-2-p(11)-(C-78-D-3h(5))(CF3)(12), *Angew. Chem. Int. Ed.* **2007**, 46, 4111.
- f) N.B. Tamm; L.N. Sidorov; E. Kemnitz; S.I. Troyanov, Crystal Structures of C-94(CF3)(20) and C-96(C2F5)(12) Reveal the Cage Connectivities in C-94 (61) and C-96 (145) Fullerenes, *Angew. Chem. Int. Ed.* **2009**, 48, 9102.
67. P.W. Fowler and D.E. Manolopoulos. *An Atlas of Fullerenes*, Clarendon, Oxford, UK, **1995**.
68. IUPAC. *Nomenclature of Organic Chemistry: Blue Book* (IUPAC Publications), Pergamon Press, Oxford, **1979**.
69. R. Rieger; K. Muellen, Forever Young: Polycyclic Aromatic Hydrocarbons as Model Cases for Structural and Optical Studies, *J. Phys. Org. Chem.* **2010**, 23, 315–325.
70. R. G. Harvey, *Polycyclic Aromatic Hydrocarbons*, Wiley and Sons, New York, **1997**.
71. M. J. Stump; R. C. Fleming; et. al., Matrix-assisted laser desorption mass spectrometry, *Applied Spectroscopy Reviews* **2002**, 37, 275–303.

72. S. B. Howerton; J. V. Goodpaster; V. L. McGuffin, Characterization of polycyclicaromatic hydrocarbons in environmental samples by selective fluorescence quenching, *Anal. Chim. Acta* **2002**, 459, 61-73.
73. W. E. Barth; R. G. Lawton, Synthesis of corannulene, *J. Am. Chem. Soc.* **1971**, 93, 1730.
74. V.M. Tsefrikas and L. T. Scott, Geodesic Polyarenes by Flash Vacuum Pyrolysis, *Chem. Rev.* **2006**, 106, 4868-4884.
75. R. F. C. Brown; K. J. Harrington; G. L. McMullen, Benzylidenecarbene as a probable intermediate in the interconversion of Ph¹³CCH and PhC¹³CH at 550 °C and 700 °C, *J. Chem. Soc. Chem. Commun.* **1974**, 123.
76. L. T. Scott; M. M. Hashemi; D. T. Meyer; H. B. Warren, Corannulene. A convenient new synthesis, *J. Am. Chem. Soc.* **1991**, 113, 7082.
77. G. Mehta; G. Panda, A new synthesis of corannulene, *Tetrahedron Letters* **1997**, 38, 2145.
78. G. Zimmermann; U. Nuechter; S. Hagen; M. Niichter, Synthesis and hydrolysis of bis-trimethylsilyl substituted 3-(4H-cyclopenta[def]phenanthrylidene)-1,4-pentadiene. A new route to corannulene, *Tetrahedron Letters* **1994**, 35, 4747.
79. L. T. Scott; P.-C. Cheng; M. M. Hashemi; M. S. Bratcher; D. T. Meyer; H. B. Warren, Corannulene. A Three-Step Synthesis, *J. Am. Chem. Soc.* **1997**, 119, 10963.
80. L. T. Scott, Fragments of fullerenes: novel syntheses, structures and reactions, *Pure Appl. Chem.* **1996**, 68, 291.
81. H. E. Bronstein; N. Choi; L. T. Scott, Practical Synthesis of an Open Geodesic Polyarene With a Fullerene-Type 6:6-Double Bond at the Center: Diindeno[1,2,3,4-defg;1',2',3',4'-mnop]chrysene, *J. Am. Chem. Soc.* **2002**, 124, 8870-8875.
82. S. Hagen; U. Nuechter; M. Nuechter; G. Zimmermann, *Polycyclic Aromat. Compd.* **1995**, 4, 209-217.
83. L. T. Scott; M. S. Bratcher; S. Hagen, Synthesis and Characterization of a C₃₆H₁₂ Fullerene Subunit, *J. Am. Chem. Soc.* **1996**, 118, 8743.
84. G. Mehta; G. Panda; P. V. V. S. Sarma, A short synthesis of 'bucky-bowl' C₃-hemifullerene (triindenotriphenylene), *Tetrahedron Lett.* **1998**, 39, 5835.
85. S. Hagen; M. S. Bratcher; M. S. Erickson; G. Zimmermann; L. T. Scott, Novel Syntheses of Three C₃₀H₁₂ Bowl-Shaped Polycyclic Aromatic Hydrocarbons, *Angew. Chem. Int. Ed.* **1997**, 36, 406.

86. G. Mehta; G. Panda, Buckybowls: a simple, conceptually new synthesis of C-2 n-semibuckminsterfullerene (C₃₀H₁₂, [5,5]-fulvalene circulene), *Chem. Comm.* **1997**, 2081.
87. L. T. Scott; M. M. Boorum; B. J. McMahon; et. al., A Rational Chemical Synthesis of C₆₀, *Science* **2002**, 295, 1500-1503.
88. K. Y. Amsharov; M. Jansen, A C(78) fullerene precursor: Toward the direct synthesis of higher fullerenes, *J. Org. Chem.* **2008**, 73, 2931 – 2934.
89. K. Y. Amsharov; M. Jansen, Synthesis of a higher fullerene precursor-an "unrolled" C-84 fullerene, *Chem. Comm.* **2009**, 2691 – 2693.
90. R. Scholl; J. Mansfeld, *Ber. Dtsch. Chem. Ges.* 1910, 43, 1734-1746.
91. A. T. Balaban; C. D. Nenitzescu, Dehydrogenation Condensation of Aromatics (Scholl and Related Reactions). In *Friedel-Crafts and Related Reactions*; Olah, G., Ed.; Wiley: New York, **1964**, 2, 979.
92. R. Pschorr, Neue Synthese des Phenanthrens und seiner Derivate, *Chem. Ber.* **1896**, 29, 496.
93. J. March, *Advanced Organic Chemistry: Reactions, Mechanisms, and Structure (3rd ed.)*, New York, Wiley **1985**.
94. K. K. Laali and M. Shokouhimehr, The Pschorr Reaction, a Fresh Look at a Classical Transformation, *Current Organic Synthesis* **2009**, 6, 193–202.
95. J. March, *Advanced Organic Chemistry 5th edition*, 535.
96. P.E. Fanta, The Ullmann Synthesis of Biaryls, *Synthesis* **1974**, 9-21.
97. F. B. Mallory; J. T. Gordon; C. S. Wood; et. al., *J. Am. Chem. Soc.* **1962**, 84, 4361.
98. F. B. Mallory; C. W. Mallory, Photocyclization of Stilbenes and Related Molecules, *Organic Reactions*, NJ, United States, **1984**.
99. http://en.wikipedia.org/wiki/Stilbene_photocyclization#cite_note-9 (accessed the 13.06.2012)
100. S. Xiao; M. Myers; et. al., Molecular Wires from Contorted Aromatic Compounds, *Angew. Chem. Int. Ed.* **2005**, 44, 7390.
101. R. Pummerer; E. Prell; A. Rieche, *Ber. Dtsch. Chem. Ges.* **1926**, 59, 2159.

102. T. S. Navale; K. Thakur; R. Rathore, Sequential Oxidative Transformation of Tetraarylethylenes to 9,10-Diarylphenanthrenes and Dibenzo[g,p]chrysenes using DDQ as an Oxidant, *Org. Lett.* **2011**, 13 (7), 1634.
103. L. Zhai; R. Shukla; R. Rathore, Oxidative C–C Bond Formation (Scholl Reaction) with DDQ as an Efficient and Easily Recyclable Oxidant, *Org. Lett.* **2009**, 11 (15), 3474.
104. V. S. Iyer; M. Wehmeier; et. al., From hexa-peri-hexabenzocoronene to "superacenes", *Angew. Chem. Int. Ed.* **1997**, 36.
105. L. Ackermann (Ed.). *Modern Arylation Methods*, Wiley-VCH, Weinheim **2009**.
106. A. M. Echavarren; B. Gomez-Lor; J. J. Gonzalez; O. De Frutos, Palladium-catalyzed intramolecular arylation reaction: Mechanism and application for the synthesis of polyarenes, *Synlett* **2003**, 585 – 597.
107. D. Alberico; M. E. Scott; M. Lautens, Palladium-Catalyzed Intramolecular Arylation Reaction: Mechanism and Application for the Synthesis of Polyarenes, *Chem. Rev.* **2007**, 107, 174 – 238.
108. S. Pascual; P. de Mendoza; A. M. Echavarren, Palladium catalyzed arylation for the synthesis of polyarenes, *Org. Biomol. Chem.* **2007**, 5, 2727 – 2734.
109. B. D. Steinberg; E. A. Jackson; A. S. Filatov; A. Wakamiya; M. A. Petrukhina; L. T. Scott, Aromatic π -Systems More Curved Than C₆₀. The Complete Family of All Indenocorannulenes Synthesized by Iterative Microwave-Assisted Intramolecular Arylations, *J. Am. Chem. Soc.* **2009**, 131, 10537 – 10545.
110. K. Yu. Amsharov; M. A. Kabdulov; M. Jansen, Facile Bucky-Bowl Synthesis by Regiospecific Cove-Region Closure by HF Elimination, *Angew. Chem.* **2012**, 124, 4672.
111. K. T. Rim; M. Siaj; et. al., Forming Aromatic Hemispheres on Transition-Metal Surfaces, *Angew. Chem. Int. Ed.* **2007**, 46, 7891.
112. G. Otero; G. Biddau; et. al., Fullerenes from aromatic precursors by surface-catalysed cyclodehydrogenation, *Nature* **2008**, 454, 865 – 868
113. K. Y. Amsharov; N. Abdurakhmanova; et. al., Towards the Isomer-Specific Synthesis of Higher Fullerenes and Buckybowls by the Surface-Catalyzed Cyclodehydrogenation of Aromatic Precursors, *Angew. Chem. Int. Ed.* **2010**, 49, 9392 – 9396.

2. Direct Fullerene synthesis

2.1. FVP approach

2.1.1. Introduction

As it was shown previously, many geodesic PAHs can be obtained by intramolecular Aryl-Aryl coupling under FVP conditions.^[1-4] The presence of a chlorine or bromine functionality in the initial precursor is essential for effective radical formation which is the driving force of the reaction. Non-halogenated analogues frequently do not undergo intramolecular cyclization or give only trace amounts of the target products.

As it was shown above this approach has proven to be effective for the synthesis of small non-planar PAHs but high-yield synthesis of fullerenes still remains challenging. Although the principal possibility of rational fullerene formation by FVP has been demonstrated by the examples of C₆₀,^[5-9] C₇₈,^[10] and C₈₄,^[11] the rates of conversion to the target molecules have remained disappointingly low. Thus C₆₀ has been obtained with 0.1-1% yield,^[7-9] whereas higher fullerenes were only detected by mass spectrometry.^[10,11] The low yields result from a lack of efficient promoters of Aryl-Aryl coupling. The frequently employed bromine or chlorine functionalizations reach their limits in the case of large molecules because of decomposition of such precursors under heating. The molar masses will generally be high, since the large numbers of new C-C bonds that need to be formed in the precursor necessitate the introduction of a big number of promoter groups. Moreover, the introduction of halogens atoms such as chlorine or bromine in the large molecules causes serious synthetic difficulties. Availability of alternative ring-closure promoters which do not have these disadvantages is a key prerequisite for successful rational fullerene synthesis via intramolecular Aryl-Aryl coupling under FVP conditions.

2.1.2. Alternative radical promoters for efficient intramolecular condensation

The conversion of benzo[*c*]phenanthrene to benzo[*ghi*]fluoranthene was chosen as a model reaction for the investigation of new ring closure promoters. Benzo[*c*]phenanthrene represents the smallest molecule bearing a cove region, where the new C-C bond should be established. Importantly, the efficiency of condensation for chlorobenzo[*c*]phenanthrene demonstrated previously has been proven transferable to the synthesis of large buckybowls structures.^[12]

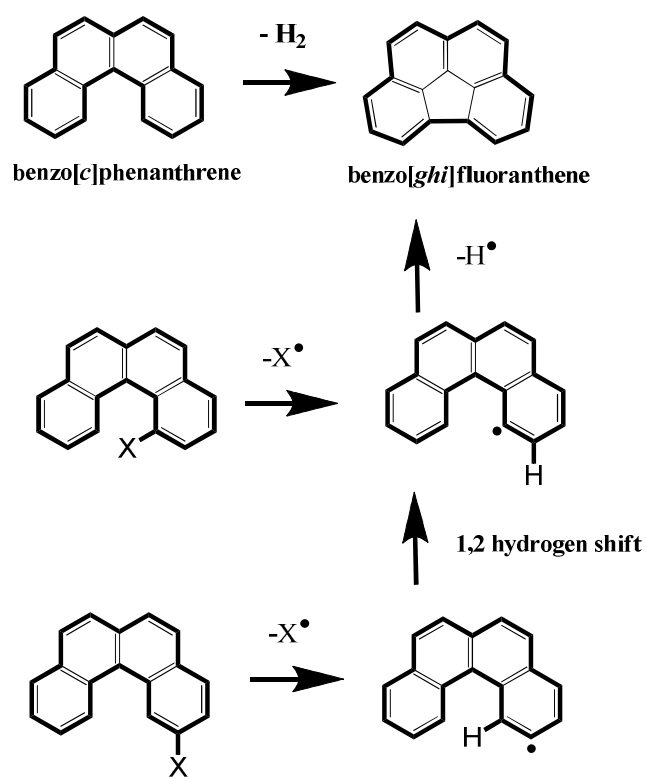


Figure 2.1. (top) Model reaction: The conversion of benzo[*c*]phenanthrene to benzo[*ghi*]fluoranthene through a cove region closure. (bottom) Two possible ways for activation of ring closure process in benzo[*c*]phenanthrene. X-denotes the ring closure promoter.

The best position for activation is the carbon atoms where the new carbon-carbon bond should be established. In the system under consideration, those carbon atoms always belong to the cove region. According to the proposed mechanism, the radical formed attacks the neighboring carbon atom with formation of a new C-C bond. Alternatively, the promoter group can be introduced to α -positions as it is presented in Figure 2.1. After homolytic cleavage of the corresponding C-X bond and subsequent 1,2- hydrogen shift, the radical position will be displaced into the cove region.^[13] Although such activation is less effective, it avoids synthetic difficulties associated with the introduction of the halogens in the sterically hampered cove/fjord regions.

Considering the routes to the synthesis of fullerene related PAHs, two approaches have been proven to be effective. The first route is based on the trimerization of cyclic ketones.^[14,15] This approach meets some limits in the case of large molecules such as precursors of higher fullerenes, mostly because of the low solubility of intermediate products.^[15,16] The reaction frequently stops after dimerization and the product often is contaminated by a considerable amount of insoluble side products. An alternative route, which avoids the solubility problem, is based on the Pd-catalyzed arylation, giving the desired product with high purity.^[17,18] Unfortunately the Pd-catalyzed cyclization excludes the option to introduce chlorine or bromine in the structure and none of these approaches can provide a way to the required precursors bearing chlorine or bromine in the structure. To solve this problem we have examined alternative promoters which can be introduced in the structure taking the above mentioned synthetic approaches into consideration.

Benzo[c]phenanthrene was chosen as a model compound for intramolecular Aryl-Aryl coupling. All benzo[c]phenanthrene derivatives (**5**) (Figure 2.2) were synthesized by four step synthesis according the synthetic route given in Figure 2.3. Two positions in benzo[c]phenanthrene can be used for activation of ring closure process, which are coded as R₃ and R₁ in compound **5** (Figure 2.2) The R₁ position was chosen preferably because of the more convenient synthetic access.

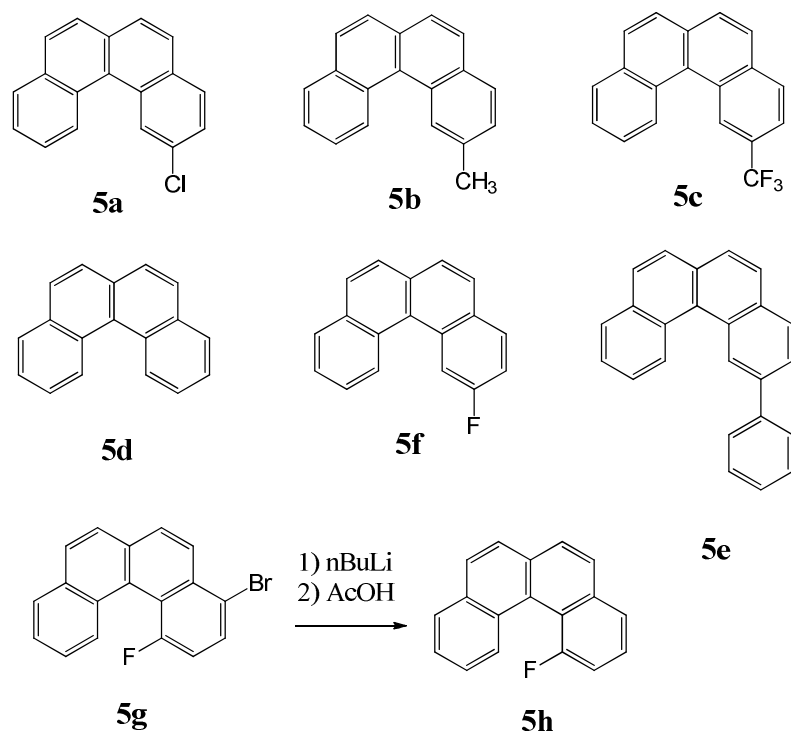
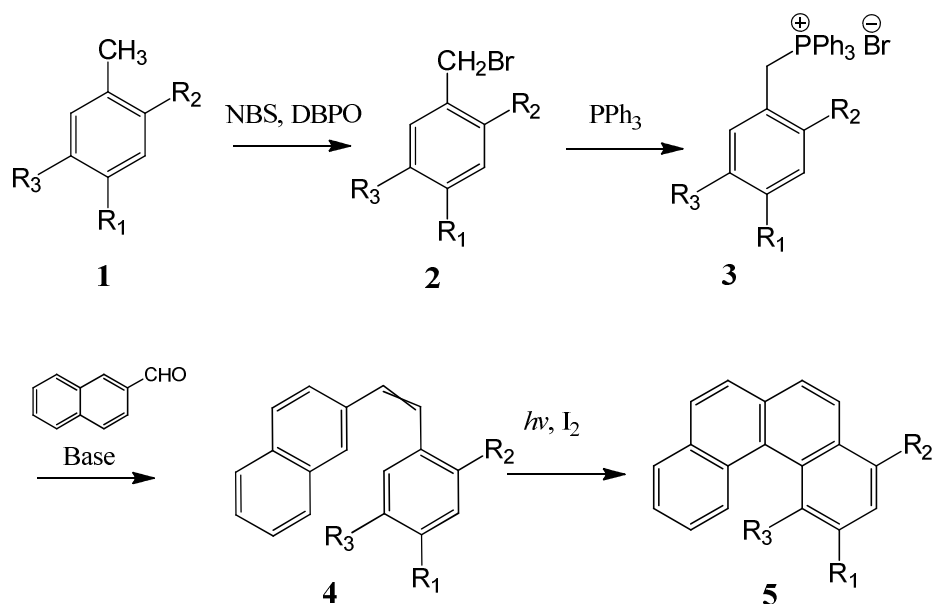


Figure 2.2. Benzo[*c*]phenanthrene derivatives **5a-5h** used in this study. (**5h** was synthesized by debromination of **5g**).

Benzyl bromides (**2**) were obtained by free radical bromination of corresponding methylbenzenes (**1**) with N-bromosuccinimide (NBS) in the presence of dibenzoylperoxide (DBPO) in CCl_4 . The solution of corresponding benzyl bromide and triphenylphosphine in toluene was refluxed to form the corresponding phosphonium salt (**3**), which was filtered and used for the next step without additional purification. Wittig reactions were carried out in anhydrous THF using *n*-butyllithium as a base (ethanol and potassium *tert*-butoxide were used for the synthesis of fluoro-derivatives). Following chromatographic separation gives benzostilbene (**4**) in form of a *cis/trans* isomer mixture. No additional separation steps were performed since the isomers interconvert photochemically in the next

step. Benzo[*c*]phenanthrenes (**5**) were synthesized using the Katz improvement of the Mallory photocyclization reaction from corresponding benzostilbenes.^[19]



Compound	R ¹	R ²	R ³
a	Cl	H	H
b	CH ₃	H	H
c	CF ₃	H	H
d	H	H	H
e	Ph	H	H
f	F	H	H
g	H	Br	F
h	H	H	F

Figure 2.3. The synthetic route to benzo[*c*]phenanthrenes **5**.

Pyrolysis experiments were carried out at typically 800-1100 °C in an improved FVP furnace allowing the simultaneous control of carrier gas flow, pressure in the system and sublimation speed. The products of FVP were analyzed by means of HPLC. As a result of harsh reaction conditions, besides desired benzo[*ghi*]fluoranthene the formation of several side products was observed. The major reaction products are summarized in Figure 2.4.

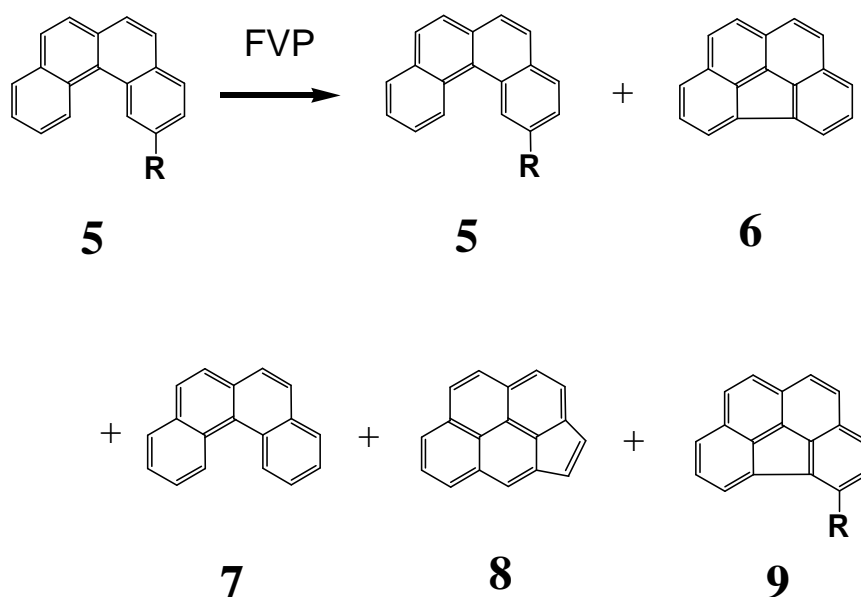


Figure 2.4. The major products of FVP pyrolysis of benzo[*c*]phenanthrene derivatives.

Benzo[*c*]phenanthrene (**5d**) and 2-chloro benzo[*c*]phenanthrene (**5a**) were selected as reference compounds. FVP of **5a** shows that the efficiency of condensation increases with increasing the temperature of pyrolysis and decreasing pressure in the system. At the same time the selectivity decreases due to conversion of benzo[*ghi*]fluoranthene (**6**) to the thermodynamically more stable

cyclopenta[*cd*]pyrene (**8**), which is in agreement with literature data.^[12,20,21] Thus, the pyrolysis of **5a** at 1100 °C and a pressure of 2.5 mbar with N₂ flow of 12 mL/min gives **8** with 50% yield, whereas **6** forms only with 20 % yield (molar percentages). The optimal conditions for condensation of **5a** to **6** were found to be T = 1000 °C, p = 2 mbar and N₂ flow of 8 mL/min. In this case **6** can be obtained with 80 % yield. Pyrolysis of benzo[*c*]phenanthrene (**5d**) at the same conditions gave only 3 % of the product **6**. The efficiency of alternative promoters was investigated in comparison with the efficiency as determined for **5a** and **5d**, under conditions required for the sublimation of large fullerene precursor molecules (p = 0.5 mbar, T = 1100 °C). The results of FVP experiments are summarized in Table 2.1. It was found, that the efficiency of the ring closure is in good correlation with the C-R₁ bond dissociation energy which is a result of effective homolytic cleavage of the corresponding bond, Table 2.1. At the same time phenyl and fluorine derivatives fall out of the correlation.

According to the data obtained, the methyl group can be considered as a prospective ring-closure promoter. The most probable mechanism of cyclization in methylbenzo[*c*]phenanthrene includes homolytic cleavage of the ArCH₂-H bond with formation of a stable benzylic radical which stimulates the ring closure without loss of the methyl group.^[22] Thus, low temperature pyrolysis results mostly in the formation of methylbenzo[*ghi*]fluoranthene **9b**. Increasing the temperature results in the subsequent cleavage of the Aryl-CH₃ bond with formation of a benzo[*ghi*]fluoranthene radical which finally results in **6**. Importantly, remarkable transformation of **6** and **9** to the corresponding cyclopenta[*cd*]pyrenes takes place already at 1000 °C (Figure 2.5), although such a transformation usually needs a temperature of more than 1150 °C.^[20] The formation of trace amounts of **7** confirms that no direct Aryl-Me bond cleavage takes place at “low” temperatures.

Table 2.1. The effect of promoters on the condensation of benzo[*c*]phenanthrenes. Pyrolysis at 1100 °C (p = 0.1 mbar). The yields are given as a molar ratio to benzo[*ghi*]fluoranthene (**6**). Bond energy (Ph-R₁) according references.^[22,23]

Compound	R ₁	Ph-R ₁ bond energy (kcal/mol)	Compound				
			5	6	7	8	9
5a	Cl	97.1	4.56	1	0.82	1.7	0
5b	CH ₃	103.5 (89.7) ^[b]	6.69	1	1.79	0.94	(0.6) ^[a]
5c	CF ₃	110.5	16.27	1	0.80	1.53	(0.2) ^[a]
5d	H	112.9	22.5	1	-	1.1	-
5e	Ph	118	13.02	1	2.07	1.25	(0.7) ^[a]
5f	F	127.2	8.36	1	0.07	1.19	(0.1) ^[a]

[a] concentrations are estimated on the assumption of equal sorption with benzo[*ghi*]fluoranthene. [b] The weakest bond in **5b** (PhCH₂-H).

Importantly, the methyl group promotes rather selective ring closure, but not directly involved in the sterically hampered cove region. The subsequent cleavage of the methyl group could provide activation for the next step of cyclization, which makes the Me group a rather promising candidate for the activation of the cyclization process in the precursor molecule where a big number of new bonds should be created.

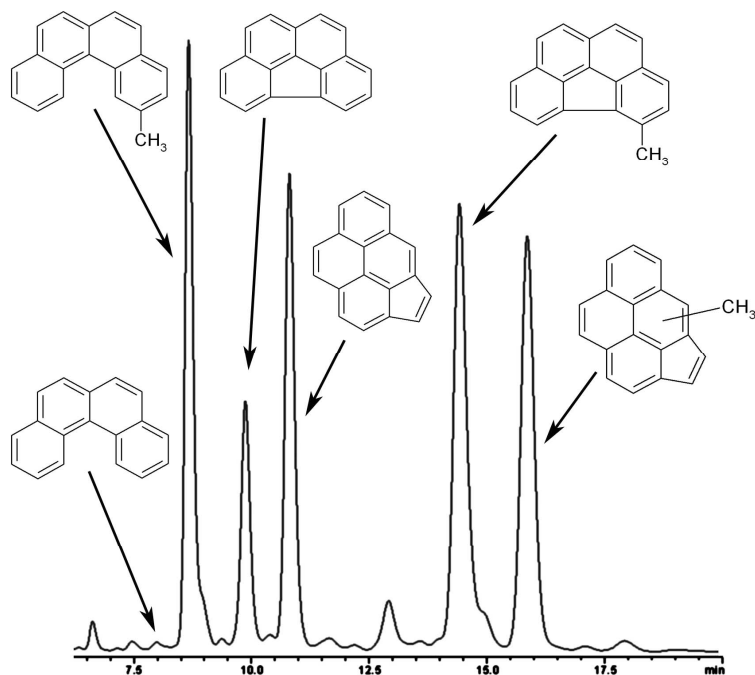


Figure 2.5. HPLC profile of products of FVP of **5b**. ($T = 1000\text{ }^{\circ}\text{C}$, $p = 0.1\text{ mbar}$).

The deviation from the correlation between bond dissociation energy and efficiency of cyclization in the case of **5e** is probably caused by the lower dissociation energy of the C-H bond in the cove region, stimulating ring closure without losing of the Ph group. Indeed, a significant amount of phenyl benzo[*c*]phenanthrene (**9e**) was observed in the pyrolysis product. Unfortunately a low degree of conversion and the formation of many side products are limiting the use of a phenyl group as a ring-closure promoter. In contrast to Ph and Me groups a CF_3 group does not show activation and gave a complex mixture of the products.

Unexpectedly, fluorine has show rather high efficiency in the activation. The results of FVP of fluorinated benzo[*c*]phenanthrenes are presented in Table 2.2. The

activity in the case of 2-fluoro-benzo[*c*]phenanthrene (**5f**) is highly unexpected. Since the C-F bond is considered as a very stable bond,^[24] and according to the proposed radical mechanism should strongly inhibit the condensation. High fluorine activity in ring closure pointed out that the mechanism of condensation is different from that proposed for other halogens.

The condensation of 1-fluoro-benzo[*c*]phenanthrene (**5h**) gave even more exciting results. In this case, a high selectivity, not typical for pyrolysis, was observed in the low temperature FVP experiment (Figure 2.6). Although only 10 % of **5h** were converted to target **6**, the selectivity of condensation has been found to be more than 97 %. In other words, the unreacted **5h** can be, principally, recovered and can be condensed to the targeted product with close to quantitative yield by repetitive pyrolysis.

Table 2.2. Relative yields of pyrolysis products (molar %).

Compound	T (°C)	5	7	6	8
5h	800	92.6	0	7.6	0.2
	850	89.5	0	10	0.5
	900	85.3	0	13	1.6
	1000	81.8	0	14.8	3.4
	1100	59.6	0	28.4	11.8
5f	900	100	0	0	0
	1000	96.7	0.05	1.3	1.6
	1100	79.3	0.7	9.4	11.3

The potential for fullerene precursor closing offered by functionalization of the precursors with fluorine is obviously promising. First of all, fluorine does not increase the molecular weight of the precursor drastically. Moreover the high stability of C-F bond excludes decomposition of the precursor during sublimation. Because of the small size of the fluorine atom it can be easily introduced in the sterically hampered cove and fjord regions of the precursor molecule. The resistance of the C-F bond remarkably extends the scope of reactions that can be applied for the precursor synthesis.

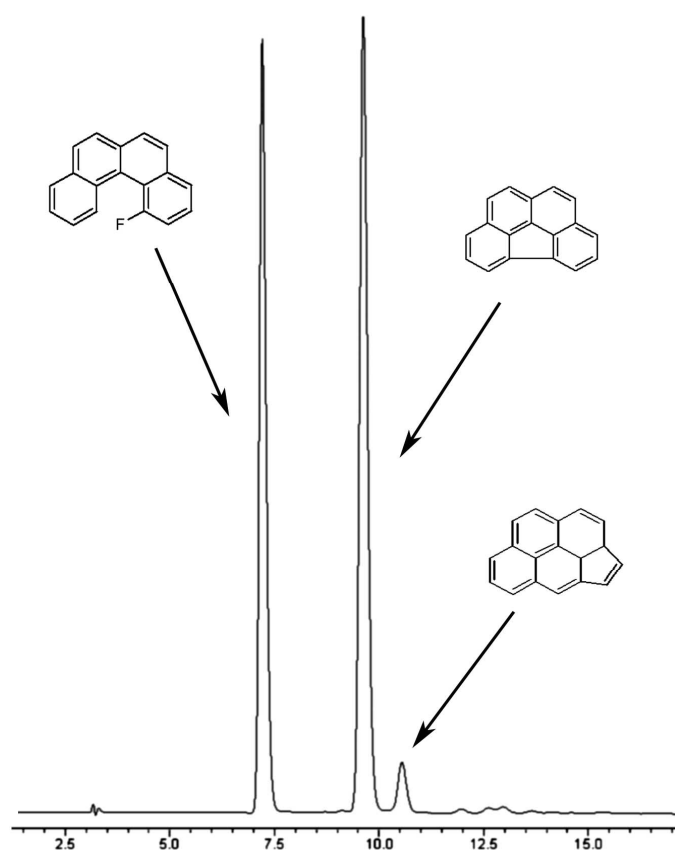


Figure 2.6. HPLC profile of FVP of **5h**. (T = 850 °C, p = 0.1 mbar).

As stated above, the mechanisms of ring closure in benzo[*c*]phenanthrenes are different for different functional groups. The most probable mechanisms of condensation for **5a**, **5b**, **5f** and **5h** are summarized in Figure 2.7.

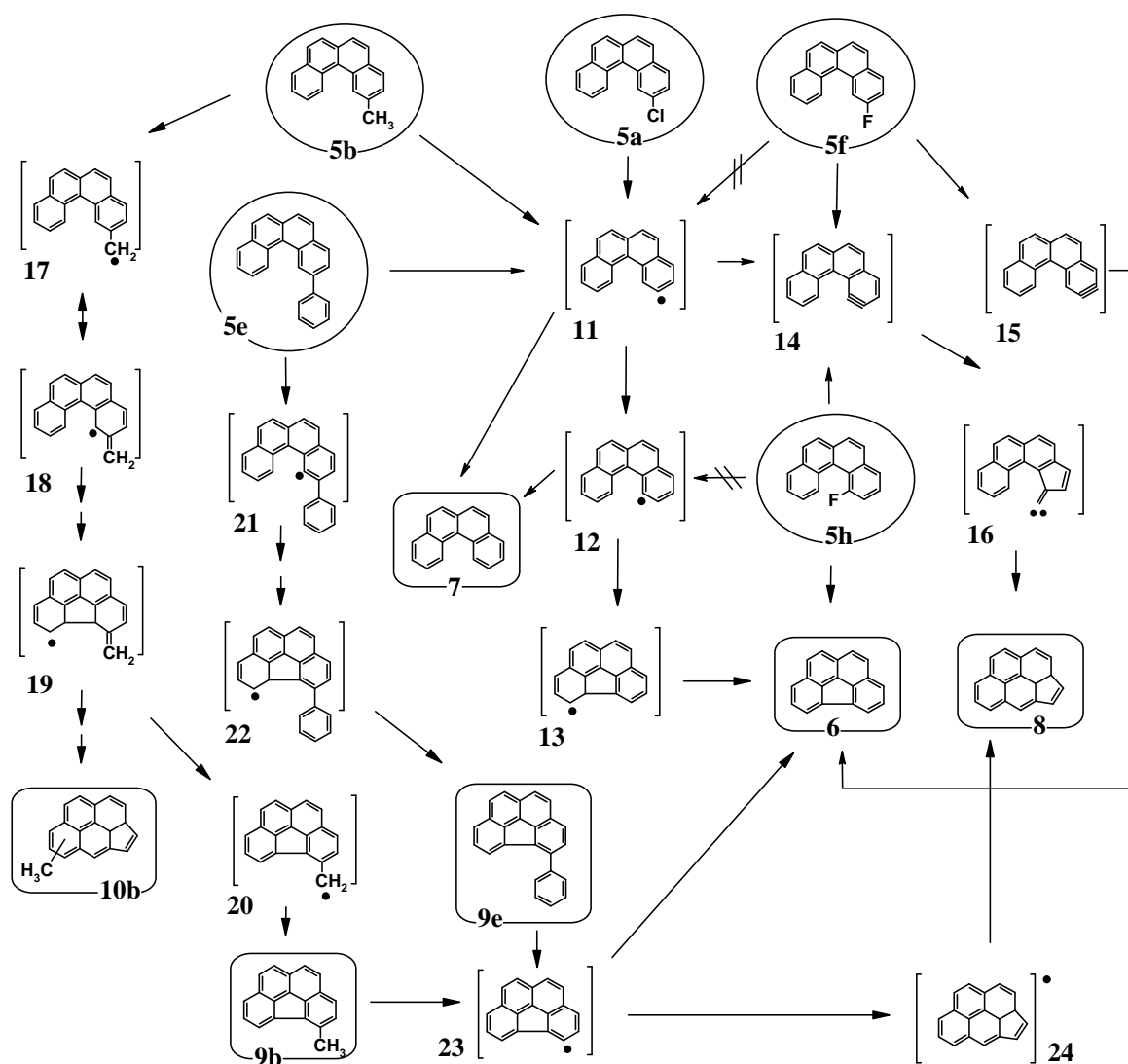


Figure 2.7. The proposed mechanism of condensation of **5a**, **5b**, **5f**, **5f** and **5h** under FVP conditions.

In the case of **5a** the mechanism of condensation seems to be the same as for its brominated analogue.^[14] As a first step, the homolytic dissociation of the weak C-Cl bond takes place. The formed radical (**11**) can be recombines with a hydrogen radical with formation of benzo[*c*]phenanthrene (**7**) or can be rearranged to **12** or **14**. Since the β -scission of the phenyl radical is less favorable (82.2 kcal/mol) than a 1-2 hydrogen shift (58.4 kcal/mol), **11** converts to radical **12**.^[14] Subsequent ring closure gives intermediate **13**, which finally converts to the targeted **6**. Increasing the pyrolysis temperature reduces the selectivity of transformation of **11** to **12**. In this case, both species (**12** and **14**) can be formed from **11** with similar probability. Whereas **12** leads to formation of benzo[*ghi*]fluoranthene **6** the intermediate **14** rearranges to carbene **16**, cyclization of which results in cyclopenta[*cd*]pyrene **8**.

In the case of methylarenes the ArCH₂-H bond dissociation (89.7 kcal/mol) is favored over Ar-CH₃ bond breaking (103.5 kcal/mol). Thus pyrolysis of **5b** preferably gives benzylic radical **17** which undergoes 1,3-sigmatropic shift with formation of **18** and subsequent ring closure to **19**. The radical **19** can be transformed to **20**, which finally yields benzo[*ghi*]fluoranthene **9b**. Although the low temperature pyrolysis results mostly in formation of **9b**, a remarkable amount of methylcyclopenta[*cd*]pyrene **10b** was observed in the product mixture. The most probable way of formation of **10b** is the rearrangement of **9b**. Increasing the pyrolysis temperature up to 1000 °C results in considerable formation of cyclopenta[*cd*]pyrene **8**. This can be a result of cleavage of the CH₃ group in **9b** and subsequent rearrangement of benzo[*ghi*]fluoranthene **23** to **24**. Additionally, this confirms that the benzo[*ghi*]fluoranthene radical **19** could rather easily be transformed in to corresponding cyclopenta[*cd*]pyrene **10b**. Pyrolysis at 1100 °C is not selective and results in a complex product mixture. Formation of benzo[*c*]phenanthrene **7** under these conditions indicates the direct Ar-CH₃ bond dissociation in **5b** under FVP conditions.

The Ph group also shows enhanced activity in ring closure. Indeed, according to quantum chemical calculations the phenyl group decreases the C-H bond

dissociation energy in the cove region. Thus the formation of **21** from **5e** requires only 106.78 kcal/mol instead of 112.9 kcal/mol, which is typical for homolytic C_{Ar}-H bond dissociation. The radical formed (**21**) leads to the ring closure (**22**) and finally results in **9e**.

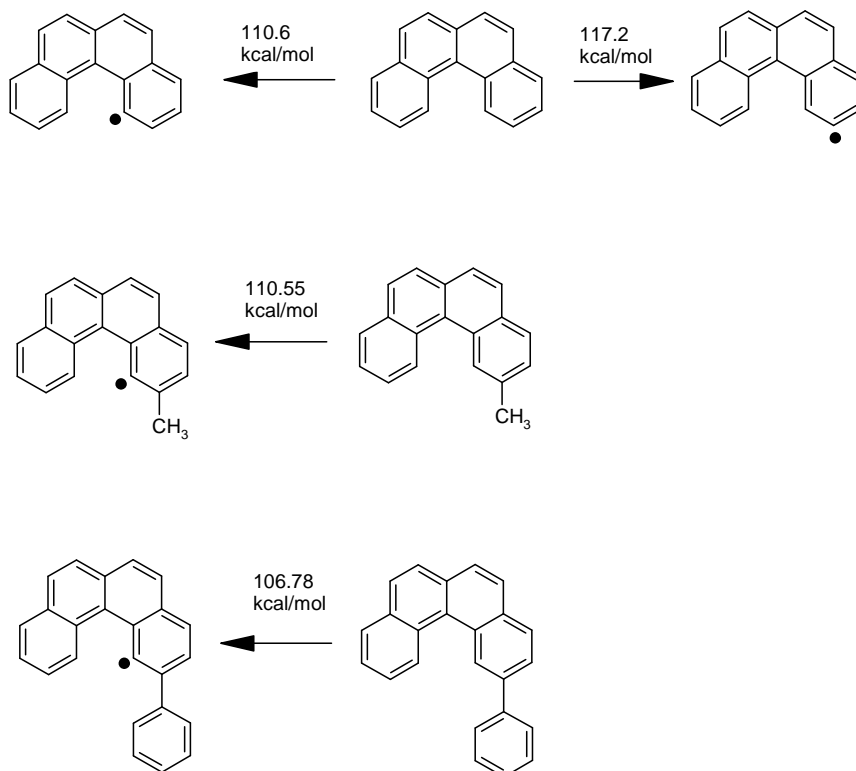


Figure 2.8. Relative activation of C-H bond cleavage in the cove region. The energies given correspond to the C-H bond dissociation energy obtained on DFT level calculation (B3LYP/6-31G basis set).

Because of the high stability of the C-F bond, the formation of radical **11** from fluorinated benzo[*c*]phenanthrene **5f** is highly unlikely. Indeed, the experiments

have shown that HF elimination does not take place through the intermediate **11**, since no benzo[*c*]phenanthrene **7** was found in the pyrolysis products. The most probable mechanism involves direct HF elimination from the cove region. Fluorine seems to be an excellent candidate for an efficient intramolecular condensation and possess all the required properties of an “ideal promoter”. High selectivity and moderate conversion together with other attractive properties of fluorine makes it a very promising group for condensation of the precursor molecules to buckybowls and fullerenes.

2.1.3. HF - homoelimination

In order to understand the effect of fluorine functionalization on the selectivity of thermally activated Aryl-Aryl coupling, the HF elimination process has been investigated further theoretically and experimentally. According to the experimental data the activation barrier for conversion of **5h** to **6** is rather low. As it was stated before, the most probable mechanism includes synchronous HF elimination. The HF elimination is a well known decomposition process in the photolysis of fluoroethylenes.^[25-30] Although the photofragmentation would be expected to proceed from an excited electronic state, it has been shown that direct dissociation most likely occurs through the ground state.^[30] This is supported by the fact that thermal fragmentation of fluoroethylenes shows a similar result, and the main decomposition process is the unimolecular 1,2-HF elimination.^[31] Theoretical studies have revealed that 1,2-HF elimination is the main decomposition channel which passes through a four- or three-centered transition state, as it presented in the Figure 2.9.

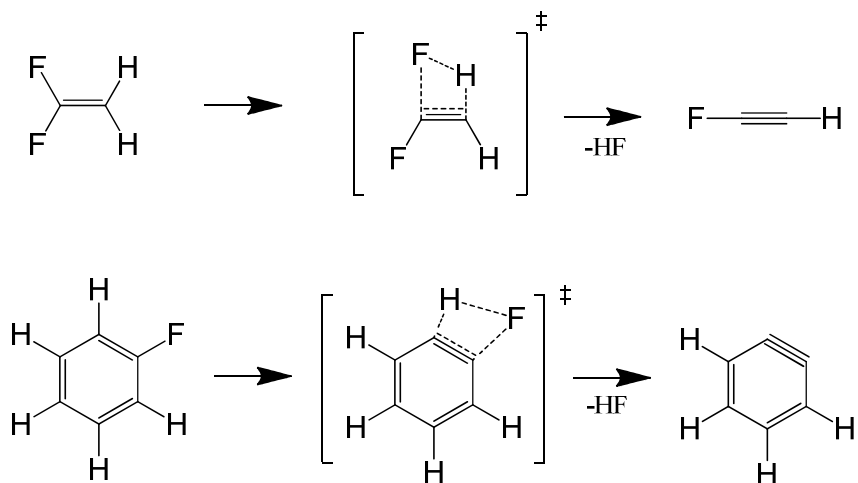


Figure 2.9. 1,2-HF elimination via four-centered transition state - the main channel of difluoroethene and fluorobenzene decomposition.

The activation barrier for HF elimination in fluoroethylenes has been found to be only 74 kcal/mol.^[32] A similar elimination process has been identified as the main channel of fluorobenzene decomposition. The activation barrier in the latter case is higher and amounts to 92 kcal/mol (Figure 2.9).^[33]

Considering the pyrolysis of **5h** and **5f**, the formation of benzyne **14** as an intermediate via 1,2-HF elimination appears to be possible (Figure 2.10). The highly reactive intermediate **14** could be stabilized by ring closure, resulting in the benzo[ghi]fluoranthene **6**. According to this mechanism both **5h** and **5f** should provide comparable activity in intramolecular condensation. However the FVP experiments show, that **5h** is much more reactive than **5f**. At low temperature pyrolysis (850 °C) **5f** remains virtually unchanged whereas compound **5h** yields about 10 % of **6** with very high selectivity (more than 97 %). Increasing the pyrolysis temperature up to 1000 °C results in 15 % of **6** in the case of **5h**, whereas pyrolysis of **5f** gave only 1 % of the product. Moreover, pyrolysis of **5f** preferably results in cyclopenta[cd]pyrene **8** whereas **5h** almost exclusively leads to the desired **6**. Such a large difference in the reactivities of **5h** and **5f** indicates that **14** is not a relevant intermediate in the condensation path from **5h** to **6**. The effective cyclisation of **5h** can only be understood as a 1,5-elimination of HF from the cove region of the 1-fluorobenzo[c]phenanthrene molecule which leads directly to the target molecule without any intermediates. (This process is energetically more favorable than the competing 1,2-elimination). The benzyne **14** is considered to be the major product of pyrolysis of **5f**. Formally **14** could give **6**, or could rearrange to the more stable carbene **16** which finally leads to **8**. The low molar ratio **6/8** at low temperature pyrolysis of **5f** indicates that rearrangement to **8** is the more favorable process. Increasing the pyrolysis temperature decreases the selectivity of the reaction and both processes occur with comparable probability. As a result the **6/8** molar ratio starts to approach the value of 1 (Figure 2.11). On the other hand, compound **5h** can either give **6** by direct 1,5-HF elimination or can produce **14** via 1,2-HF elimination. The preferred formation of **6** at low temperature indicates that the

activation barrier for 1,5-HF elimination is remarkably lower than the barrier for 1,2-elimination. At high temperature both processes become equiprobable, but the molar ratio of **6/8** in the pyrolysis products of **5h** remains higher than 1. This is in good agreement with the proposed mechanism, since there are two channels to **6** and only one to **8**.

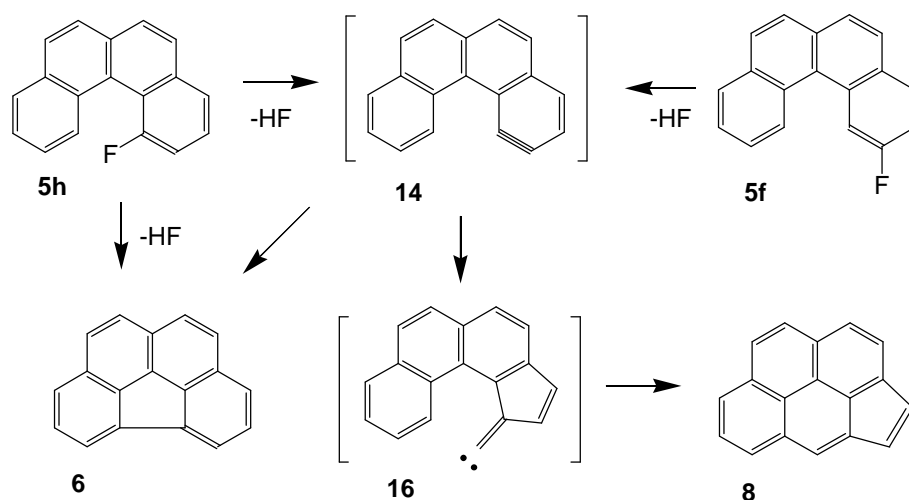


Figure 2.10. Possible transformations of 1- and 2-fluoro benzo[*c*]phenanthrenes under FVP conditions.

In order to corroborate the presented hypothesis, and to prove the principal possibility of 1,5-HF elimination experimentally, 1,2,3,4-tetrafluorobenzo[*c*]phenanthrene (**26**) has been synthesized and subjected to FVP at the same conditions. The synthetic route to compound **27** is summarized in Figure 2.12. None of the fluorine atoms in **26** has immediate hydrogen neighbours, and therefore **26** is not able to eliminate HF via conventional 1,2-elimination. Thus, the formation of benzo[*ghi*]fluoranthene would unambiguously confirm direct 1,5-HF elimination to have occurred.

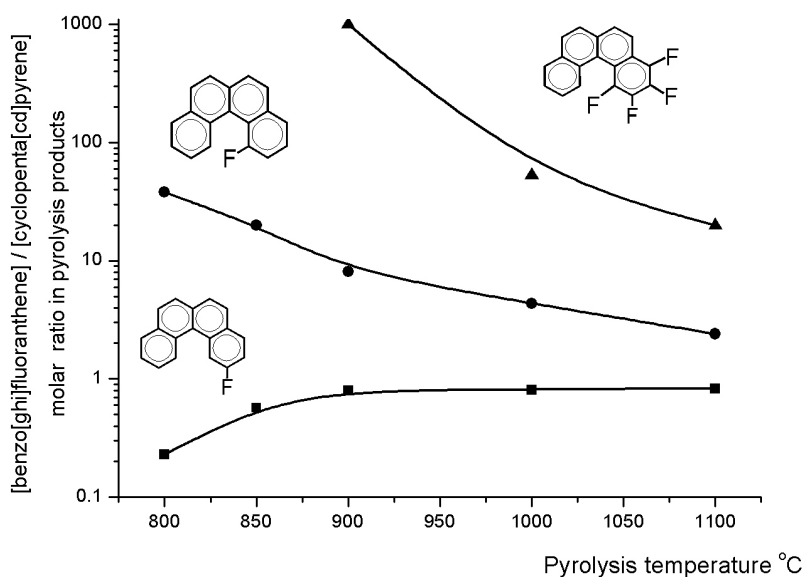


Figure 2.11. Temperature-dependent dynamic of benzo[*ghi*]fluoranthene/cyclopenta[*cd*]pyrene molar ratio in FVP of fluorinated benzo[*c*]phenanthrenes **5h**, **5f** and **26**. The molar ratios are obtained from HPLC data of the pyrolysis product. The concentration of trifluoro-cyclopenta[*cd*]pyrene is estimated on the assumption of equal sorption with unsubstituted cyclopenta[*cd*]pyrene.

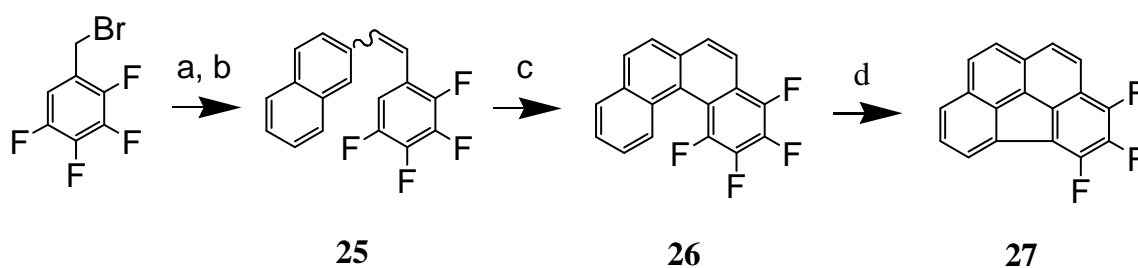


Figure 2.12. The synthetic route to 1,2,3,4-tetrafluoro-benzo[*c*]phenanthrene **26** and its condensation to trifluoro-benzo[*ghi*]fluoranthene **27**. a) PPh_3 , toluene 97 % b) 2-naphthaldehyde, KOTBu , EtOH, 87 % c) $h\nu$, I_2 , propylene oxide, cyclohexane, 43 % d) FVP, 1100 °C, 60 %.

Indeed, FVP of **26** has resulted in highly selective benzo[*c*]phenanthrene formation. Importantly, no cyclopenta[*cd*]pyrene derivatives were found in the pyrolysis products, which is in good agreement with the proposed mechanism. The evolution of the benzo[*ghi*]fluoranthene/cyclo[*cd*]pyrene ratio with temperature for compounds **5h**, **5f** and **26** are summarized in Figure 2.13.

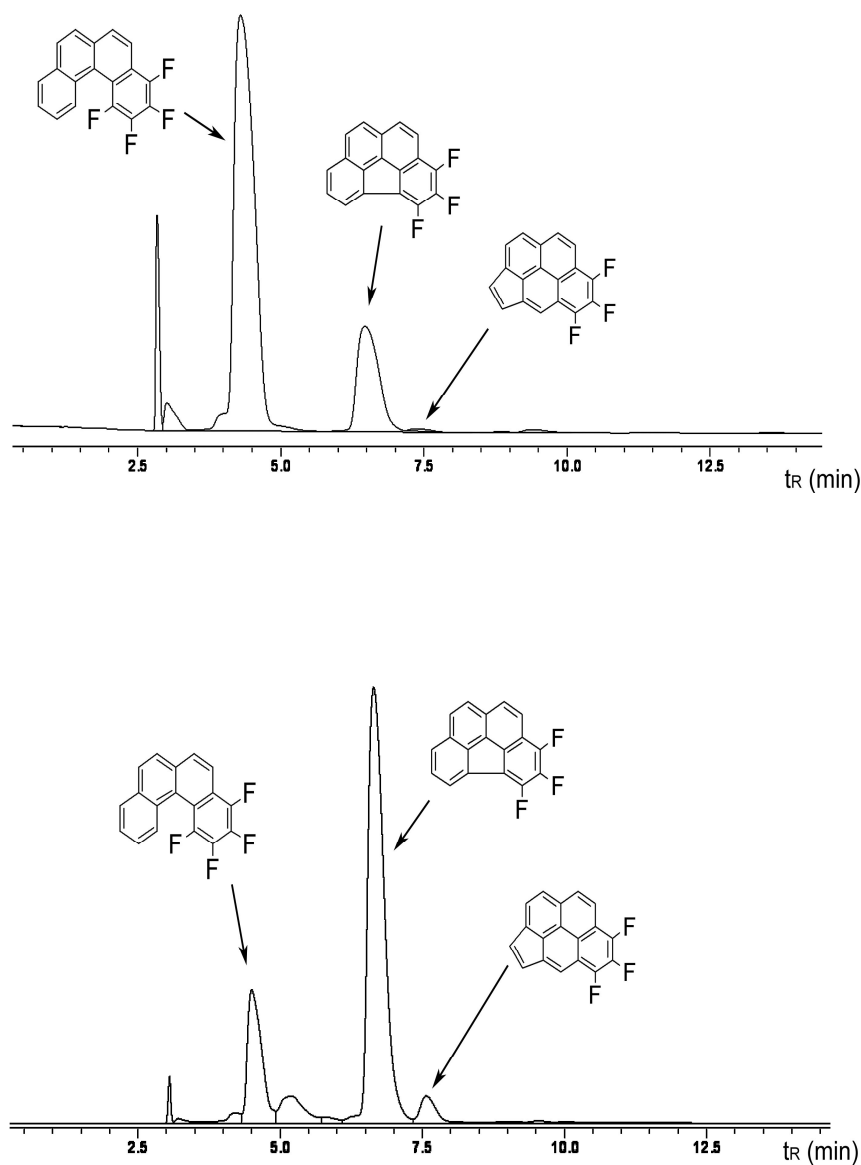


Figure 2.13. HPLC profile of products of FVP of **26** at 900 °C (top) and 1100 °C (bottom).

As can be seen from Figure 2.11, even high temperature pyrolysis does not result in a noticeable cyclopenta[*cd*]pyrene formation in case of **26**. Only a small amount of trifluorinated cyclopenta[*cd*]pyrene was observed in the pyrolysis products which is a result of the expected rearrangement in the non-fluorinated benzene ring at high temperatures. Since all other channels of HF elimination are “blocked” in **26**, increasing the pyrolysis temperature does not affect the selectivity substantially. This has made it possible to achieve a remarkably selective and efficient condensation of **26** to **27** under FVP conditions with up to 60 % yield. Almost no side products were detected in the pyrolysis product (Figure 2.13).

The quantum chemical calculations show that 1,5-elimination in the 1-fluorobenzo[*c*]phenanthrene molecule is possible via the four-centered transition state. The transition state and its optimum geometrical parameters are presented in Figure 2.14.

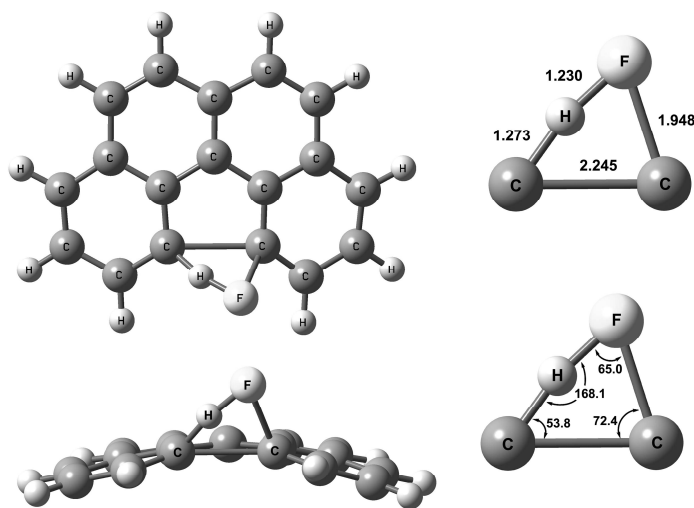


Figure 2.14. Transition state geometry for HF homo-elimination predicted with the DFT B3LYP/6-311G(d,p) method. On the right, only those bonds broken or formed during the reaction are shown. Bond lengths are given in Å, angles in degrees. The geometry of the benzo[*c*]phenanthrene moiety in the transition state is characterized by sufficient deviation from planarity. The four centered transition state is highly distorted from square geometry, and the H atom is placed virtually on the C-F axis.

The activation energy for this process was found to be 80.2 kcal/mol. The 1,5-HF elimination is thus substantially favored over the 1,2-elimination (92 kcal/mole). Interestingly, none of the carbon atoms involved changes its hybridization during reaction, which is atypical for an elimination reaction. The formal increase in unsaturation, which is a necessary prerequisite of any elimination, is realized through the formation of a new ring in the system. The π -system of benzo[c]phenanthrene is not involved in the condensation process and the elimination process can thus be considered as four-centered *homo*-elimination reaction. In order to estimate the influence of the π -system on the condensation process, the model reaction between benzene and fluorobenzene has been investigated theoretically. Indeed, a low energetic path to biphenyl with a similarly low activation energy barrier (84.2 kcal/mol) was also found in this case. This confirms our conclusion that HF elimination in the system considered is a *homo* reaction takes place directly through the space. Ordinarily, inter-molecular process cannot possibly occur due to entropic reasons in the case of fluorobenzene, but it becomes possible in the case of benzo[c]phenanthrene, in which benzene rings are already oriented in an appropriate way in space. In other words *C_{sp2}-H and C_{sp2}-F groups can interact directly through space whereas the rest of the molecule is not involved in the process but is just interconnecting the reacting atoms. This interaction finally results in formation of a new C_{sp2}-C_{sp2} bond and elimination of HF.* The geometries of the transition states for benzene–fluorobenzene condensation and for cyclisation in **5h** were found to be rather similar, except for a higher deviation from planarity in the case of the biphenyl system. The angular orientation of benzene rings with 113° angle was found to be optimal for homo HF elimination (Figure 2.15). Such an orientation of benzene rings in benzo[c]phenanthrene requires partial perturbation of the aromatic system, but according to calculations the deviation from planarity does not contribute significantly to the activation energy.

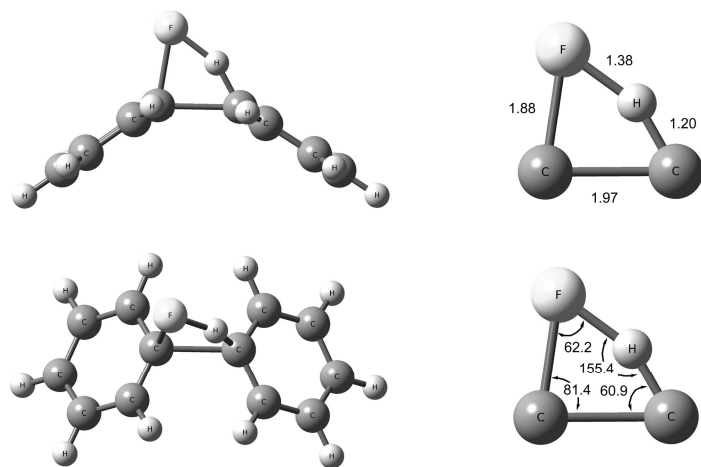


Figure 2.15. Transition state geometry for HF elimination for hypothetical intermolecular benzene-fluorobenzene condensation predicted with the DFT B3LYP/6-311G(d,p) method. On the right, only those bonds broken or formed during the reaction are shown. Bond lengths are given in Å, angles in degrees.

As an important consequence, the cyclisation occurs via a transition state with an already curved π -system, which is required for buckybowls and fullerenes. Regarding the condensation of fullerene precursors such a bent geometry seems to be suitable for condensation and the activation barrier for HF elimination is expected to be even lower than found for benzo[c]phenanthrene.

Taking into consideration that fluorine can promote the desired ring closure only if hydrogen is placed neighbouring in the precursor structure, it seems to be possible to fully control the direction of the condensation. According to our results highly efficient intramolecular condensations of appropriately functionalized PAH to non-planar PAHs via homo-HF elimination can be achieved. Use of fluorine as an activating group could solve the problem of selectivity in FVP and should provide an

effective conversion of respective planar PAH precursors to the desired fullerene cage.

2.1.4. Synthesis of fullerene precursors containing fluorine in key positions

The small size and low molecular weight of fluorine, as well as high thermostability of the C-F bond, make fluorine a “perfect” activating group for rational fullerene synthesis. As a next step towards the direct fullerene synthesis, several C₆₀ fullerene precursors containing fluorine atoms in key positions have been synthesized and investigated as a precursor for synthesis of C₆₀ fullerene.

Two general strategies were chosen for the synthesis of fullerene related PAHs. The first route starts from the heptacyclic hydrocarbon truxene, the trianion of which can be alkylated by treatment with bromomethyl-bromoarene. The corresponding trialkylated truxene can be converted to the fullerene-related PAH by intramolecular palladium-catalyzed arylation via HBr elimination.^[18,34] An alternative approach is based on the acid catalyzed head-to-tail cyclotrimerization of cyclic ketones,^[14,15] which leads directly to the precursor molecule. In his work both approaches for the synthesis of C₆₀ fullerene precursors containing a varying number of fluorine atoms in the key positions have been examined.

2.1.4.1. Synthesis on the base of truxene

The starting fluorinated truxenes was obtained in one step synthesis by acid catalyzed aldol cyclotrimerization of corresponding fluoroindanones (**31a**, **31b**, **31c**) as it is presented on Figure 2.16. Indanone **31c** (5,6,7-trifluoro-1-indanone) was prepared in several steps from 3,4,5-trifluorobenzyl bromide. 3,4,5-trifluoro-hydrocinnamic acid was synthesized analogously using the known procedure for hydrocinnamic acid.^[35] On the final step, the trifluoro-hydrocinnamic acid was directly cyclized by heating in polyphosphoric acid (PPA).

6,11,16-trifluorotruxene (compound **32a**) was prepared in 27 % yield by the classical route consisting in refluxing of 7-fluoro-1-indanone (**31a**) in a 1:2 mixture of concentrated HCl and acetic acid (HOAc).^[36] All attempts to trimerize **31b** and **31c** under the same conditions failed. Condensation of 5,7-difluoro indanone (**31b**) in a HCl/HOAc mixture e.g. results in the formation of the dimer (2-(2,3-dihydro-5,7-difluoro-1H-inden-1-ylidene)-2,3-dihydro-5,7-difluoro-1H-Inden-1-one) (**33**) with 44 % yield (Figure 2.16). The reaction probably stops after dimerization because of the low solubility of the dimer, which precipitates out of the reaction mixture as soon as it is formed. Sterical reasons can be excluded since the trifluorotruxene **32a** containing three fluorine atoms in sterically hampered regions readily forms by trimerization of fluoroindanone **31a**. Applying the improved protocol for aldol trimerization (p-toluenesulfonic acid (TsOH) in *o*-dichlorobenzene (ODCB),^[14] gave the desired truxene **32b**, but the product is contaminated by the dimer and tetramer, according to MS data. Pure **32b** was obtained after recrystallization from boiling *o*-xylene (or *o*-dichlorobenzene) with an overall yield of about 30%. Condensation of **31b** in aprotic medium, using TiCl₄ in ODCB,^[15] gave the pure product with more than 50 % yield. Introducing a third fluorine atom in the indanone molecule additionally reduces the ability to undergo aldol trimerization. Thus, whereas difluoro-indanone **31b** trimerizes to hexafluorotruxene **32b** in fair yield using TsOH/ODCB system under relative mild conditions (110 °C), the trifluoro-indanone **31c** gives no more than traces of the trimer, in a wide range of temperatures. In contrast, the condensation of **31c** in ODCB in presence of TiCl₄ gave truxene **32c** with moderate yield (45 %).

The fluorinated truxenes represent useful building blocks for synthesis of various fluorine-containing fullerene precursors.

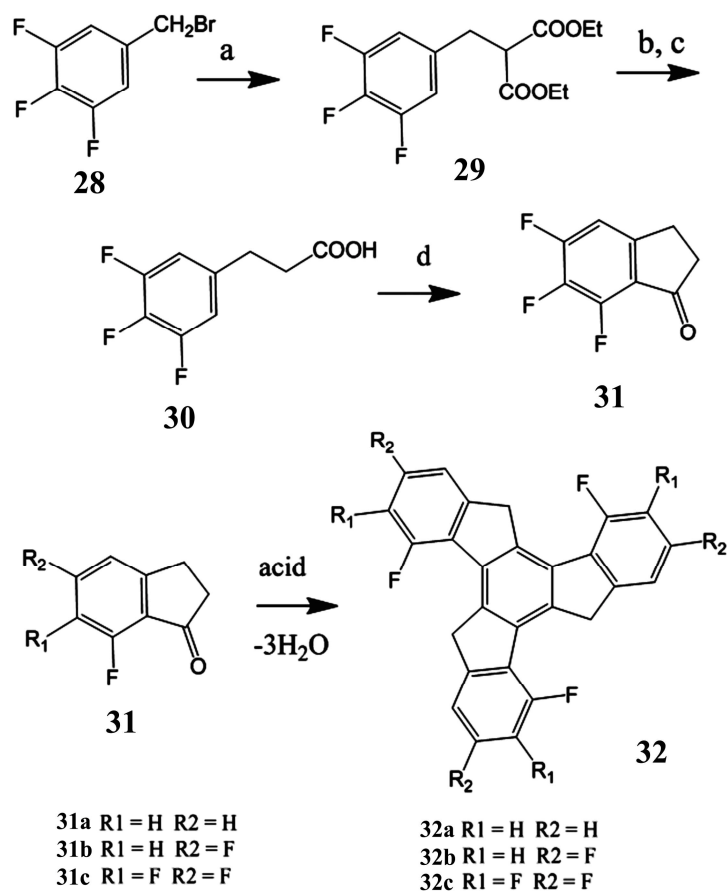


Figure 2.16. Synthetic route to 5,6,7-trifluoro-1-indanone a) NaOEt/EtOH; b) KOH; c) H₂SO₄ (overall yield 32 %); d) PPA 80°C (40 %). Synthesis of fluorinated truxenes by aldol cyclotrimerization (**32a**: 27 %, **32b**: 31 %, **32c**: 45 %).

Thus a C₆₀ precursor containing 3 fluorine atoms in the fjord regions (compound **35**) has been obtained in just two steps starting from trifluorinated truxene **31a** (Figure 2.17) analogously to the previously reported procedure.^[17,34] On the first step 1-bromo-2-bromomethylnaphthalene was added to the trifluorinated truxene trianion, which was generated in situ by treatment of **32** with three equivalents of *n*-BuLi. Compound **34** was obtained as a mixture of *syn* and *anti* isomers. Interestingly, both *syn* and *anti* isomers show good solubility in common organic solvents, whereas the *syn* isomer of the nonfluorinated analog is a highly insoluble compound. As a final step, palladium-catalyzed intramolecular arylation of the *anti/syn* mixture of **34** and the subsequent sublimation gave the compound **35**.

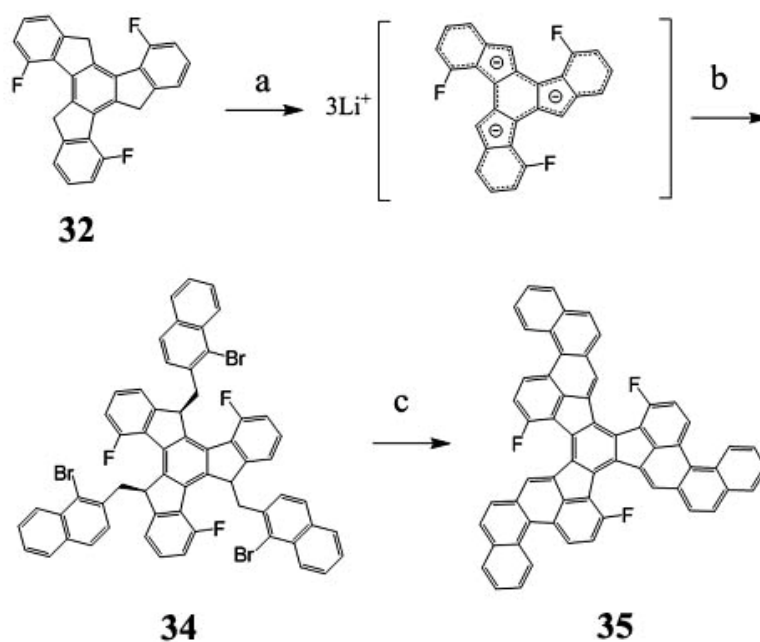


Figure 2.17. The synthetic route to the trifluorinated C₆₀ precursor - C₆₀H₂₇F₃. a) *n*BuLi/THF, -78 °C; b) 1-bromo-2-bromomethylnaphthalene (61 %) c) Pd(OAc)₂, DMA, Cs₂CO₃, Me₃BzNBr, 140 °C (67 %).

It is easy to see that additional fluorine atoms can be introduced in all other key positions by using appropriately fluorinated bromomethyl arenes. For instance, the C₆₀ fullerene precursor in which six regions are activated can be obtained starting from **32a** and 1-bromo-8-fluoro-2-bromomethylnaphthalene.

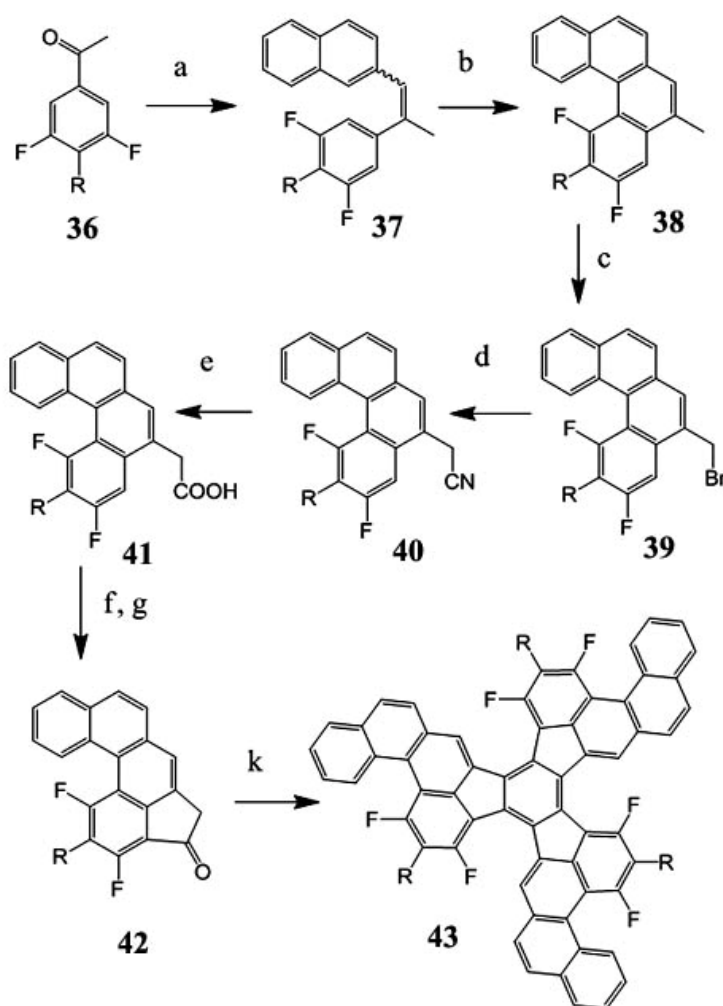
Hexa- and nona-fluorinated truxenes represent alternative building blocks for synthesis of multi-fluorinated precursors. However, all attempts to synthesize hexa- and nona-fluorinated precursor starting from truxenes **32b** and **32c** failed on the alkylation step. This is probably because of low stability of the corresponding truxene trianion and/or enhanced acidity of protons neighboring to fluorine. The reaction of 1-bromo-2-bromomethylnaphthalene with the corresponding fluorinated truxene trianion results in a complex mixture, which is difficult to analyze.

2.1.4.2. Synthesis on the base of aldol trimerization of cyclic ketones

An alternative way to fullerene related PAHs is based on the aldol trimerization of cyclic ketones. Although this reaction was discovered more than 100 years ago, it only recently became a powerful method for the synthesis of large molecules. It was demonstrated that large PAHs can be obtained effectively via aldol trimerization of cyclic ketones using TsOH in ODCB,^[16,37] or TiCl₄ in ODCB.^[7,15,38] Both methods have been examined for synthesis of fluorinated precursors.

The synthetic route to hexa- and nona-fluorinated precursors is summarized in Figure 2.18. Fluorinated methylbenzo[c]phenanthrenes (**38a** and **38b**) were synthesized by standard Wittig olefination of correspondingly fluorinated acetophenones with subsequent photocyclization. Benzylic bromination with NBS and subsequent treatment with aqueous ethanolic sodium cyanide gave cyanomethylbenzophenanthrenes (**40a**, **40b**) which were hydrolyzed into acid (**41a**, **41b**). Ketones **42a** and **42b** were obtained after transforming the acids (**41a**, **41b**) to

the corresponding acid chlorides with subsequent intramolecular Friedel-Crafts acylation in the presence of AlCl_3 .



a: R = H b: R = F

Figure 2.18. The synthetic route to the hexa and nona fluorinated C_{60} precursors. a) $\text{Ph}_3\text{PCH}_2\text{Ph}^+ \text{Br}^-$, NaOEt/EtOH ; b) $h\nu$, I_2 , propylene oxide (**38a**: 67 %; **38b**: 65 %); c) NBS, DBPO, CCl_4 (**39a**: 68 %; **39b**: 72 %); d) NaCN , $\text{EtOH}/\text{H}_2\text{O}$ (**40a**: 75 %; **40b**: 85 %); e) H_2SO_4 , H_2O , HOAc (**41a**: 90 %; **41b**: 84 %); f) SOCl_2 ; g) AlCl_3/DCM (**42a**: 30 %; **42b**: 23 %); k) $\text{TiCl}_4/\text{ODCB}$ (**43a**: 57 %; **43b**: 85 %).

Despite the quite smooth trimerization conditions needed for indanones **31b** and **31c**, the condensation scenario changes drastically in the case of structurally related benzacephenanthrylenones **42a** and **42b**. Thus, the condensation of **42a** in ODCB in presence of TsOH at 100-140 °C gave a complex mixture containing mainly dimer, tetramer and hexamer according to MS data. Interestingly only a trace amount of trimer and pentamer were detected in MS. Condensation at 160 °C gave a highly insoluble product which shows three groups of signals at 858.3, 856.3 and 854.3 m/z (Figure 2.19).

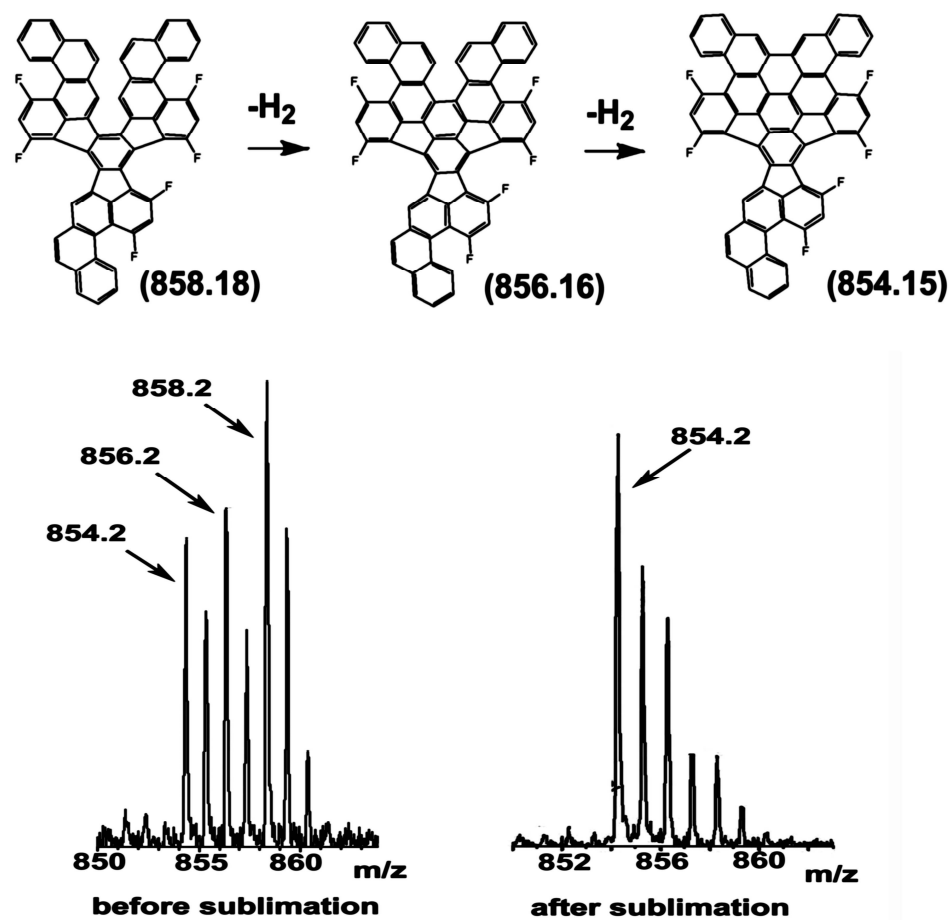


Figure 2.19. The MS spectra of condensation products of **42a** in TsOH/ODCB system.

The sample was purified by sublimation and analyzed. MS analyses have shown almost exclusively the ion peak at 854.2 m/z which is 4 Da less than the mass of the expected trimer (Figure 2.19). However, for the targeted structure a respective hydrogen elimination can not take place since all possible condensation ways are blocked by the fluorine atoms (formation of new C-C bond requires HF elimination). The elimination of hydrogen atoms would have only become possible if one of the benzophenanthrene fragments is “wrongly” oriented, as it shown in Figure 2.20. Indeed, the analysis of intermediate products confirms this supposition. A more detailed MS analysis of the reaction mixture shows the presence of a dimer containing two carbonyl groups confirming the possibility of **42a** for atypical tail-to-tail dimerization.

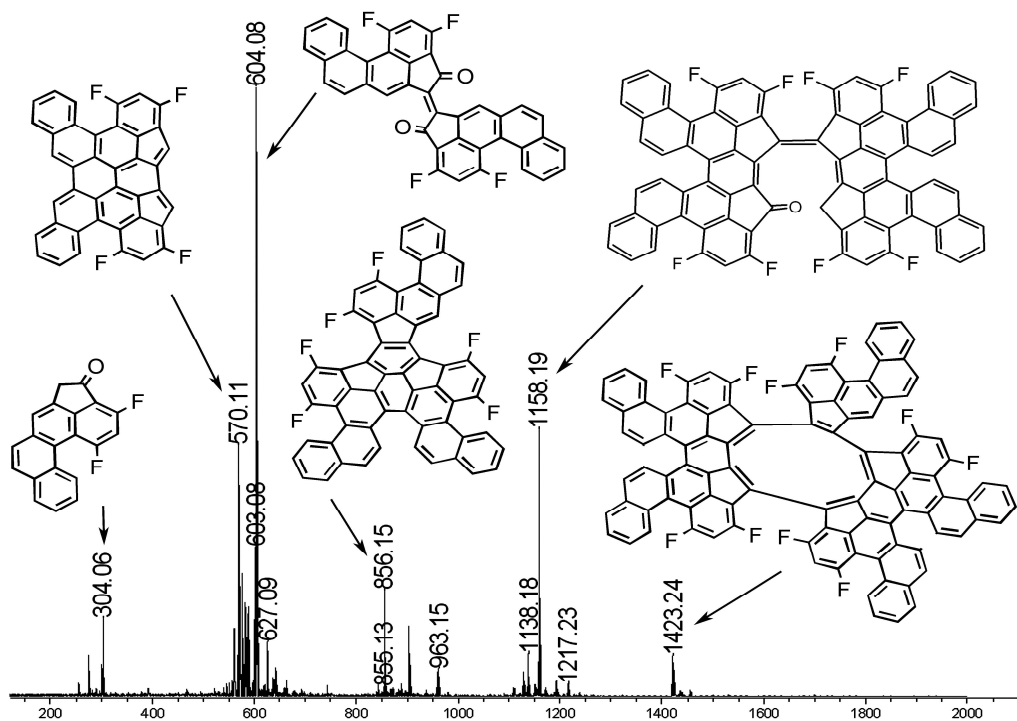


Figure 2.20. MS analysis of the intermediate products of condensation of **42a** in HCl/AcOH, 72 h, reflux (more probable structures are given).

More information about the mechanism can be obtained by analysis of reaction products obtained at mild conditions (HCl/AcOH, 100 °C or TsOH/ODCB, 100 °C). In this case all intermediates can be easily detected in the MS spectra. According to MS data the reaction mixture contains the dimer and several products of its subsequent condensation. The molecular masses of trimer, tetramer and pentamer are slightly less than expected which additionally confirms the presence of “wrongly” connected benzacephenanthrylenone fragments (Figure 2.20 and Figure 2.21). Although the mechanism of condensation is not fully clear, it obviously involves unusual tail-to-tail ketone condensation and is accompanied by numerous redox processes. The presence of such a condensation product has been confirmed by detail MS/MS/MS analysis of **42a** dimer (Figure 2.22).

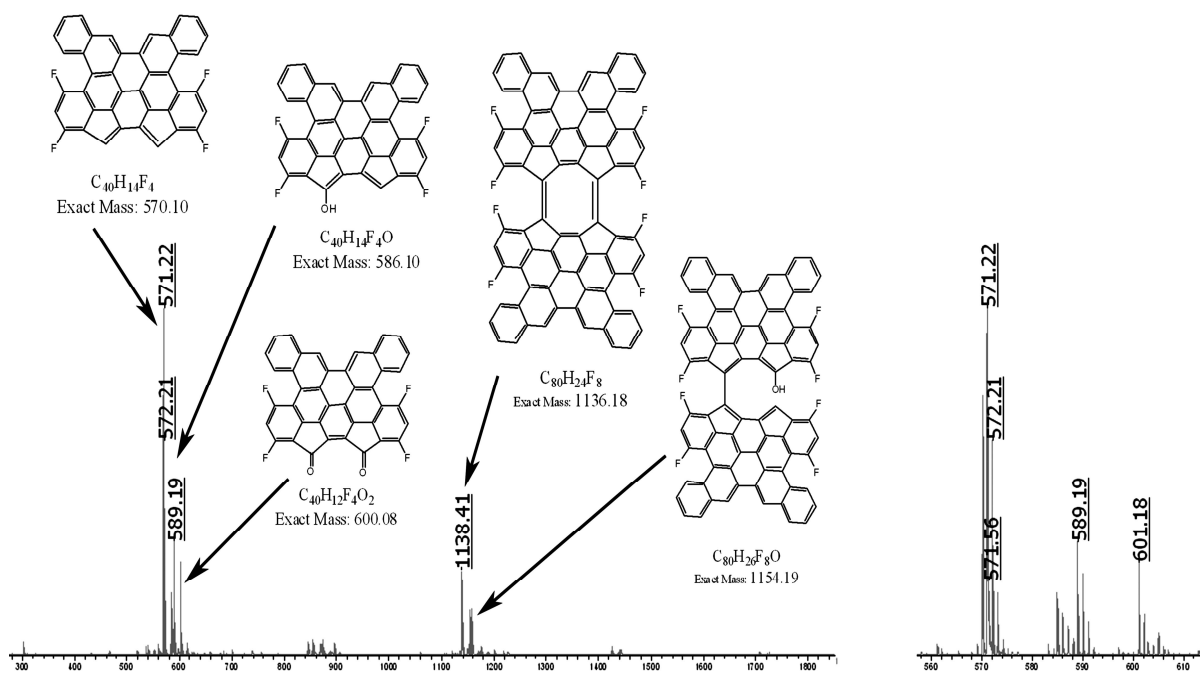


Figure 2.21. MS analysis of the intermediate products of condensation of **42a** in TsOH/ODCB 20 min, 100 °C (more probable structures are given).

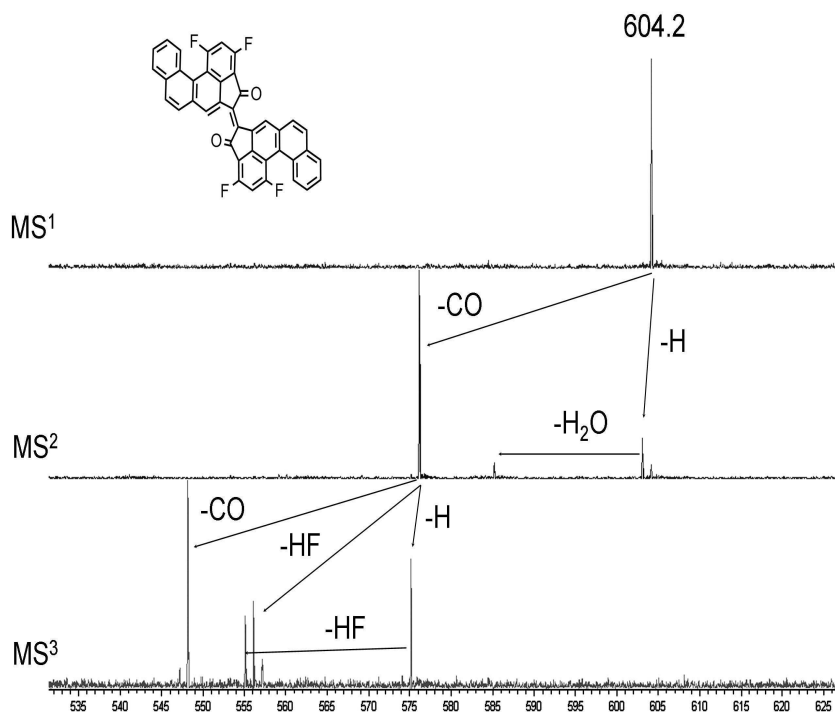


Figure 2.22. MS/MS/MS analysis of dimer of **42a**. The presence of two carbonyl groups in the molecule confirms tail-to-tail condensation of ketone **42a**.

On the other hand the condensation of **42a** and **42b** in an aprotic medium, using TiCl_4 in ODCB, gave the desired products with good yields (60-80 %), and in high purity. In both cases, the MS analyses shows the single ion peaks at 858.2 m/z for the hexafluorinated precursor (**43a**) and 912.2 m/z for nonafluorinated precursor (**43b**), which corresponds to the expected structures (Figure 2.23). Both compounds show poor solubility and can not be analyzed by NMR spectroscopy. However, MS and MS/MS analyses have provided sufficient structural information. Thus, applying a higher ionization energy causes partial condensation of the precursor exclusively

by HF elimination. No loss of two hydrogen atoms under high energy ionization confirms the expected structure (absence of “wrongly” oriented benzophenanthrene fragments), because only in this case there is no possibility for intramolecular condensation via H₂ elimination. In the MS/MS experiment the monoisotopic precursor ions were selected and subjected to collision-induced dissociation with argon. The respective analyses show that H₂ elimination is a main fragmentation process for the non-substituted precursor C₆₀H₃₀, which is a result of intramolecular condensation in the fjord/cove regions. In the case of the trifluorinated precursor (**35**), the intramolecular condensation is accompanied by elimination of HF and H₂ molecules, which is in good agreement with the expected structure of the precursor. The hexa-fluorinated precursor (**43a**) is not able to undergo intramolecular condensation via H₂ elimination, since all fjord/cove regions contain fluorine atoms. Therefore no [M-H₂]⁺ ions are observed in the respective MS/MS spectra. Interestingly, the cyclization via HF elimination results in the formation of a new fjord region and H₂ elimination as a subsequent step become possible. Indeed, the corresponding ion peak ([M-HF-H₂]⁺) was detected in the MS/MS spectra of **43a** (Figure 2.25). In contrast, the nonafluorinated precursor (**43b**) does not show any H₂ elimination since the new fjord/cove region which forms after HF elimination still contains a fluorine atom. The MS/MS patterns obtained indicate that all fjord regions in **43a** and **43b** contain fluorine atoms, which confirm the absence of “wrongly” orientated benzophenanthrene fragments in the structure. Additionally, the comparison of UV-spectra of nona-fluorinated (**43b**), hexa-fluorinated (**43a**), tri-fluorinated (**35**) precursors with well characterized C₆₀H₃₀ precursor, reveals the similarity of π-system for all four compounds (Figure 2.26)

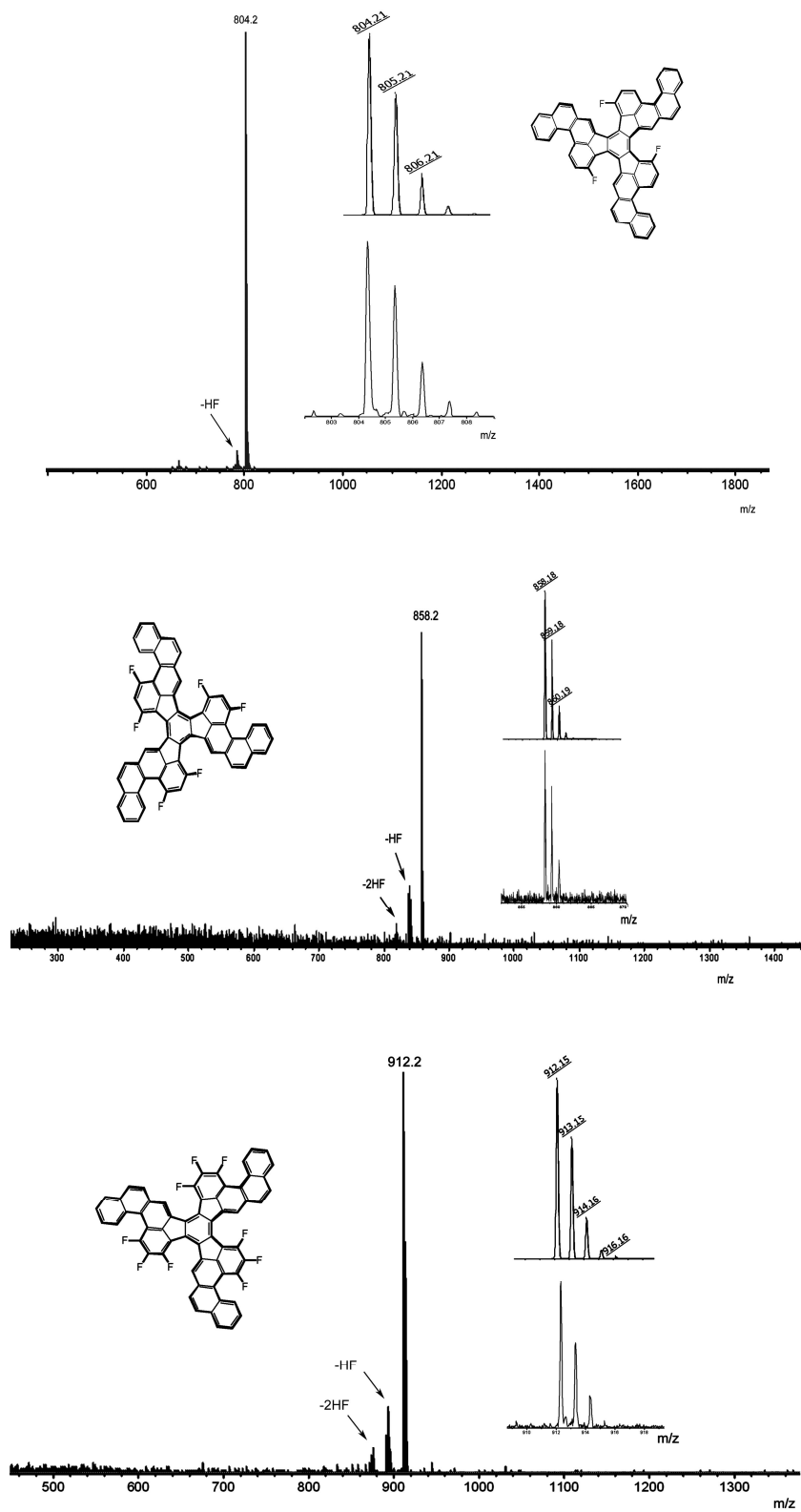


Figure 2.24. LDI mass spectrum of **35** ($C_{60}H_{27}F_3$), **43b** ($C_{60}H_{21}F_9$) and **43a** ($C_{60}H_{24}F_6$) (positive mode).

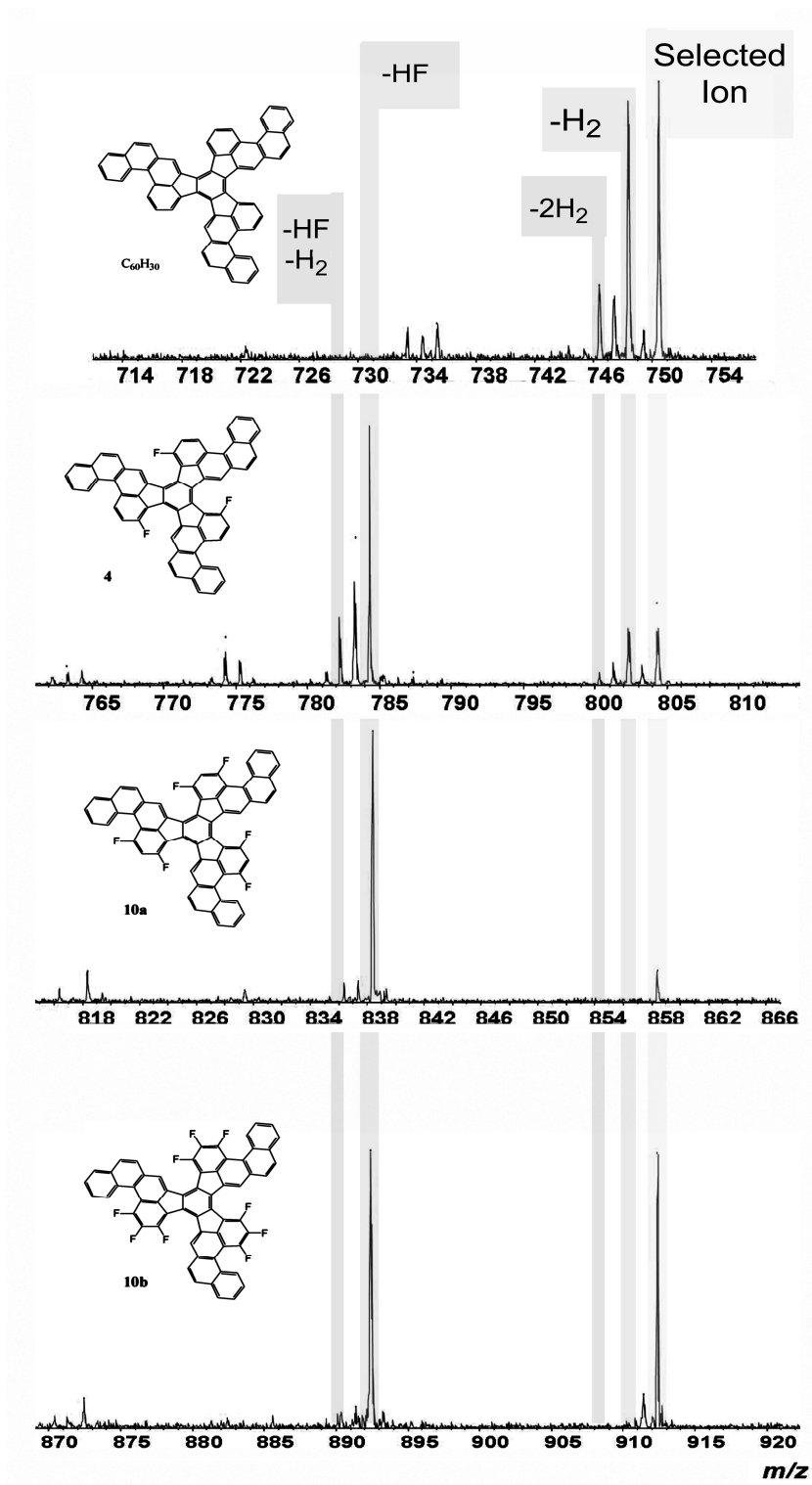


Figure 2.25. MS/MS spectra of precursors **35**, **43a**, **43b** and $C_{60}H_{30}$.

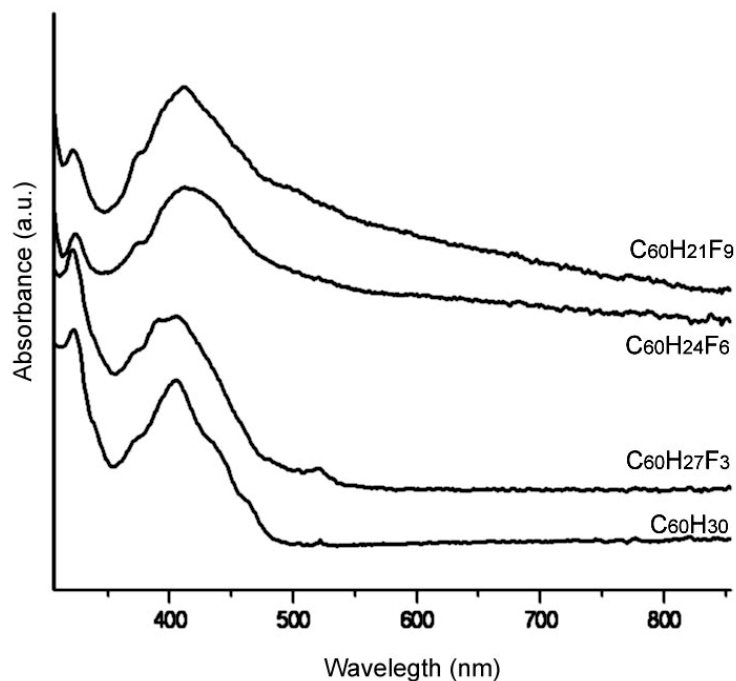


Figure 2.26. UV/VIS spectra of C_{60} fullerene precursors: $C_{60}H_{30}$, **35** ($C_{60}H_{27}F_3$), **43a** ($C_{60}H_{24}F_6$) and **43b** ($C_{60}H_{21}F_9$) (1,2,4-trichlorobenzene, 60 °C).

Thus fullerene precursors containing a different number of fluorine atoms in the key positions can be synthesized from trifluorinated truxene or by aldol cyclotrimerization of cyclic ketones. In contrast to chlorine, the fluorine can be introduced quite easily into the sterically hampered regions of the precursor molecules as a result of the small size. The aldol condensation of fluorinated cyclic ketones using $TiCl_4/ODCB$ was found to be an effective route for synthesis of fluorine containing PAHs, whereas the condensation using $TsOH/ODCB$, which is the best route for synthesis of related chlorinated PAHs completely failed.

2.1.5. Condensation of fluorinated C₆₀ precursor to C₆₀ fullerene

The fluorinated PAHs obtained represent attractive precursor molecules for rational fullerene synthesis by flash vacuum pyrolysis. Taking into consideration that fluorine can promote the ring closure only if hydrogen is placed in a neighboring position in the precursor structure it appears to be possible to fully control the direction of the process.

2.1.6. Condensation under FVP conditions

Compound **35**, **43a**, and **43b** were found to be thermally stable and can be easily sublimed without visible decompositions, which is an important prerequisite for the FVP procedure. The FVP experiments indeed have shown a selective transformation of the precursors **35**, **43a**, and **43b** to the C₆₀ fullerene. As it was expected, the best results were obtained for compound **43b** in which nine positions are “activated” by fluorine.

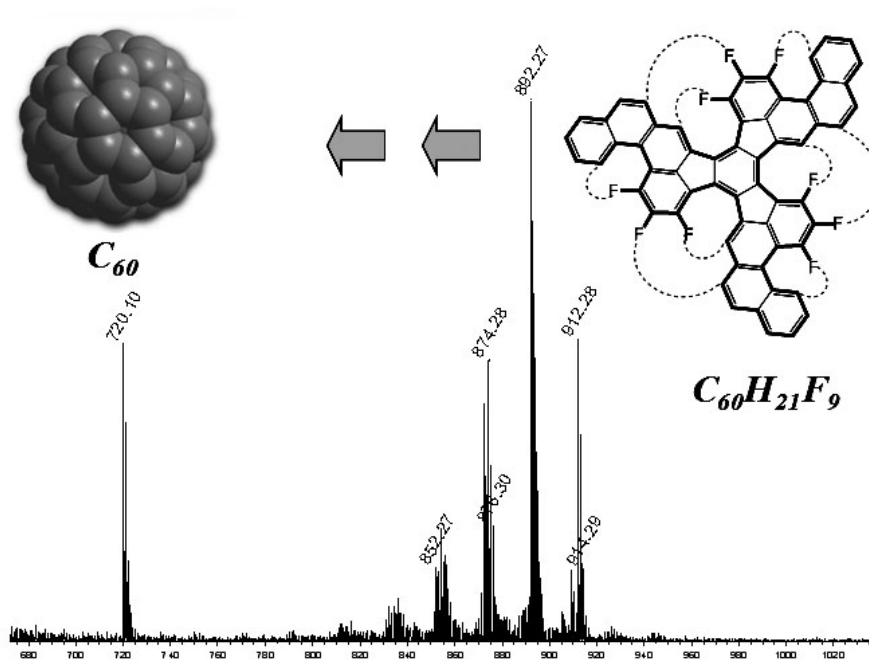


Figure 2.27. The LDI-MS spectrum of the toluene extract of the FVP products of **43b**.

Additionally no side 1,2-elimination in **43b** is possible, which is probably also responsible for high selectivity in the condensation process. Unfortunately, as a result of high molecular weight of the precursor molecules the pyrolysis experiment was carry out at pressure of about 10^{-2} mbar (it was not possible to carry out the experiment at optimal pressure, $p = 0.1$ mbar). Unfortunately the efficiency of conversation has been significantly reduced in this case. Thus, many products of partial condensation can be detected in extract of pyrolysis product as well as unreacted starting material (Figure 2.27). Although the C_{60} has formed very selectively (no other fullerenes were detected) the yield of target molecule was found to be low ($< 0.5\%$).

2.1.7. Condensation under LDI-MS conditions

During LDI-MS analysis of the precursors **35**, **43a**, and **43b** was found that effective HF elimination takes place if high laser energy is applied. Thus tandem cyclodehydrofluorination has been monitored directly as it can be seen from Figure 2.28. Subsequent elimination of nine HF molecules leads to the formation of metastable $C_{60}H_{12}$, which, according to quantum chemical calculations, is able to collapse spontaneously to the C_{60} fullerene. The process of six subsequent H_2 eliminations can be observed on the MS-spectrum. In order to exclude possible spontaneous C_{60} fullerene formation under laser ablation ^{13}C a labelled $C_{60}H_{21}F_9$ precursor has been synthesized and condensed under LDI-MS conditions. The labelled precursor has been synthesized in analogy to compound **43b** (using $K^{13}CN$ for nitrile synthesis). Since the resulting precursor has three ^{13}C -carbon atoms ($^{13}C_3C_{57}H_{21}F_9$) its condensation will give labelled C_{60} fullerene bearing three ^{13}C . The difference between natural C_{60} and labelled $^{13}C_3C_{57}$ (3.0 Da heavier) can be easily detected by MS. Indeed LDI-MS analysis of the labelled precursor has shown that $^{13}C_3C_{57}$ forms exclusively. This experiment gave strong evidence that fullerene

formation is a result of selective condensation of the precursor to the desired fullerenes.

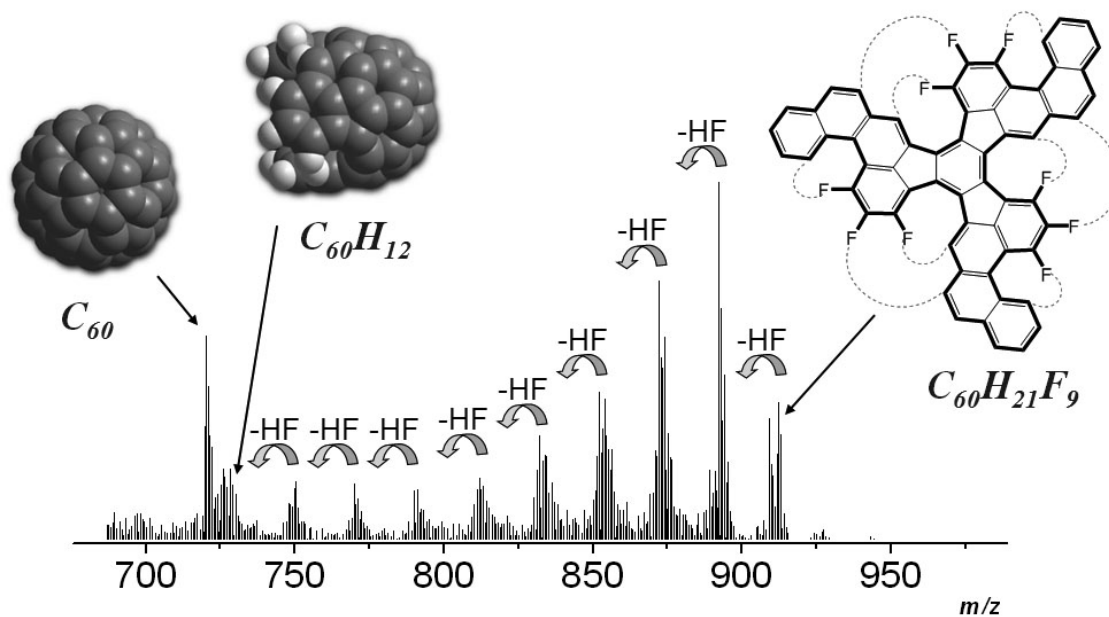


Figure 2.28. The LDI-MS spectrum of **43b** at high laser ionization energy.

2.2. Non-pyrolytical approach

2.2.1. Introduction

Fluorine group was found to be a very effective for activation of intermolecular Aryl-Aryl coupling under FVP conditions. As demonstrated above, the fluorine atom can be rather easily introduced in the sterically hampered cove/fjord regions due to its small size, and the scope of reactions which can be used for the precursor synthesis can be remarkably extended. Although, a single intramolecular condensation via HF elimination by FVP can be realized rather selectively under FVP conditions, the conversion rate is still too low (of about 60 % for a single cyclization) in order to carry out a multifold process effectively. Besides modest yield and difficulty in scale-up the main drawback of the FVP technique is minimum functional group tolerance and numerous side reactions caused by the harsh reaction conditions. To overcome these disadvantages several alternative liquid-phase intermolecular Aryl-Aryl coupling techniques have been developed during the last years. Thus the Pd(0) catalyzed arylation utilizing bromo- or chloro- derivatives has been found to be effective for the synthesis of various buckybowls.^[18,39-41] Unfortunately, this methodology can not be extended to fluorinated analogues because of low reactivity of C-F bond. Moreover, the main drawback of the approach is aggressive reaction conditions with respect to the fullerene species. The discovery of C-F bond activation under transition-metal free conditions utilizing silylium-carborane catalysis might be a good alternative.^[42] Recently this strategy has been successfully applied for to intramolecular Aryl-Aryl coupling.^[43] Unfortunately, the yield, in the case of non-planar PAHs, drops from 99 % to 50-80 % already for single condensation, which limits the application for multifold condensation. Moreover all solution approaches might be not effective in the case of extra large hydrocarbons which are typically insoluble compounds. It is worth mentioning that the intramolecular Aryl-Aryl coupling cannot be realized in a domino fashion neither by Pd(0) catalyzed arylation nor by silylium-carborane catalysis.

2.2.2. Al₂O₃ mediated Cove-Region-Closure via HF elimination

In the search for a more effective method for ring closure, applicable for highly insoluble fullerene precursors, we have turned our attention to solid state reactions. It has been found that several metal oxides show activity in Aryl-Aryl coupling through HF-elimination. Thus Al₂O₃, SiO₂, Ga₂O₃ and GeO₂ have shown activity in HF elimination at 300–350 °C. The highest activity has been observed for γ -Al₂O₃ which has been investigated further in detail.

The conversion of 1-fluorobenzo[*c*]phenanthrene (**5h**) to benzo[*ghi*]fluoranthene (**6**) was chosen as a model reaction for the investigation. In this system the γ -Al₂O₃ displays pronounced activity above 300 °C. In the case of benzo[*ghi*]fluoranthene the rather high temperature does not cause further decomposition and **5h** can be (effectively) converted to **6**. Nevertheless the condition is too harsh for synthesis of buckybowls and fullerenes. During the optimization of the reaction conditions it was found that the high temperature is only required for γ -Al₂O₃ activation whereas the condensation process can proceed smoothly at lower temperatures. The best results were obtained after activation of γ -Al₂O₃ by annealing at 500 °C for 15 min at 10⁻³ mbar pressure. Using such activated γ -Al₂O₃, compound **5h** can be quantitatively transformed to **6** at amazingly low temperatures. Thus, quantitative conversion of **5h** to **6** was observed after 20 h at 150 °C. Full conversion has even been achieved at 100 °C after 60 h. The same process can be completed in 1 h or in just several minutes at 200 °C and 250 °C respectively. For practical purpose the condensation temperature of about 150 – 200 °C was found to be the most appropriate.

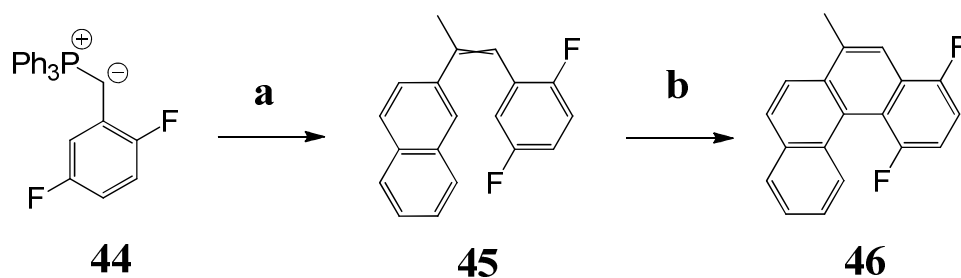


Figure 2.29. The synthetic route to 1,4-difluoro-6-methyl-benzo[*c*]phenanthrene (**46**). (a) 2-acetonaphthone, *t*-BuOK/EtOH, reflux (60 %); (b) $h\nu$, I_2 , propyleneoxide, cyclohexane (89 %)

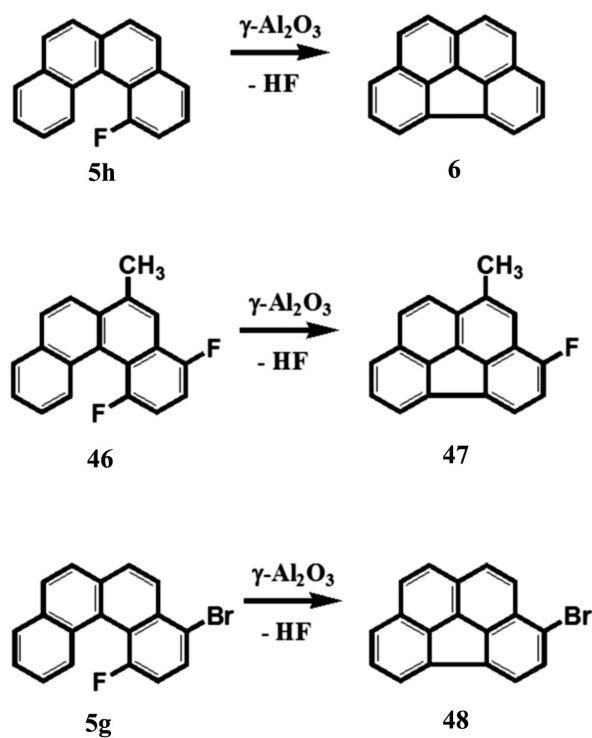


Figure 2.30. Cove-Region-Closure (CRC) mediated by Al_2O_3 . CRC via HF elimination in 1-fluorobenzo[*c*]phenanthrene derivatives, demonstrating high chemoselectivity and regioselectivity of the process. Compounds **6**, **47** and **48** were obtained with quantitative or close to quantitative yield.

The process discovered has demonstrated an unexpectedly high chemoselectivity and regioselectivity. Thus, if the fluorine atom is not involved in the cove region (2-fluorobenzo[*c*]phenanthrene), no reaction takes place and the compound remains completely intact. The regioselectivity has been demonstrated on the synthesis of **47** where condensation in **46** has been realized with quantitative yield (Figure 2.30). Importantly, chlorinated and even brominated analogues (2-chlorobenzo[*c*]phenanthrene and 2-bromobenzo[*c*]phenanthrene) have shown no activity and both cases starting compound remain completely intact. The high chemoselectivity has been demonstrated by the synthesis of **48** where HF elimination has been realized in the presence of a C-Br bond. Importantly, no exchange of fluorine to hydrogen has been detected and no evidence of any side reactions has been obtained during the condensation. The desired **48** has formed exclusively and has required no further purification (Figure 2.31).

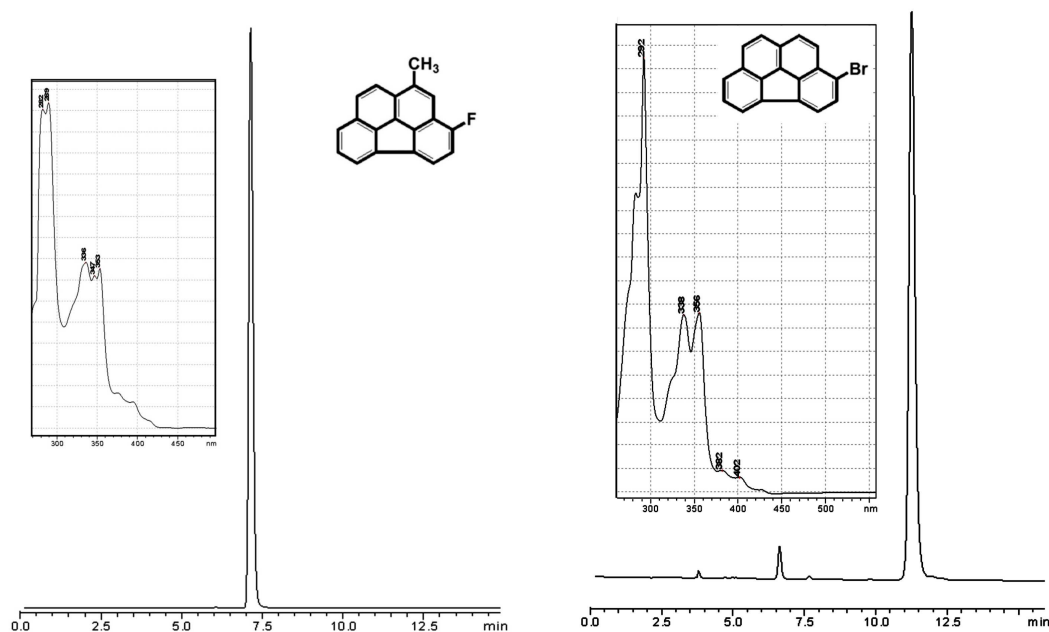


Figure 2.31. HPLC profile of the compound **47** (left) and compound **48** (right) as obtained after reaction (200 °C, 2h). 5PYE column, toluene:MeOH 1:4 as eluent. (inset) UV-Vis spectra (toluene/MeOH).

The driving force of the reaction is the formation of exceptionally strong Al-F bond. On the other hand, the results obtained exclude direct C-F bond activation and indicate that no reactive intermediates form during the reaction. The most probable mechanism of condensation includes aromatic transition states (the condensation takes place in a concerted fashion) (Figure 2.32).

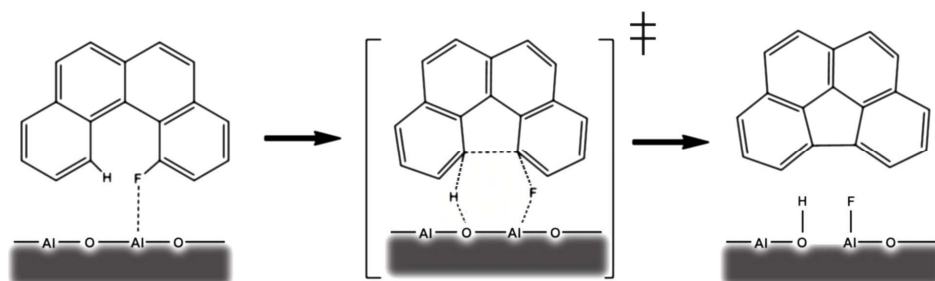


Figure 2.32. A schematic representation of the most probable mechanism of the CRC. The mechanism of the CRC at the example of benzo[*c*]phenanthrene condensation representing the key points of the process: coordination on the aluminium oxide surface, aromatic transition state and high energy gain due to Al-F bond formation.

2.2.3. Synthesis of extended buckybowls

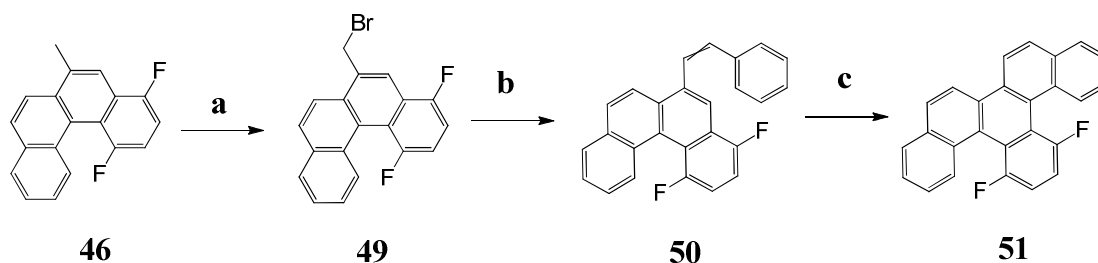


Figure 2.33. The synthetic route to the 13,16-difluoro-Benzo[*s*]picene. (a) NBS, DBPO, CCl₄, reflux (97 %); (b) 1) Ph₃P, toluene, reflux 2) PhCHO, *t*-BuOK/EtOH, reflux (58 %); (c) *hν*, I₂, propyleneoxide, cyclohexane (84 %).

Since bond dissociation and bond formation takes place simultaneously, no reactive intermediates (which might cause side reactions) form. An aromatic transition state explains the low activation barrier allowing the reaction to take place under rather low temperatures. Regiospecificity can also be explained in terms of the assumed mechanism, since 1,2-HF elimination is unfavorable due to high energy of 1,2-didehydrobenzene which should be formed.

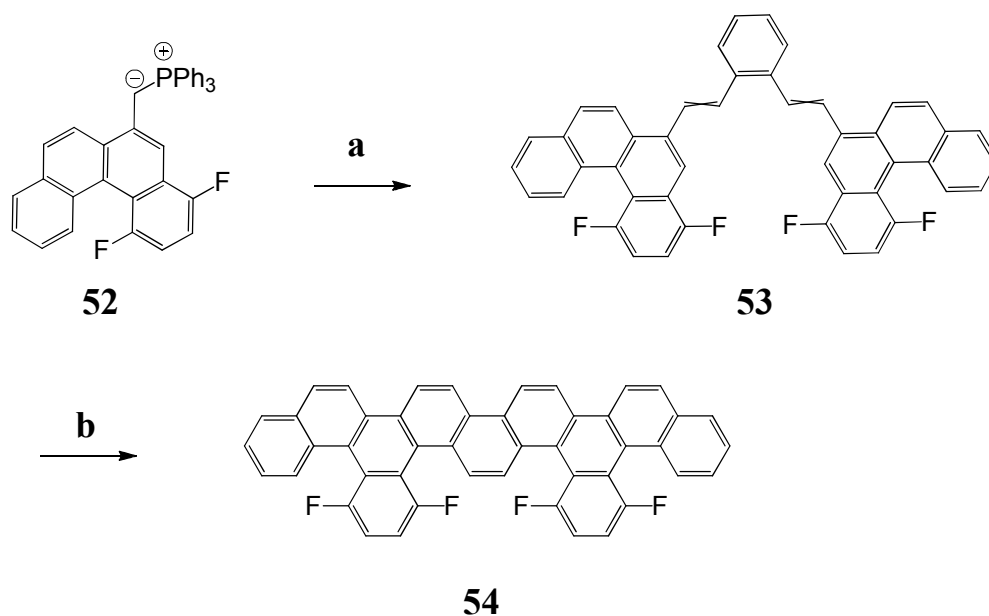


Figure 2.34. The synthetic route to the compound **54**. (a) 1,2-Benzenedicarboxaldehyde, *t*-BuOK/EtOH, reflux (20 %); (b) $h\nu$, I_2 , propyleneoxide, cyclohexane (52 %).

Considering the multifold condensation, each new pentagon formation imposes remarkable strain to the system because of perturbation of the aromatic system. Typically, each subsequent condensation step requires harder condition and frequently the condensation process stops.

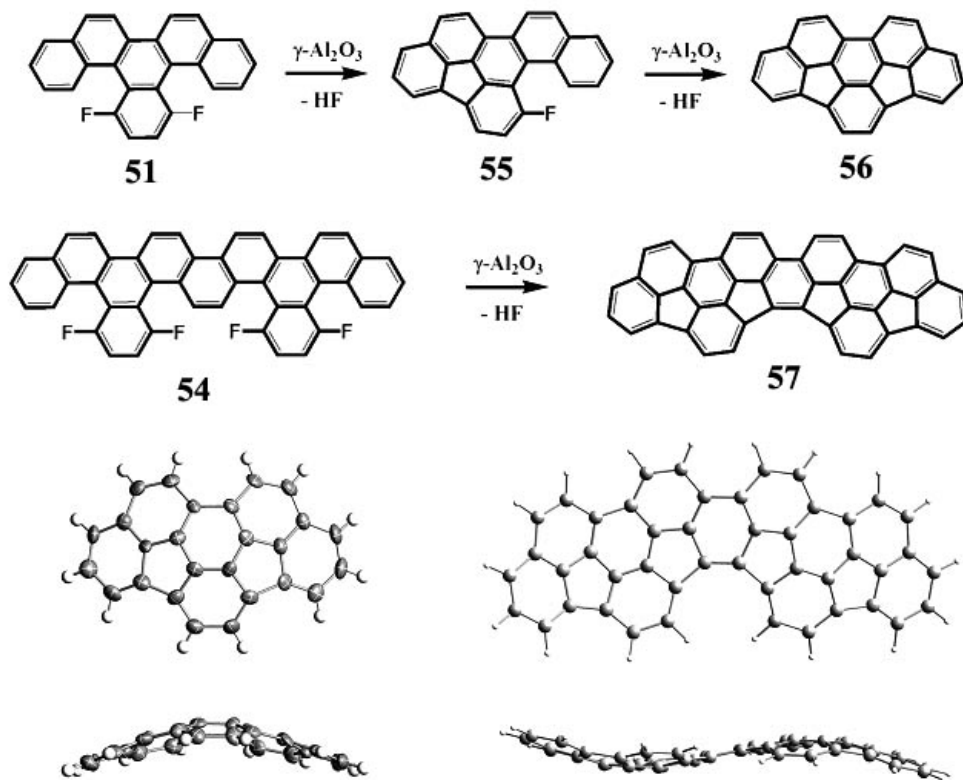


Figure 2.35. Synthesis of buckybowls by CRC approach. (top) Buckybowl synthesis by two- and fourfold Fjord-Region-Closure. (bottom) ORTEP plot of compound **56** (top and side view) and DFT optimized structure of **57** (top and side view) demonstrating the geodesic shapes. Compounds **56** and **57** were obtained with quantitative yield.

The suitability of the $\gamma\text{-Al}_2\text{O}_3$ for construction of non-planar PAHs via HF-elimination has been examined on the synthesis of indacenoprene (**56**). Despite of the strain imposed, compound **51** was converted to the buckybowl **56** quantitatively at 150 °C after 60 h. At 250 °C the process was completed after 60 min. Interestingly, the product of mono condensation **55** was not detected in the reaction even if the starting material was not fully converted. This indicates that the HF elimination in **55** proceeds much faster than in compound **51**. Indacenoprene **56** was obtained in

pure form by extraction with hot toluene (isolated yield 99 %). Single-crystal X-ray analysis unambiguously confirms the structure and reveals the geodesic shape of **56** (Figure 2.35-2.38).

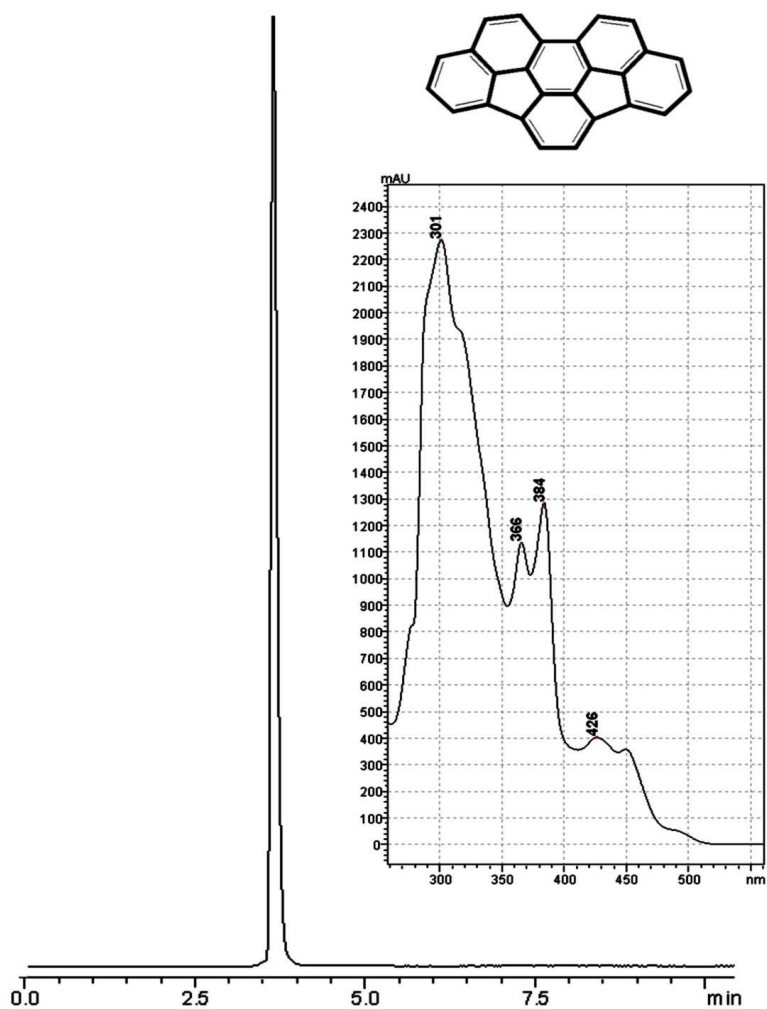


Figure 2.36. HPLC profile of the compound **56** as obtained after reaction (150 °C, 48h). 5PYE column, toluene as eluent. (inset) UV-Vis spectrum of **56** (toluene).

To address the solubility issue we investigated the discovered reaction for the badly soluble precursor **54**. It was found that the four-fold HF elimination proceeds very effectively. After annealing (10 h, 250 °C) of **54** deposited on an activated $\gamma\text{-Al}_2\text{O}_3$ and subsequent Soxhlet extraction with o-xylene, the desired buckybowl **57** was obtained in pure form as a hardly soluble red powder (isolated yield 98 %). Importantly, no side products and no products of partial condensation were found in the sample (Figure 2.39).

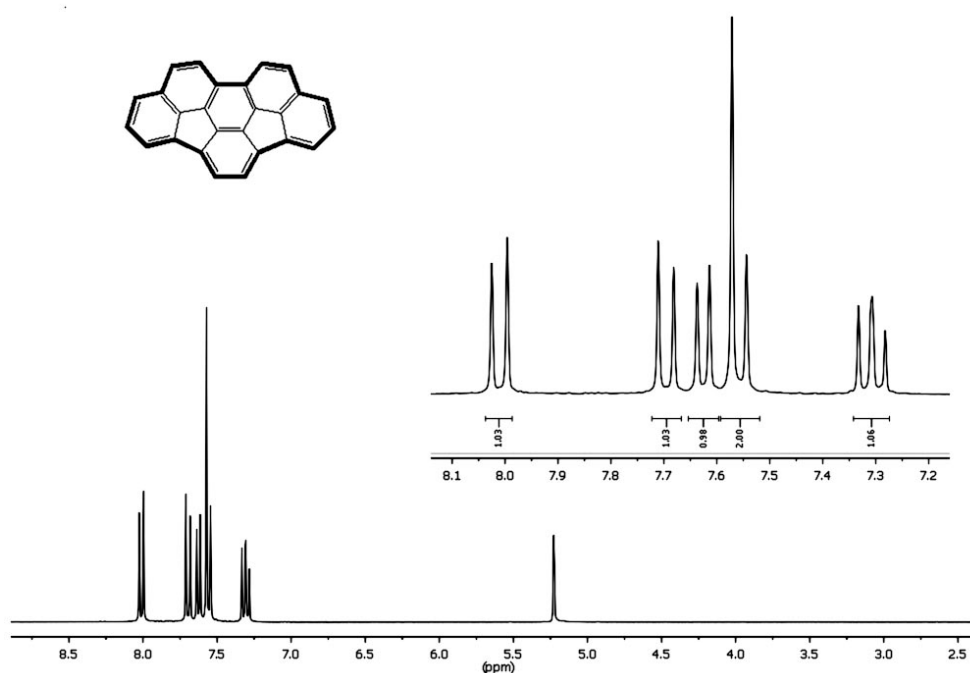


Figure 2.37. ^1H spectra of the compound **56** (CD_2Cl_2).

Quantitative transformation of the precursor molecules to the desired buckybowl structures demonstrates high efficiency of the approach. The high conversion level to extended buckybowl **57**, which formally represents more than 75 % of the C_{60} fullerene surface, demonstrates high potential of the technique for synthesis of

extended non-planar carbon based nanostructures, including higher fullerenes, giant buckybowls and nanotubes.

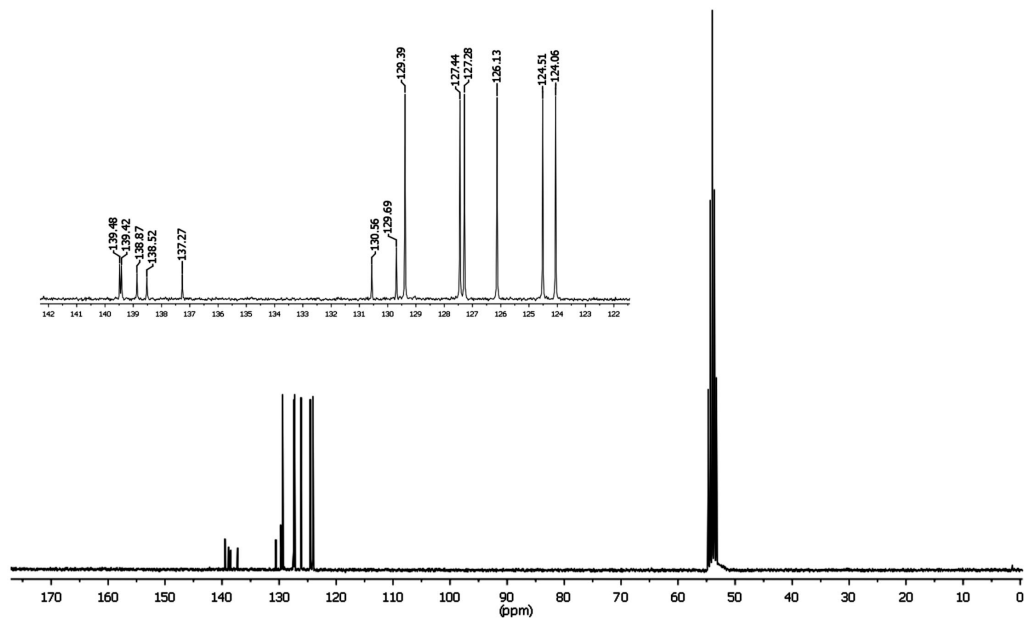
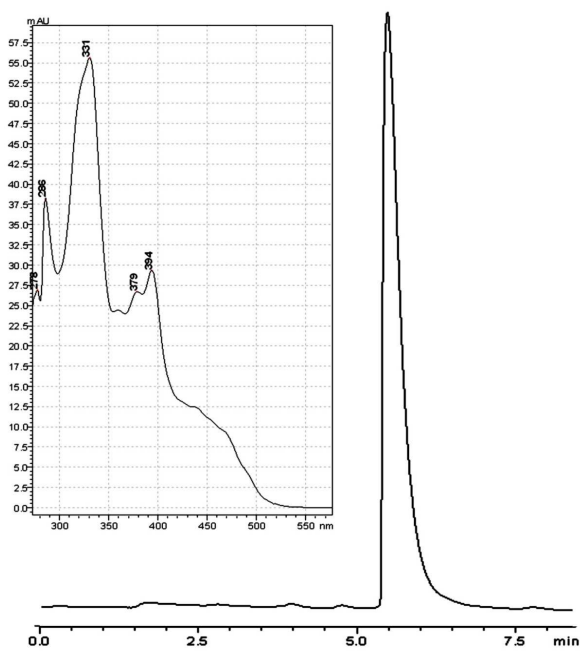


Figure 2.38. ^{13}C -NMR spectra of the compound **56** (CD_2Cl_2).



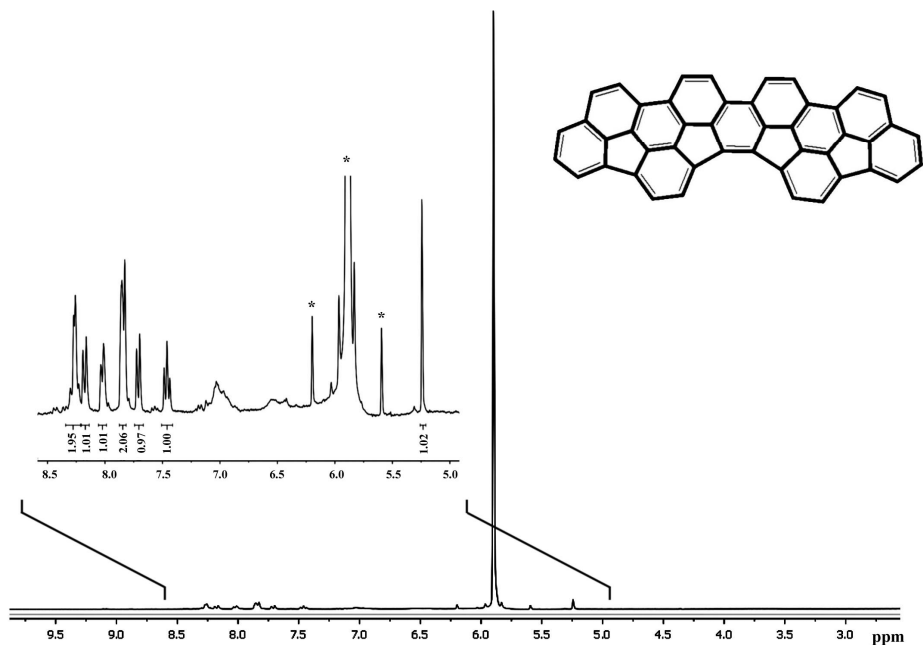


Figure 2.39. (top) HPLC profile of the compound **57** as obtained after reaction (250 °C, 10 h). 5PYE column, column temperature 60 °C, toluene as eluent. (inset) UV-Vis spectrum of **57**. (bottom) $^1\text{H-NMR}$ spectrum of the compound **57** measured in $\text{C}_2\text{D}_2\text{Cl}_4$ at 110 °C.

2.2.4. Perspectives of Al_2O_3 media for synthesis of fullerenes, nanotubes and other carbon based structure

The high tolerance to chlorine and bromine functionalities makes the approach a very powerful synthetic tool for synthesis of functionalized buckybowls representing useful building blocks for the synthesis of more complex carbon based nanostructures.

2.3. References

1. L.T. Scott, Fragments of fullerenes: Novel syntheses, structures and reactions, *Pure Appl. Chem.* **1996**, 68, 291-300.
2. M. J. Plater; M. Praveen; D. M. Schmidt, Buckybowl synthesis: A novel application of flash vacuum pyrolysis, *Fullerene Sci. Technol.* **1997**, 5, 781-800.
3. G. Mehta; H. S. P. Rao, Synthetic studies directed towards bucky-balls and bucky-bowls, *Tetrahedron Lett.* **1998**, 54, 13325-13370.
4. V.M. Tsefrikas; L.T. Scott, Geodesic polyarenes by flash vacuum pyrolysis, *Chem. Rev.* **2006**, 106, 4868-4884.
5. M. M. Boorum; Y. V. Vasil'ev; T. Drewello; L. T. Scott, Groundwork for a rational synthesis of C-60: Cyclodehydrogenation of a C₆₀H₃₀ polyarene. *Science* **2001**, 294, 828-831.
6. B. Gomez-Lor; C. Koper; R. H. Fokkens; et al., Zipping up 'the crushed fullerene' C₆₀H₃₀: C-60 by fifteen-fold, consecutive intramolecular H-2 losses, *Chem. Comm.* **2002**, 4, 370-371.
7. L. T. Scott; M. M. Boorum; B. J. McMahon; et. al., A Rational Chemical Synthesis of C₆₀, *Science* **2002**, 295, 1500-1503.
8. K. Y. Amsharov; M. Jansen, C-48 buckybowl and C-60 fullerene precursors on the basis of truxenone, *Z. Naturforsch. B Chem. Sci.* **2007**, 62, 1497-1508.
9. K. Y. Amsharov; K. Simeonov; M. Jansen, Formation of fullerenes by pyrolysis of 1,2'-binaphthyl and 1,3-oligonaphthylene, *Carbon* **2007**, 45, 337-343.
10. K. Y. Amsharov; M. Jansen, A C(78) fullerene precursor: Toward the direct synthesis of higher fullerenes, *J. Org. Chem.* **2008**, 73, 2931-2934.
11. K. Y. Amsharov; M. Jansen, Synthesis of a higher fullerene precursor-an "unrolled" C-84 fullerene, *Chem. Comm.* **2009**, 19, 2691-2693.
12. M. J. Plater, Fullerene tectonics .2. Synthesis and pyrolysis of halogenated benzo[c]phenanthrenes, *J. Chem. Soc. Perkin Trans 1.* **1997**, 19, 2903-2909.
13. M. A. Brooks; L. T. Scott, 1,2-shifts of hydrogen atoms in aryl radicals, *J. Am. Chem. Soc.* **1999**, 121, 5444-5449.
14. A. W. Amick; L. T. Scott, Trisannulated benzene derivatives by acid catalyzed aldol cyclotrimerizations of cyclic ketones. Methodology development and mechanistic insight, *J. Org. Chem.* **2007**, 72, 3412-3418.

15. M. M. Boorum; L. T. Scott, In *Modern Arene Chemistry*; Astruc, D., Ed.; Wiley-VCH: Weinheim, Germany, **2002**, 20-31 and references cited there.
16. T. J. Hill; R. K. Hugher; L. T. Scott, Steps toward the synthesis of a geodesic C₆₀H₁₂ end cap for a C-3v carbon [6,6]nanotube, *Tetrahedron Lett.* **2008**, 64, 11360-11369.
17. B. Gomez-Lor; O. de Frutos; A. M. Echavarren, Synthesis of 'crushed fullerene' C₆₀H₃₀, *Chem. Commun.* **1999**, 23, 2431-2432.
18. A. M. Echavarren; B. Gomez-Lor; J. J. Gonzalez; O. de Frutos, Palladium-catalyzed intramolecular arylation reaction: Mechanism and application for the synthesis of polyarenes, *Synlett* **2003**, 5, 585-597 and references cited there.
19. L.B. Liu; B.W. Yang; T.J. Katz; M.K. Poindexter, Improved methodology for photocyclization reactions *J. Org. Chem.* **1991**, 56, 3769-3775.
20. M. Sarobe; L.W. Jenneskens; U.E. Wiersum, Thermolysis of benzo[c]phenanthrene: Conversion of an alternant C₁₈H₁₂ PAH into non-alternant C₁₈H₁₀ PAHs, *Tetrahedron Lett.* **1996**, 37, 1121-1122.
21. M.J. Plater; Synthesis of benzo[ghi]fluoranthenes from 1-halobenzo[c]phenanthrenes by flash vacuum pyrolysis, *Tetrahedron Lett.* **1994**, 35, 6147-6150.
22. S.J. Blanksby; G.B. Ellison, Bond dissociation energies of organic molecules, *Acc.Chem.Res.* **2003**, 36, 255-263.
23. J.W. Coomber; E. Whittle, Bond dissociation energies from equilibrium studies. Part 3.—D(CF₃—Cl), D(C₂F₅—Cl) and the enthalpy of formation of CF₃Cl, *Trans. Faraday Soc.* **1967**, 63, 2656-2667.
24. D. O'Hagan, Understanding organofluorine chemistry. An introduction to the C-F bond, *Chem. Soc. Rev.* **2008**, 37, 308-319.
25. B. A. Balko; J. Zhang; Y. T. Lee, The 193 nm photodissociation of 1,1- and 1,2- difluoroethylene, *J. Phys. Chem. A* **1997**, 101, 6611-6618.
26. M. J. Berry; G. C. Pimentel, Hydrogen Halide Photoelimination Chemical Lasers, *J. Chem. Phys.* **1969**, 51, 2274.
27. D. J. Donaldson; D. G. Watson; J. J. Sloan, Detailed energy partitioning in the decomposition of chemically energized C₂H₃F, *Chem. Phys.* **1982**, 68, 95-107.
28. J. Gonzalez-Vazquez; A. Fernandez-Ramos; E. Martinez-Nunez; S. A. Vazquez, Dissociation of difluoroethylenes. I. Global potential energy surface, RRKM, and VTST calculations, *J. Phys. Chem. A* **2003**, 107, 1389-1397.

29. J. Gonzalez-Vazquez; E. Martinez-Nunez; A. Fernandez-Ramos; S. A. Vazquez, Dissociation of difluoroethylenes. II. Direct Classical Trajectory Study of the HF elimination from 1,2-difluoroethylene, *J Phys. Chem. A* **2003**, 107, 1398-1404.
30. J. J. Lin; S. M. Wu; D. W. Hwang; Y. T. Lee; X. Yang, Photodissociation dynamics of 1,1-difluoroethylene at 157 nm excitation, *J. Chem. Phys.* **1998**, 109, 10838-10846.
31. J. M. Simmie; E. Tschuiko, Kinetics of the shock-initiated decomposition of 1,1-difluoroethylene, *J. Phys. Chem.* **1970**, 74, 4075.
32. E. Martinez-Nunez; S. A. Vazquez, Ab initio calculations on the vinyl fluoride fragmentation reactions, *Struct. Chem.* **2001**, 12, 95-100.
33. C. Y. Wu; Y. J. Wu; Y. P. Lee, Molecular elimination in photolysis of fluorobenzene at 193 nm: Internal energy of HF determined with time-resolved Fourier-transform spectroscopy, *J. Chem. Phys.* **2004**, 121, 8792-8799.
34. O. de Frutos; B. Gomez-Lor; T. Granier; M.A. Monge; E. Gutierrez-Puebla; A.M. Echavarren, Syn-trialkylated truxenes: Building blocks that self-associate by arene stacking, *Angew. Chem. Int. Ed.* **1999**, 38, 204-207.
35. A. I. Vogel, A Textbook of Practical Organic Chemistry, 3rd ed., Wiley, New York, N. Y., **1956**, 768.
36. E.V. Dehmlow; T. Kelle, Synthesis of new truxene derivatives: Possible precursors of fullerene partial structures?, *Synth. Commun.* **1997**, 27, 2021-2031.
37. A. Mueller; K.Yu. Amsharov; M. Jansen, Synthesis of end-cap precursor molecules for (6,6) armchair and (9,0) zig-zag single-walled carbon nanotubes, *Tetrahedron Lett.* **2010**, 51, 3221-3225.
38. M. M. Boorum; Y. V. Vasil'ev; T. Drewello; L. T. Scott, Groundwork for a rational synthesis of C-60: Cyclodehydrogenation of a C₆₀H₃₀ polyarene. *Science* **2001**, 294, 828-831.
39. D. Alberico; M. E. Scott; M. Lautens, Palladium-Catalyzed Intramolecular Arylation Reaction: Mechanism and Application for the Synthesis of Polyarenes, *Chem. Rev.* **2007**, 107, 174 – 238.
40. S. Pascual; P. de Mendoza; A. M. Echavarren, Palladium catalyzed arylation for the synthesis of polyarenes, *Org. Biomol. Chem.* **2007**, 5, 2727 – 2734.
41. B. D. Steinberg; E. A. Jackson; A. S. Filatov; A. Wakamiya; M. A. Petrukhina; L. T. Scott, Aromatic pi-Systems More Curved Than C-60. The Complete Family of All ndenocorannulenes Synthesized by Iterative Microwave-Assisted Intramolecular Arylations, *J.Am.Chem. Soc.* **2009**, 131, 10537-10545.

42. C. Douvris; O. V. Ozerov, Hydrodefluorination of perfluoroalkyl groups using silylium-carborane catalysts, *Science* **2008**, 321, 1188-1190.
43. O. Allemann; S. Duttwyler; P. Romanato; K.K. Baldrige; J. S. Siegel, Proton-Catalyzed, Silane-Fueled Friedel-Crafts Coupling of Fluoroarenes, *Science* **2011**, 332, 574-577.

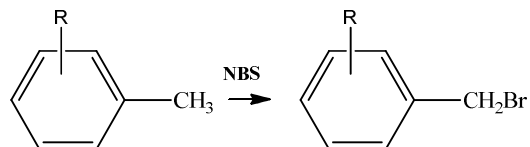
3. Experimental Part

3.1. Measurements

LDI-Mass spectra were recorded with a Shimadzu AXIMA resonance spectrometer. ^1H - (300 MHz) and ^{13}C -NMR (75.5 MHz) spectra were measured on Bruker ARX-300 instrument, δ were determined in ppm relative to TMS (0.00 ppm). All NMR spectra were measured at 20 °C (if not otherwise indicated). X-ray experimental intensity data of the single crystals were collected with a Smart APEX I diffractometer (Bruker AXS, Karlsruhe, Germany, Mo- K_α radiation, $\lambda = 0.71073 \text{ \AA}$) and a dual wavelength three circle single crystal diffractometer - Smart APEX II (Bruker AXS, Karlsruhe, Germany) equipped with a CCD-detector, a Siemens X-ray sealed tube (Mo- K_α radiation, $\lambda = 0.71073 \text{ \AA}$), an Incoatec (Geesthacht, Germany) microfocus X-ray source ImS (Cu- K_α radiation, $\lambda = 1.54178 \text{ \AA}$). The X-ray beam of the copper-source was generated with Incoatec IG150 and monochromatized by using a Montel optic monochromator (Incoatec, Geesthacht, Germany). The collection and reduction of data were carried out with the Bruker Suite software package.^[1] Intensities were corrected for absorption effects applying a semi-empirical method.^[2] The structures were solved by direct methods and refined by full-matrix least-squares fitting with the SHELXTL software package.^[3] HPLC analyses were carried out using a Shimadzu HPLC system (CBM-20A), equipped with an UV-Vis DAD (SPD-M20A) detector. Cosmosil Buckyprep (4.6 mm x 250 mm) and Cosmosil 5-PYE (4.6 mm x 250 mm) columns were used for analysis (flow rate 1 mL/min). Flash chromatographic purifications were carried out using flash grade silica gel Kieselgel 60 (0.06-0.2 mm). R_f values were determined on TLC-PET sheets coated with silica gel with fluorescent indicator 254 nm (layer thickness 0.25 mm, medium pore diameter 60 \AA), Fluka. Elemental analyses were performed with an Elementar VARIO EL elemental analyser. Quantum chemical calculations were performed by the DFT method with B3LYP/6-31G using the Gaussian03 software package. The commercially available reagents were used as received without further purification (if not otherwise stated).

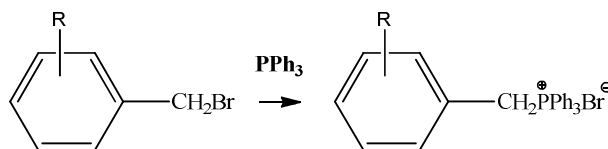
3.2. General procedures

3.2.1. Synthesis of bromomethylarenes



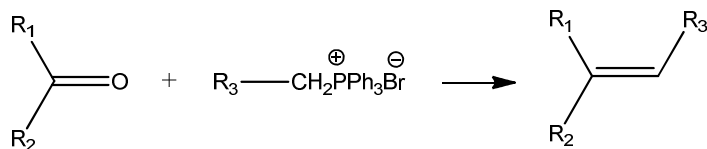
100 mmol of the respective methylarene was dissolved in 150-200 mL of CCl₄. 100 mmol of N-bromosuccinimide (NBS) with catalytic amounts (5-10 mg) of dibenzoylperoxide (DBPO) were added and the mixture was refluxed until completion as monitored by TLC (2 - 6 h). The reaction mixture was then allowed to cool, filtered and evaporated. The crude product was purified chromatographically on silica gel.

3.2.2. Synthesis of phosphonium salts



The respective bromomethylarene (100 mmol) and triphenylphosphine (110 mmol) were dissolved in 100-200 mL of toluene, and mixture was reflux with vigorous stirring for 12 h. During this time a white crystalline solid precipitated from solution. The reaction mixture was cooled to room temperature and then filtered. The solid was washed with toluene and hexane to give a total of 85 - 95 % yield of the phosphonium salt as a white powder. The resulting salt was used in a next step without additional purification.

3.2.3. Synthesis of diarylethenes



Method 1:

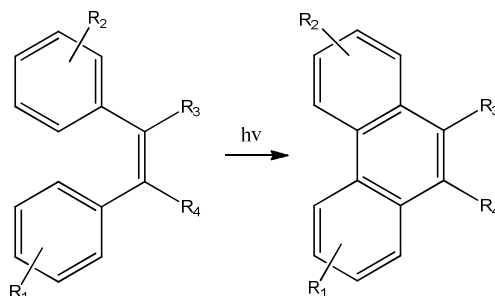
The whole procedure was carried out under argon atmosphere. Respective phosphonium salt (30 mmol) and aldehyde (or ketone) (30 mmol) were dissolved in 100 mL of absolute ethanol. The mixture was stirred while *t*-BuOK (34 mmol) in ethanol was added dropwise for 5-10 min. The solution obtained was refluxed for 10-20 h (TCL monitoring). The reaction mixture was cooled to room temperature and neutralized by addition of 1M HCl. After concentration by evaporation under reduced pressure, the mixture was diluted with water and the product was extracted with DCM. The DCM solution was dried over MgSO₄ and filtered through a short silica gel plug using a DCM:PE mixture as the eluent. After evaporation the diarylethene was obtained as a white solid with yield of 65 - 80 % (mixture of *cis/trans* isomers). The resulting diarylethene was used in the next step without additional purification.

Method 2:

The whole procedure was carried out in a round-bottomed flask under argon atmosphere. The phosphonium salt (34 mmol) was dissolved in anhydrous THF (100 mL). The mixture was cooled to -78 °C and stirred while *n*-butyllithium (38 mmol) 1.6M solution in hexane was added dropwise over 10–20 min. The orange-red solution obtained was allowed to warm to room temperature and stirred for an additional 45 min. At this point, aldehyde or ketone (34.1 mmol) was added as a solution in anhydrous THF. After stirring for 12 h the reaction mixture turned light-yellow. THF was removed by evaporation and the resulting material was passed

through a short silica gel plug using DCM as the eluent. A white solid of the title compound as a mixture of cis/trans isomers was obtained in a yield of 65–80 %. The resulting stilbene was used in the next step without additional purification.

3.2.4. Photocyclization



The corresponding benzo-stilbene (10 mmol) as a cis/trans mixture was dissolved in cyclohexane (350 mL). The resulting solution was placed in a 500 W water-cooled quartz photochemical reactor and iodine (11 mmol) was then added. Argon was bubbled through the stirred solution for 15–20 min before an excess of propylene oxide (10 mL) was added. After irradiation for 10–30 h the colour of iodine had disappeared. The mixture was washed with aqueous Na₂S₂O₃ to remove residual traces of iodine, concentrated in vacuo and then purified by flash chromatography on silica gel. A mixture of light petroleum and dichloromethane (1:1) was used as eluent. The targeted compound was obtained with 60–95 % yield as a white solid.

3.2.5. Flash vacuum pyrolysis (FVP)

Pyrolysis experiments were carried out at typically 800–1100 °C in an improved FVP furnace that allowed simultaneous control of the pressure and the flow of the carrier gas in the system. A movable oven made it possible to regulate the sublimation temperature and tune the sublimation speed during the FVP experiments. A special construction of the injector decreases the probability of

contact between sample molecules and the walls of the heated quartz tube. Nitrogen flow and pressure in the system can be tuned independently by flow and pressure regulators (EV 016 DOS AB, Oerlikon Leybold Vacuum). The product trap is cooled by water. The second trap (cooled by liquid nitrogen) is used to protect the vacuum pump. (Figure 3.1).

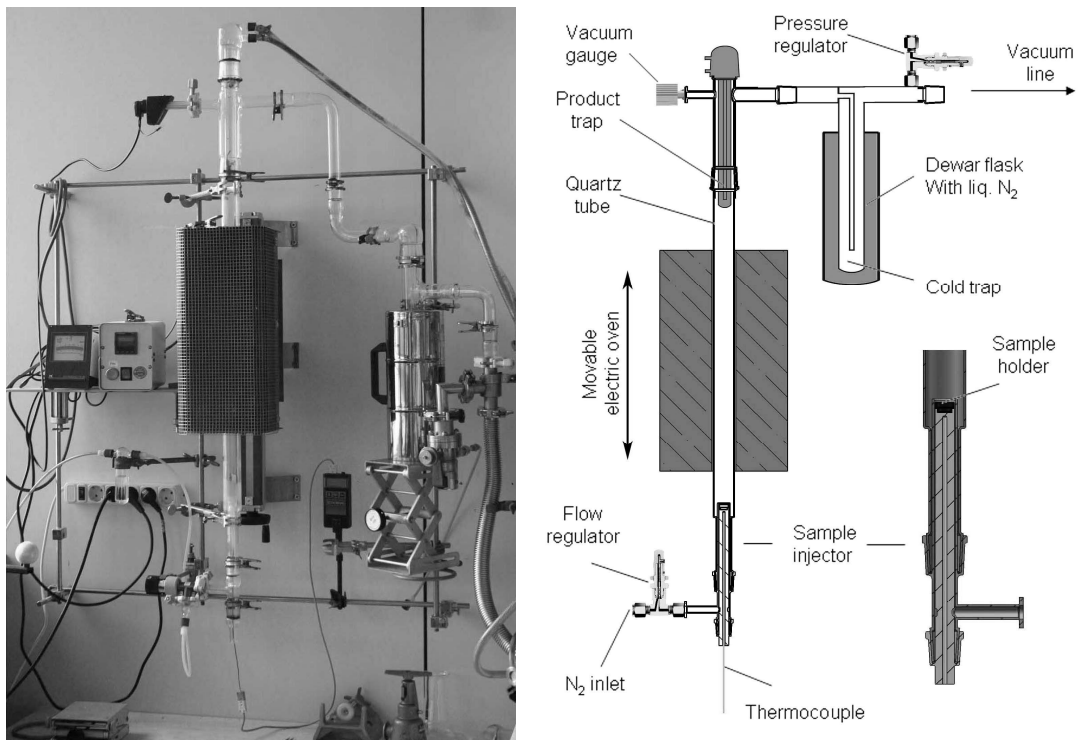
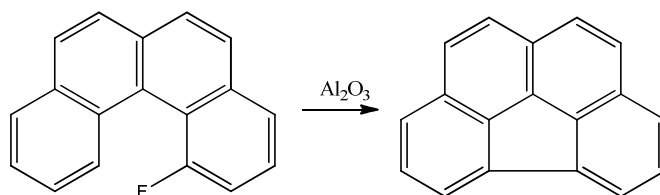


Figure 3.1. FVP apparatus (left), schematic representation (right).

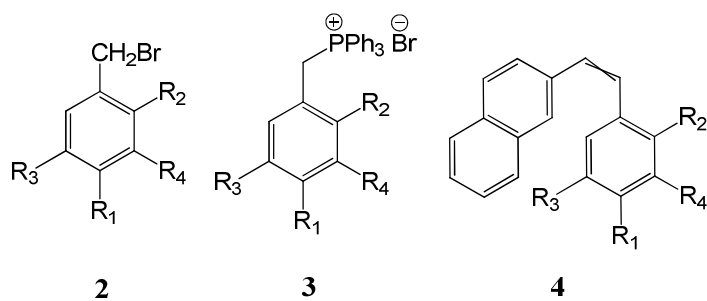
3.2.6. Cove-Region-Closure via Al₂O₃ mediated HF Elimination



Commercially available aluminium oxide (activated, neutral, 50-200 micron, Acros) has been used for HF elimination procedure. Typically 2-3 g of Al_2O_3 were placed in glass ampule and activated by annealing at 500 °C for 10-15 min in vacuum (10^{-3} mbar). 20-50 mg of the respective fluoroarene were carefully mixed with activated aluminium oxide under argon atmosphere. The ampule was evacuated (10^{-3} mbar) and sealed. The condensation was carried out typically at 150-200 °C for 2-10 h. The product was obtained after extraction with toluene (xylene) and evaporation.

3.3. Synthesis

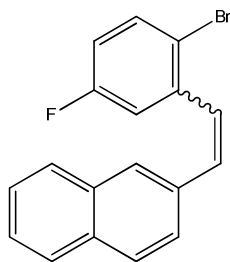
Compounds **2** - **4** (Figure 3.2) were synthesized using the general techniques **3.2.1** - **3.2.3**.



Compounds	R ¹	R ²	R ³	R ⁴
2a, 3a, 4a	Cl	H	H	H
2b, 3b, 4b	CH ₃	H	H	H
2c, 3c, 4c	CF ₃	H	H	H
2d, 3d, 4d	H	H	H	H
2e, 3e, 4e	Ph	H	H	H
2f, 3f, 4ff	F	H	H	H
2g, 3g, 4g	H	Br	F	H
2h, 3h, 4h	H	H	F	H
2i, 3i	F	F	F	F

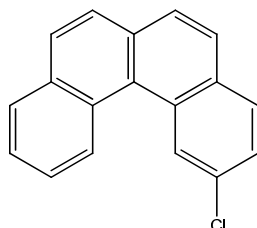
Figure 3.2. Benzo[*c*]phenanthrenes **2-4**.

(E/Z)-2-[2-(2-Bromo-5-fluorophenyl)ethenyl]-naphthalene (4g)



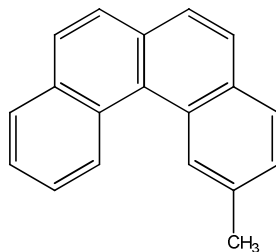
Compound **4g** was synthesized using the general procedure **3.2.4** 2-Bromo-5-fluorobenzylphosphonium bromide (9.4 g, 17.7 mmol), tBuOK (1.99 g, 17.7 mmol) and 2-naphthaldehyde (2.77 g, 17.7 mmol) were dissolved in ethanol (200 mL). The mixture was reflux overnight. White solid (4 g, 70 %).

2-Chlorobenzo[c]phenanthrene (5a)



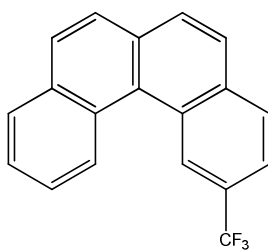
Compound **5a** was synthesized from compound **4a** according the general procedure **3.2.4**. White solid (yield 70 %). $R_f = 0.38$ (hexane). M.p. 61.4-61.8 °C. $^1\text{H-NMR}$ (CDCl_3 , 300 MHz) $\delta = 7.48$ (dd, $J_1 = 8.57$, $J_2 = 2.01$, 1H), 7.52 - 7.68 (m, 2H), 7.69 - 7.88 (m, 5H), 7.93 (dd, $J_1 = 7.87$, $J_2 = 1.36$, 1H), 8.96 (d, $J_1 = 8.43$, 1H), 9.03 (d, $J_2 = 1.82$, 1H). $^{13}\text{C-NMR}$ (CDCl_3 , 75 MHz) $\delta = 126.12$, 126.41, 126.64, 126.67, 126.94, 127.05, 127.18, 127.36, 128.14, 128.69, 129.91, 130.11, 131.15, 131.48, 131.73, 132.35, 133.52. LDI-TOF MS: $m/z = 262.06$ [$\text{M}]^+$ (Exact Mass: 262.0549). Anal. Calcd. for $\text{C}_{18}\text{H}_{11}\text{Cl}$: C, 82.29; H, 4.22; Found: C, 81.9; H, 4.2.

2-Methylbenzo[*c*]phenanthrene (5b)



Compound **5b** was synthesized from compound **4b** according to the general procedure **3.2.4**. White solid (yield 57 %). $R_f = 0.31$ (hexane). M.p. 75.8-76.2 °C. $^1\text{H-NMR}$ (CDCl_3 , 300 MHz) $\delta = 2.57$ (s, 3H), 7.34 (d, $J = 8.13$, 1H), 7.48 - 7.86 (m, 7H), 7.93 (dd, $J_1 = 6.5$, $J_2 = 1.42$, 1H), 8.86 (s, 1H), 9.01 (d, $J = 10.6$, 1H). $^{13}\text{C-NMR}$ (CDCl_3 , 75 MHz) $\delta = 22.24$, 125.65, 125.90, 125.97, 126.88, 126.95, 127.23, 127.26, 127.39, 127.65, 127.82, 128.37, 128.5, 130.42, 130.49, 131.14, 131.58, 133.45, 135.83. LDI-TOF MS: $m/z = 242.11$ $[\text{M}]^+$ (Exact Mass: 242.1096). Anal. Calcd. for $\text{C}_{19}\text{H}_{14}$: C, 94.18; H, 5.82; Found: C, 94.1; H, 5.9.

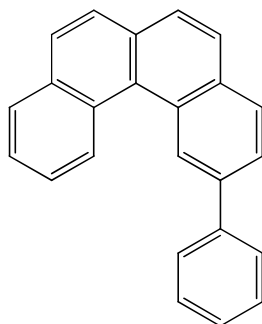
2-Trifluoromethylbenzo[*c*]phenanthrene (5c)



Compound **5c** was synthesized from compound **4c** according to the general procedure **3.2.4**. White solid (yield 73 %). $R_f = 0.40$ (hexane). M.p. 109.6-110.0 °C. $^1\text{H-NMR}$ (CDCl_3 , 300 MHz) $\delta = 7.55 - 7.75$ (m, 4H), 7.82 - 7.9 (m, 3H), 8 - 8.08 (m, 2H), 8.92 (d, $J = 8.48$, 1H), 9.33 (s, 1H). $^{13}\text{C-NMR}$ (CDCl_3 , 75 MHz) $\delta = 121.66$ (q, $J = 3.38$), 125.38 (q, $J = 4.5$), 126.41, 126.60, 126.84, 126.88, 127.42, 128.39, 128.79, 129.11, 129.33,

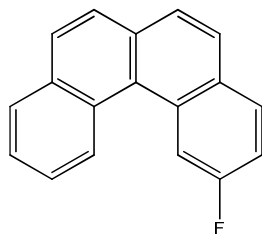
129.48, 129.94, 131.46, 133.7. LDI-TOF MS: $m/z = 296.10$ $[M]^+$ (Exact Mass: 296.0813). Anal. Calcd. for $C_{19}H_{11}F_3$: C, 77.02; H, 3.74; Found: C, 76.1; H, 4.0.

2-Phenylbenzo[c]phenanthrene (5e)



Compound **5e** was synthesized from compound **4e** according to the general procedure **3.2.4**. White solid (yield 55 %). $R_f = 0.18$ (hexane). M.p. 131.5-131.9 °C. 1H - and ^{13}C -NMR spectra are in a good agreement with the data reported previously.^[24] LDI-TOF MS: $m/z = 304.13$ $[M]^+$ (Exact Mass: 304.1252). Anal. Calcd. for $C_{24}H_{16}$: C, 94.70; H, 5.30; Found: C, 94.5; H, 5.2.

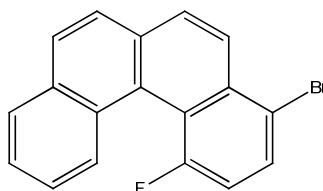
2-Fluorobenzo[c]phenanthrene (5f)



Compound **5f** was synthesized from compound **4f** according to the general procedure **3.2.4**. White solid (yield 66 %). $R_f = 0.33$ (hexane). M.p. 63.7-64.1 °C. 1H -NMR ($CDCl_3$, 300 MHz) $\delta = 7.31$ (td, $J_1 = 2.42$, $J_2 = 8.32$, 1H), 7.49 - 8.09 (m, 8H), 8.73 (dd, $J_1 = 2.1$, $J_2 = 12.37$, 1H), 8.99 (d, $J = 8.34$, 1H). ^{13}C -NMR ($CDCl_3$, 75 MHz) $\delta = 112.46$ (d, $J = 23.4$), 115.16 (d, $J = 24.23$), 126.01, 126.19 (d, $J = 2.42$), 126.51, 126.66, 126.72,

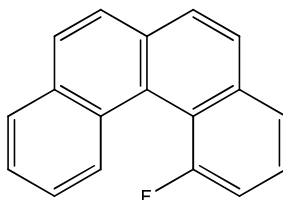
126.77, 127.08 (d, $J = 1.06$), 127.11, 128.09, 128.70, 130.29, 130.6 (d, $J = 9.13$), 131.37 (d, $J = 8.83$), 131.53, 133.4, 161.45 (d, $J = 244.15$). LDI-TOF MS: $m/z = 246.04$ $[M]^+$ (Exact Mass: 246.0845). Anal. Calcd. for $C_{18}H_{11}F$: C, 87.78; H, 4.50; Found: C, 86.1; H, 4.5.

4-Bromo-1-fluorobenzo[*c*]phenanthrene (5g)



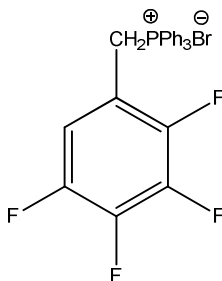
Compound **5g** was synthesized from compound **4g** according the general procedure **3.2.4**. White solid (yield 50 %). $R_f = 0.34$ (hexane). $^1\text{H-NMR}$ (CDCl_3 , 300 MHz) $\delta = 7.12 - 7.21$ (m, 1H), 7.49 - 7.59 (m, 2H), 7.69 - 7.77 (m, 1H), 7.78 - 7.86 (m, 2H), 7.87 - 7.95 (m, 2H), 8.08 - 8.28 (m, 2H). $^{13}\text{C-NMR}$ (CDCl_3 , 75 MHz) $\delta = 112.87$ (d, $J = 25.74$), 117.42 (d, $J = 3.47$), 120.3 (d, $J = 13.67$), 124.44 (d, $J = 3.25$), 125.17 (d, $J = 2.94$), 125.56, 125.93 (d, $J = 2.19$), 126.29, 127.47, 129.09, 129.22, 129.57 (d, $J = 16.9$), 129.83 (d, $J = 3.4$), 130.21 (d, $J = 8.99$), 131.82, 132.93, 133.35 (d, $J = 4.45$), 158.85 (d, $J = 254.41$). Crystal Data: monoclinic; space group $P 2_1/c$; $a = 7.2750(8)$, $b = 11.6037(12)$, $c = 15.4111(16)$ Å; $\beta = 91.147(2)$, $V = 1300.7(2)$ Å³, $Z = 4$; $2\theta_{\text{max}} = 54.26^\circ$; $-9 < h < 9$, $-14 < k < 14$, $-19 < l < 19$; $\lambda = 0.71073$ Å; $T = 137(2)$ K; final R value 0.0369 ($R_w = 0.1030$). CCDC-743279.

1-Fluorobenzo[*c*]phenanthrene (5h)



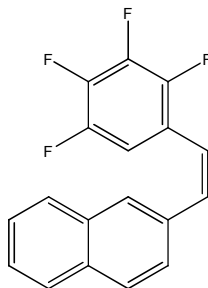
Compound **5h** was synthesized from compound **5g**. 1 g, (3.1 mmol) of 4-bromo-1-fluorobenzo[c]phenanthrene were dissolved in 50 mL of anhydrous THF. All procedures were carried out under argon atmosphere. The mixture was cooled to –78 °C and stirred while *n*-butyllithium (3.1 mmol) was added dropwise. The reaction was quenched after 3 min by addition of 3 mL of cooled acetic acid. The reaction mixture was heated to room temperature. Afterwards H₂O was added to the reaction mixture and the product was extracted with DCM, dried over Na₂SO₄ and evaporated. The compound was purified chromatographically (silica gel, PE). White solid (yield 66 %). R_f = 0.25 (hexane). M.p. 85.0-85.4 °C. ¹H-NMR (CDCl₃, 300 MHz) δ = 7.31 (td, *J*₁ = 2.42, *J*₂ = 8.32, 1H), 7.49 - 8.09 (m, 8H), 8.73 (dd, *J*₁ = 2.1, *J*₂ = 12.37, 1H), 8.99 (d, *J* = 8.34, 1H). ¹³C-NMR (CDCl₃, 75 MHz): δ 112.46 (d, *J* = 23.4), 115.16 (d, *J* = 24.23), 126.01, 126.19 (d, *J* = 2.42), 126.51, 126.66, 126.72, 126.77, 127.08 (d, *J* = 1.06), 127.11, 128.09, 128.70, 130.29, 130.6 (d, *J* = 9.13), 131.37 (d, *J* = 8.83), 131.53, 133.4, 161.45 (d, *J* = 244.15). LDI-TOF MS: *m/z* = 246.06 [M]⁺ (Exact Mass: 246.0845). Anal. Calcd. for C₁₈H₁₁F: C, 87.78; H, 4.50; Found: C, 87.3; H, 4.4.

2,3,4,5-Tetrafluorobenzyltriphenylphosphonium bromide (**3i**)



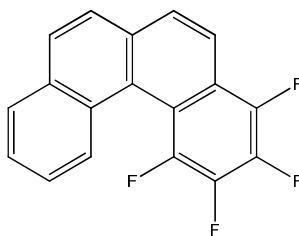
The compound **3i** was obtained according the general procedure **3.2.1**. 10.0 g (41.2 mmol) of 2,3,4,5-tetrafluorobenzylbromide and 11.8 g (45.0 mmol) triphenylphosphine were dissolved in 50 mL of toluene. The product was obtained as a white powder, 20.8 g (97 %). The resulting phosphonium salt was used in the next step without additional purification.

***cis*-2-[2-(2,3,4,5-Tetrafluorophenyl)ethenyl]-naphthalene (25)**



Compound **25** was obtained according the general procedure **3.2.3.** using 9.78 g (19.4 mmol) of 2,3,4,5-tetrafluorobenzyltriphenylphosphonium bromide, 2.17 g (19.4 mmol) of KOtBu and 3.03 g (19.4 mmol) of 2-naphthaldehyde and 300 mL of absolute ethanol. 5.1 g (87 %) (mixture of *cis/trans* isomers). R_f *cis* (hexane) = 0.20, R_f *trans* (hexane) = 0.23. The pure *cis* isomer (2.3 g, 39 %) was obtained after grinding under hexane and filtration. White solid. $^1\text{H-NMR}$ (CDCl_3 , 300 MHz) δ = 7.09 - 7.22 (m, 3H), 7.38 - 7.44 (m, 2H), 7.6 - 7.69 (m, 1H), 7.71 - 7.88 (m, 4H). $^{13}\text{C-NMR}$ (CDCl_3 , 75 MHz): δ = 118.23, 123.2, 26.53, 126.6, 127.67, 127.74, 128.18, 128.61, 133.06 (d, J = 4.5), 133.51 (d, J = 2.9), 133.62.

1,2,3,4-Tetrafluorobenzo[*c*]phenanthrene (26)



Compound **26** was obtained according the general procedure **3.2.4.** 1 g (3.3 mmol) of **25** (*cis* isomer) were dissolved in 400 mL of cyclohexane, 0.94 g of iodine (3.7 mmol) and propylene oxide (4.8 mL) were added. The product was obtained with 43 % yield (0.44 g). White solid. R_f (hexane) = 0.24. m.p. 153.1-153.2 °C. $^1\text{H-NMR}$

(CDCl₃, 300 MHz) d = 7.58 (dd, J₁ = 3.34, J₂ = 5.9, 2H), 7.75 (d, J = 8.6, 1H), 7.82 (d, J = 8.8, 1H), 7.78 - 7.98 (m, 2H), 7.99 - 8.05 (m, 1H), 8.06 - 8.19 (m, 1H). ¹³C-NMR (CDCl₃, 75 MHz): d = 125.20, 125.56, 125.76, 126.68, 127.58, 127.6, 128.51, 128.86, 129.09, 129.55 (Figure 3.3). LDI-TOF MS: m/z = 300.06 [M]⁺ (Exact Mass: 300.0562). UV spectrum see in Figure 3.4.

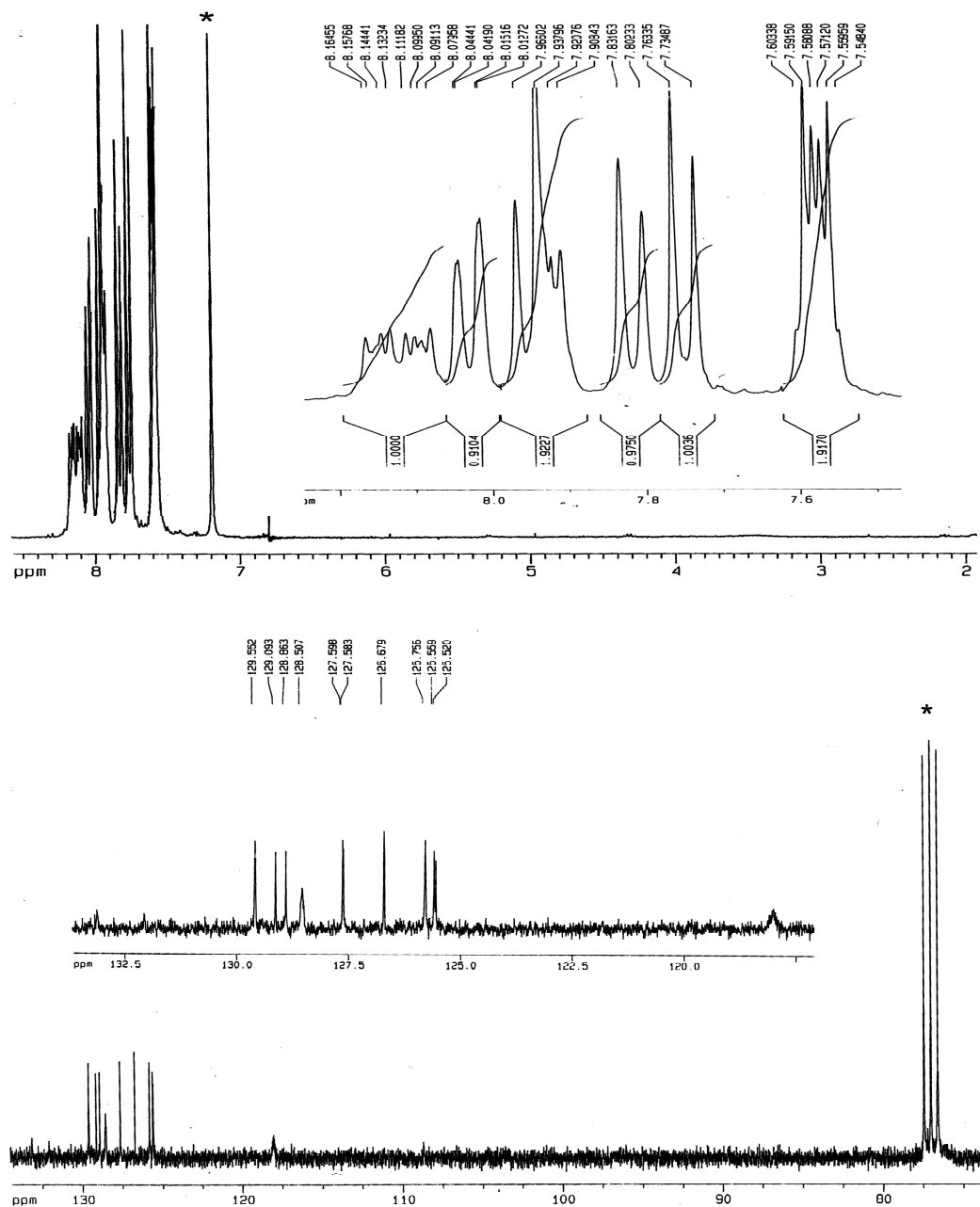


Figure 3.3. ¹H- and ¹³C-spectra of 1,2,3,4-tetrafluorobenzo[c]phenanthrene (**26**).

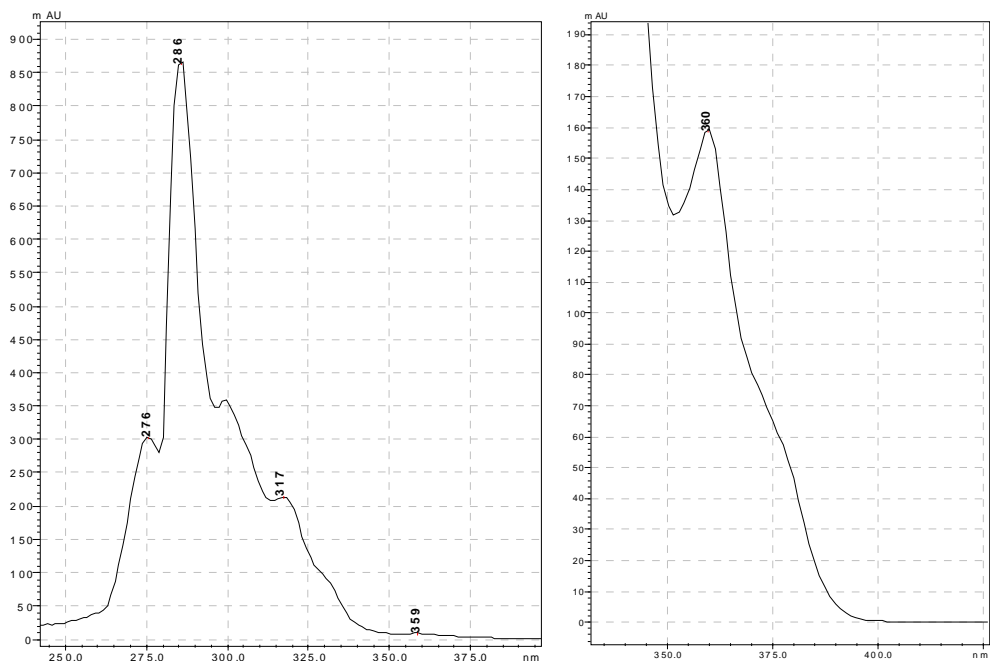
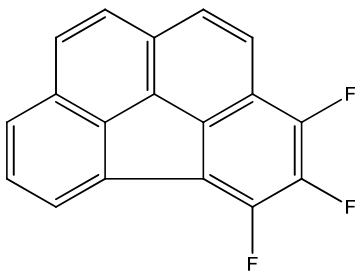


Figure 3.4. UV- spectra of 1,2,3,4-tetrafluorobenzo[c]phenanthrene (**26**).

3,4,5-Trifluorobenzo[ghi]fluoranthene (**27**)



Compound **27** was obtained according the general procedure **3.2.5**. 50 mg of **26** was subjected to FVP at 1100 °C ($p = 0.2$ bar). The target compound was obtained with 60% yield according to HPLC data (yield is given as a molar concentration in pyrolyzate). Small amounts of **27** were separated for analytical purpose by means of HPLC (Buckyprep, Toluene:Methanol 1:1). Yellow needle. $^1\text{H-NMR}$ (CD_2Cl_2 , 300 MHz) $\delta = 7.7$ (dd, $J_1 = 7.1$, $J_2 = 8.1$, 1H), 7.87 - 8.02 (m, 5H), 8.12 (d, $J = 7.0$, 1H). $^{13}\text{C-NMR}$ (CD_2Cl_2 , 75 MHz): $\delta = 120.28$, 125.26, 125.49, 125.67, 126.98, 127.65, 128.12,

129.12, 132.72 (Figure 3.5). ^{19}F -NMR (CD_2Cl_2 , 35 MHz) $d = -160.74$ (dd, $J_1 = 12.6$, $J_2 = 17.0$), -139.12 (dd, $J_1 = 12.6$, $J_2 = 9.2$), -126.85 (dd, $J_1 = 9.2$, $J_2 = 17.0$) (Figure 3.6). LDI-TOF MS: $m/z = 280.05$ $[\text{M}]^+$ (Exact Mass: 280.0500). UV spectrum see in Figure 3.7

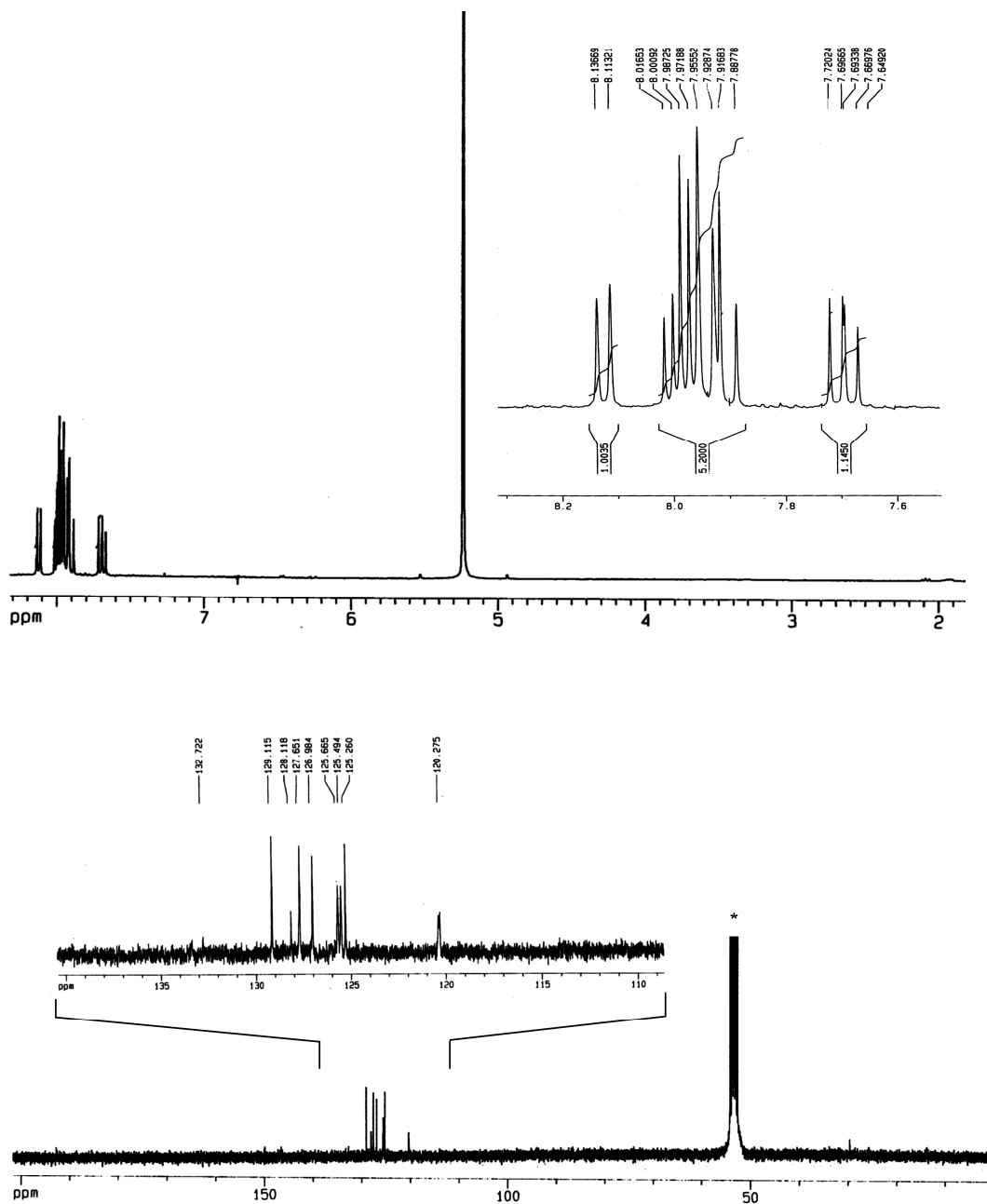


Figure 3.5. ^1H - and ^{13}C -NMR spectra (CDCl_2) of 3,4,5-trifluorobenzo[ghi]fluoranthene (**27**).

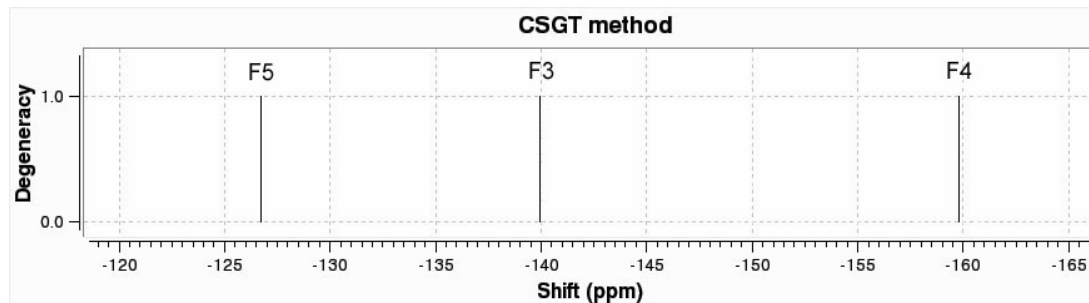
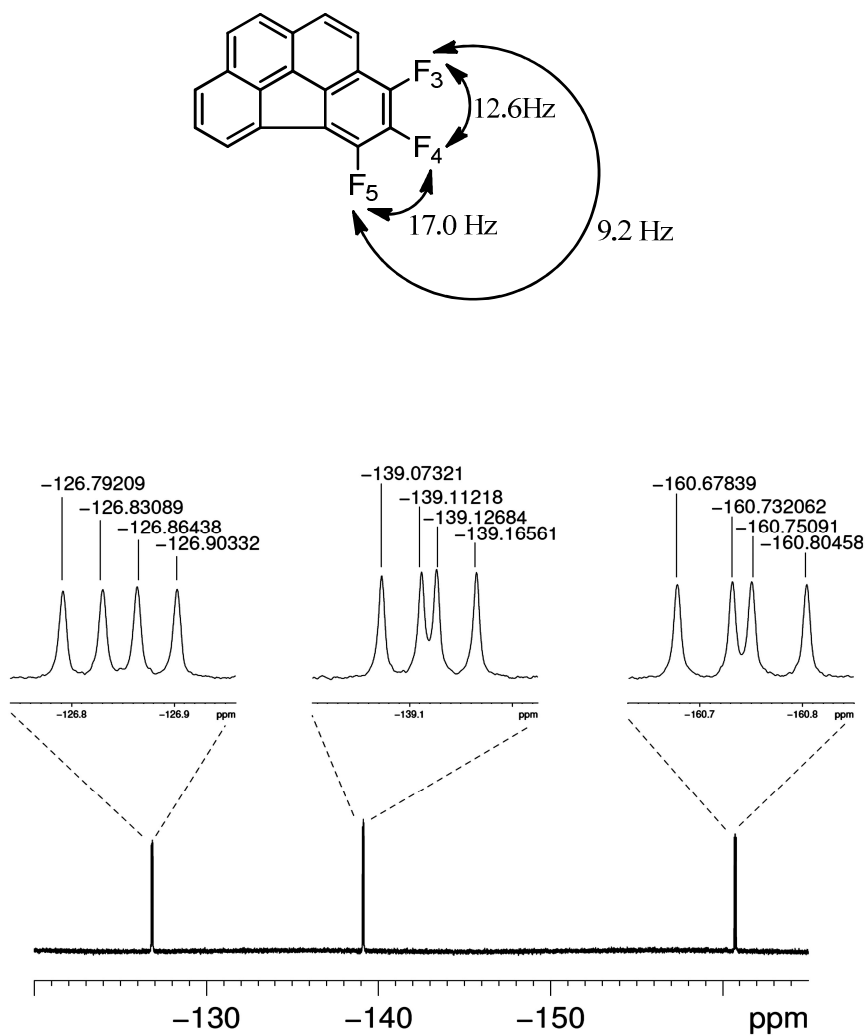


Figure 3.6. ¹⁹F-NMR experimental (CD₂Cl₂) and predicted (DFT B3LYP 6-311G(d,p) CSGT) spectra of 3,4,5-trifluorobenzo[ghi]fluoranthene (**27**) and F-F coupling constants.

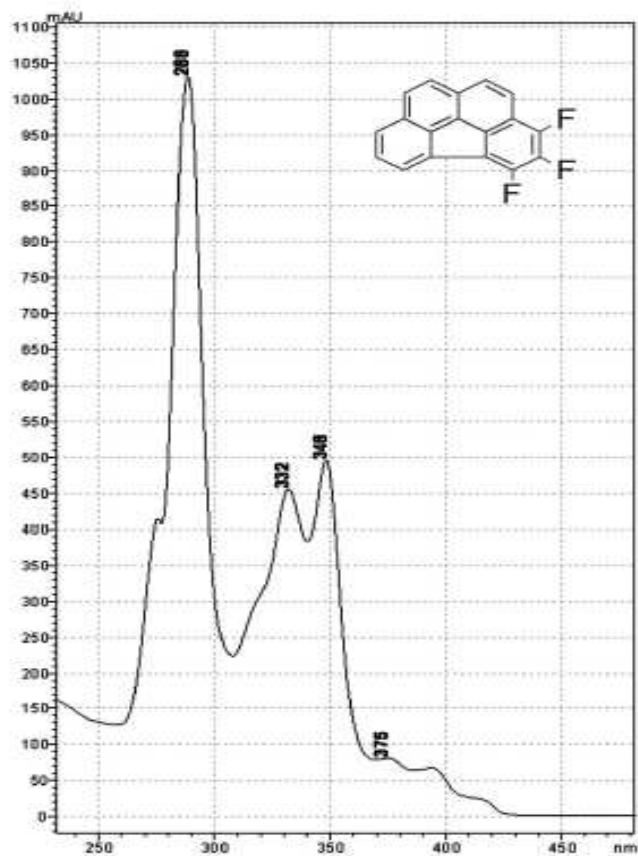
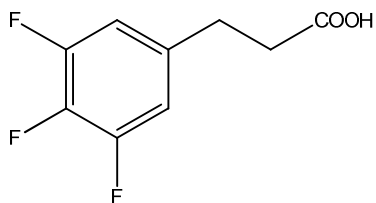


Figure 3.7. UV-spectra of 1,2,3,4-tetrafluorobenzo[c]phenanthrene (**27**).

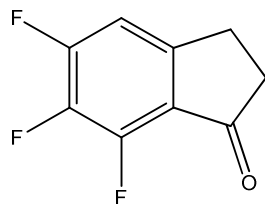
3-(3,4,5-Trifluoro)propionic acid (**30**)



1.0 g (44 mmol) of metallic sodium was dissolved in 50 mL of absolute ethanol. 7.13 g (45 mmol) of diethylmalonate were added to the stirred solution of sodium

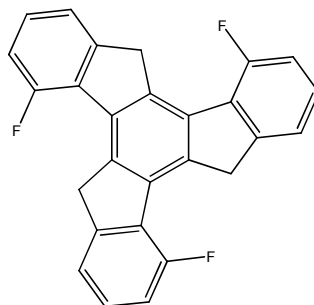
ethoxide obtained. After gradual addition of 10.0 g (44.4 mmol) of trifluorobenzylbromide the mixture was reflux for 2 h and cooled down. The sodium bromide was filtered out and the major part of ethanol was removed in vacuo. The residue was distilled under reduced pressure. The colorless oil obtained was mixed with aqueous KOH (5 g KOH in 10 mL H₂O) and reflux for 3 h. Afterwards the ethanol formed was removed under diminished pressure, 5 mL of H₂O and 25 mL of 5M H₂SO₄ were added additionally and the resulting mixture was refluxed for 5 h. After cooling the mixture was diluted with 50 mL of water, three times extracted with Et₂O, dried over MgSO₄ and evaporated. The yellowish oil had crystallized during cooling. The product was filtered, washed with hexane and dried. White crystalline powder (3.1 g, 32 % yield). ¹H-NMR (CDCl₃, 300 MHz) δ = 2.5-2.6 (m, 2H), 2.8-2.9 (m, 2H), 6.7-6.8 (m, 2H). R_f = 0.29 (DCM).

5,6,7-Trifluoro-1-indanone (31c)



2.8 g (12.8 mmol) of **30** and 25 mL of polyphosphoric acid were stirred for 24 h at 80 °C. After cooling down the mixture was diluted with 50 mL of water and extracted with DCM. The extract was dried over MgSO₄ and evaporated. The crude product was purified chromatographically using DCM as an eluent. White solid 1.0 g (40 % yield). R_f = 0.40 (DCM). ¹H-NMR (CDCl₃, 300 MHz) δ = 2.68 (t, *J* = 6.1, 2H), 3.05 (t, *J* = 5.7, 2H), 7.00 (t, *J* = 6.8, 1H). ¹³C-NMR (CDCl₃, 75 MHz) δ = 25.76, 37.11, 110.08 (dd, *J*₁ = 4.5, *J*₂ = 18.1). LDI-TOF MS: *m/z* = 186.03 [M]⁺ (Exact mass: 186.0292).

6,11,16-Trifluorotruxene (32a)



4.5 g (30 mmol) of commercially available 7-fluoro-1-indanone (**31a**) were added to a mixture of 20 mL of acetic acid and 10 mL of concentrated (34 %) HCl and stirred for 36 h at 100 ° C. After cooling down the mixture was poured into ice. The solid was filtered, washed with water, acetone, and DCM to give a white powder. White solid (1.1 g, 27% yield). $^1\text{H-NMR}$ ($\text{C}_2\text{Cl}_4\text{D}_2$, 300 MHz) δ = 4.37 (s, 6H), 7.03 (t, J = 10.6, 3H), 7.17-7.3 (m, 3H), 7.3-7.45 (m, 3H) (Figure 3.8). $^{19}\text{F-NMR}$ ($\text{C}_2\text{Cl}_4\text{D}_2$, 235 MHz) δ = -112.5 (sex, J = 6.01) (Figure 3.9). LDI-TOF MS: m/z 395.04 [M-H] $^-$ (Exactmass: 395.1048).

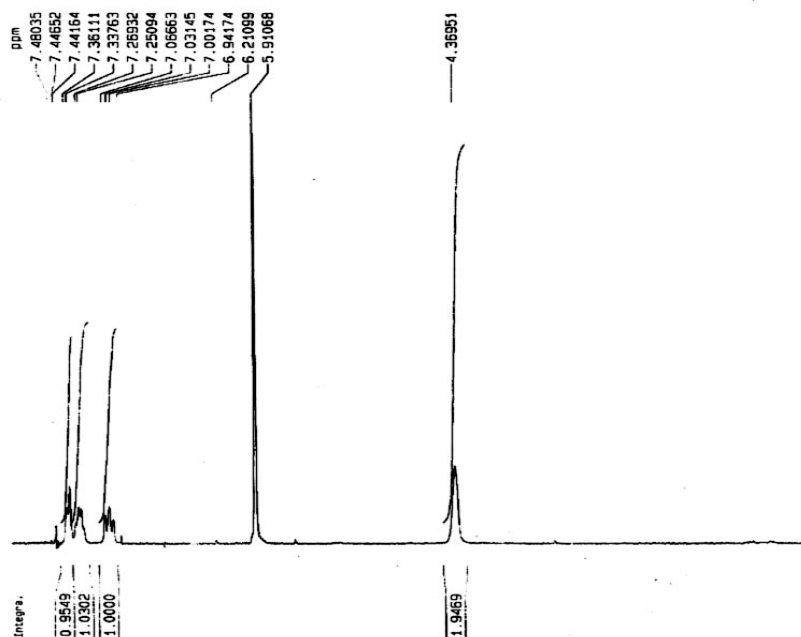


Figure 3.8. $^1\text{H-NMR}$ of 6,11,16-trifluorotruxene (**32a**) (300 MHz, $\text{C}_2\text{Cl}_4\text{D}_2$).

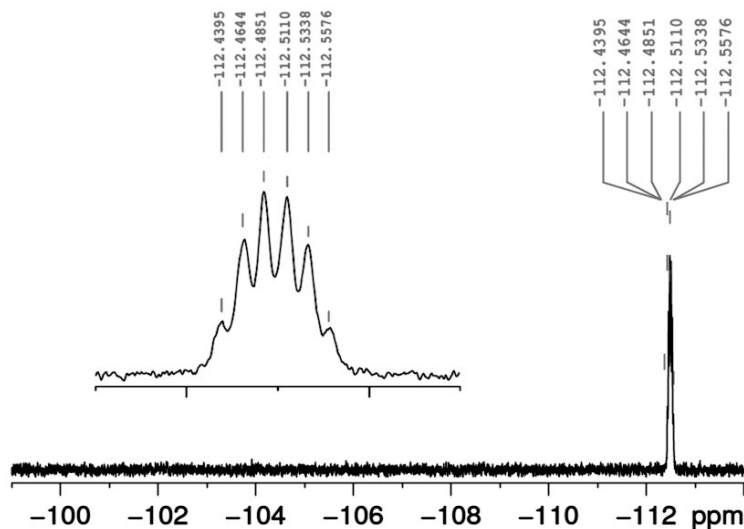
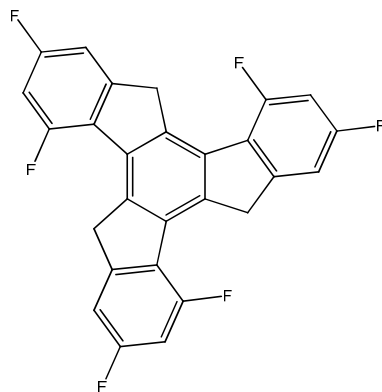


Figure 3.9. ^{19}F -NMR of 6,11,16-trifluorotruxene (**32a**) (235 MHz, $\text{C}_2\text{Cl}_4\text{D}_2$, $120\text{ }^\circ\text{C}$).

6,8,11,13,16,18-Hexafluorotruxene (**32b**)



Method 1:

A mixture of 5,7-difluoro-1-indanone (1 g, 5.95 mmol), *p*-toluenesulfonic acid monohydrate (3.45 g, 20.8 mmol), propionic acid (1.54 mL, 20.55 mmol) and *o*-dichlorobenzene (5 mL) was transferred in round-bottom flask. The mixture was heated at $110\text{ }^\circ\text{C}$ for 16 h. After cooling down the mixture was poured into 50 mL of methanol containing aqueous KOH. The precipitate was filtrated, washed with

methanol, H₂O, acetone, DCM and petroleum ether resulting in a greenish powder (0.52 g). Recrystallization from boiling *o*-xylene gave a product as a white powder (0.28 g, 31 % yield).

Method 2:

200 mg of 5,7-trifluoro-1-indanone, 6 mL of *o*-dichlorobenzene and 0.72 mL of TiCl₄ (6 molar equivalents) were transferred in a glass ampoule. The ampoule was evacuated and sealed by melting while the reaction mixture was frozen by liquid nitrogen to prevent the solvent from evaporation. The ampoule was heated at 180 °C for 20 h. After cooling down the ampoule was opened and the mixture was poured into 50 mL of acetone. The precipitate was filtrated, washed with acetone, DCM and petroleum ether. Pink crystals (92 mg, 52 % yield). ¹H-NMR (C₂Cl₄D₂, 250 MHz, 120 °C) δ = 4.38 (d, *J* = 5.75, 6H), 6.81 (t, *J* = 10.25, 3H), 7.10 (d, *J* = 7.25, 3H) (Figure 3.10). ¹⁹F-NMR (C₂Cl₄D₂, 235 MHz, 120 °C) δ = -112.04 (q, *J* = 7.29), δ = -109.2 (sex, *J* = 5.88) (Figure 3.11). LDI-TOF MS: *m/z* = 449.07 [M-H]⁻ (Exact mass: 449.0765).

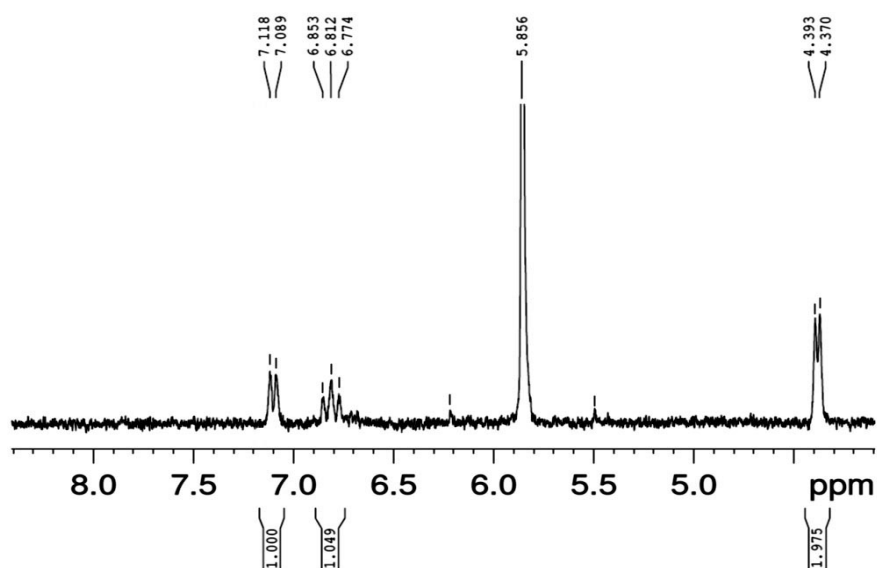


Figure 3.10. ¹H-NMR of 6,8,11,13,16,18-hexafluorotraxene (**32b**) (250 MHz, C₂Cl₄D₂, 120 °C).

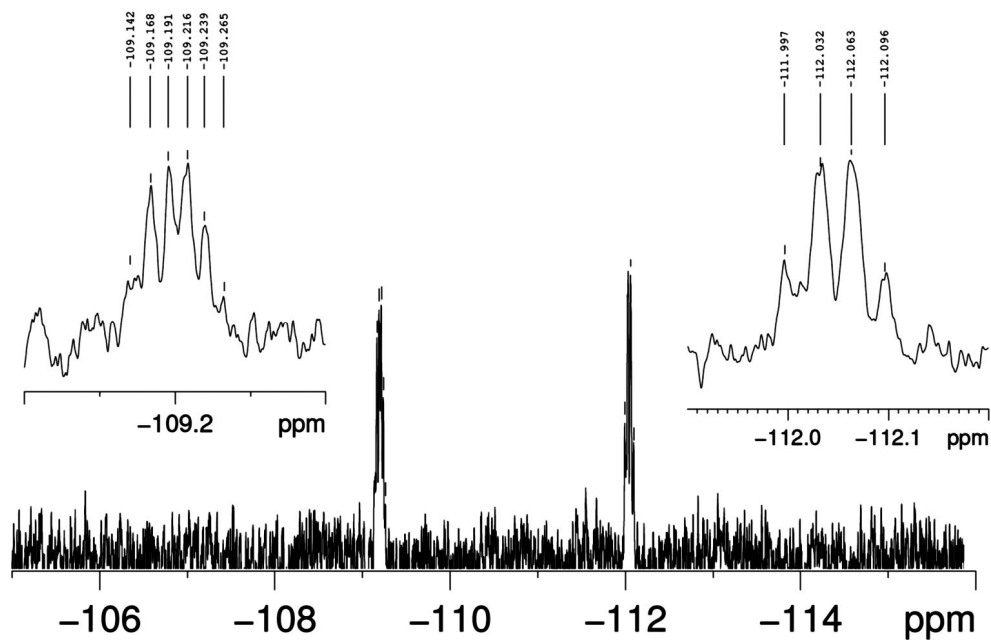
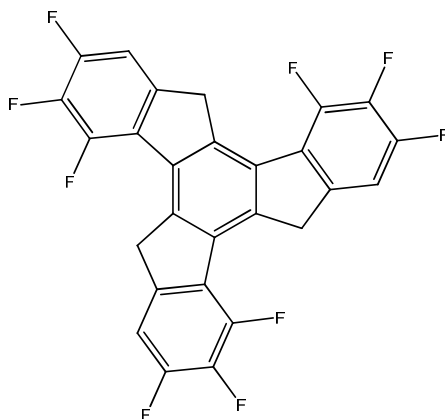


Figure 3.11. ^{19}F -NMR of 6,8,11,13,16,18-Hexafluorotruxene (**32b**) (235 MHz, $\text{C}_2\text{Cl}_4\text{D}_2$, 120°C).

6,8,9,11,12,13,16,17,18-Nonafluorotruxene (**32c**)



32c was synthesized analogously to **32b** (**route 2**) starting from 5,6,7-trifluoro-1-indanone. The mixture was heated at 170°C for 16 h. Pink crystals (50 mg, 45 %). ^1H -NMR ($\text{C}_2\text{Cl}_4\text{D}_2$, 250 MHz, 120°C) $\delta = 4.35$ (d, $J = 5.75$, 6H), 7.19 (t, $J = 7.25$, 3H)

(Figure 3.12). ^{19}F -NMR ($\text{C}_2\text{Cl}_4\text{D}_2$, 235 MHz, 120°C) $\delta = -166.57$ (td, $J_1 = 6.03$, $J_2 = 19.6$), $\delta = -152$ -(-141) (m) (Figure 3.13). LDI-TOF MS: $m/z = 503.03$ $[\text{M}-\text{H}]^-$ (Exact mass: 503.0482).

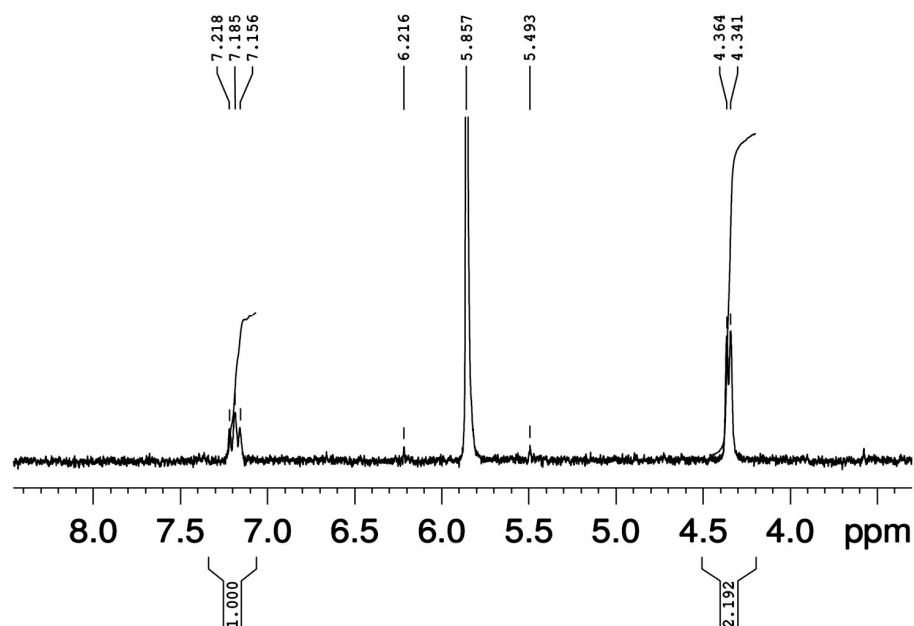


Figure 3.12. ^1H -NMR of 6,8,9,11,12,13,16,17,18-nonafluorotruxen (**32c**) (250 MHz, $\text{C}_2\text{Cl}_4\text{D}_2$, 120°C).

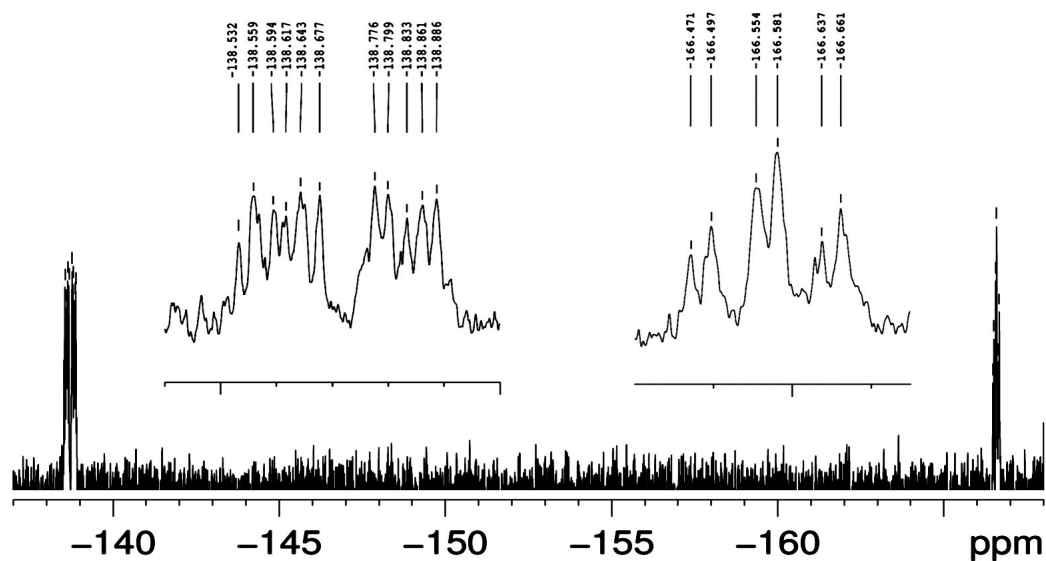
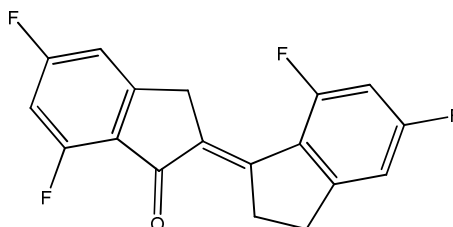


Figure 3.13. ^{19}F -NMR of 6,8,9,11,12,13,16,17,18-nonafluorotruxen (**32c**) (235 MHz, $\text{C}_2\text{Cl}_4\text{D}_2$, 120°C).

2-(2,3-Dihydro-5,7-difluoro-1H-inden-1-ylidene)-2,3-dihydro-5,7-difluoro-1H-inden-1-one (Dimer of 5,7-difluoro-1-indanone) (33)



5.0 g (29.7 mmol) of 5,7-difluoro-1-indanone were added to a mixture 20 mL of acetic acid and 10 mL of concentrated HCl. The mixture was stirred for 72 h at 100 °C, cooled down and poured into ice. The solid precipitate was filtered, washed with water, acetone and DCM to give a white powder (2.1 g, 44 % yield). ¹H-NMR (CDCl₃, 300 MHz) δ = 3.01 (t, J = 6.28, 2H), 3.5 (t, J = 6.1, 2H), 3.95 (d, J = 5.35, 2H), 6.6 - 6.8 (m, 2H), 6.88 (d, J = 7.6, 1H), 6.94 (d, J = 6.25, 1H) (Figure 3.14). ¹⁹F-NMR (C₂Cl₄D₂, 235 MHz, 120 °C) δ = -112.8 (dd, J_1 = 9.6, J_2 = 2.6), δ = -105.3 (q, J = 8.9), δ = -100.5 (7, J = 5.2), δ = -100.1 (dt, J_1 = 8.9, J_2 = 12) (Figure 3.15), LDI-TOF MS: m/z = 319.06 [M+H]⁺ (Exact mass: 319.2783).

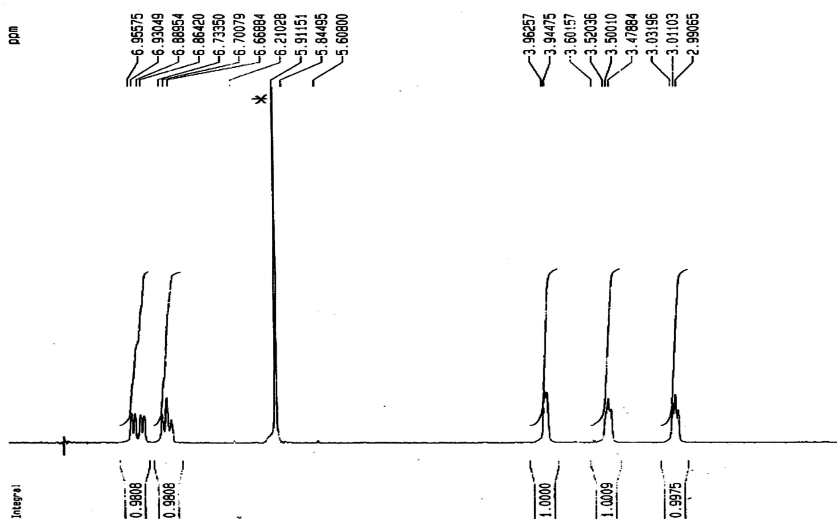


Figure 3.14. ¹H-NMR of 2-(2,3-dihydro-5,7-difluoro-1H-inden-1-ylidene)-2,3-dihydro-5,7-difluoro-1H-Inden-1-one (300 MHz, C₂Cl₄D₂).

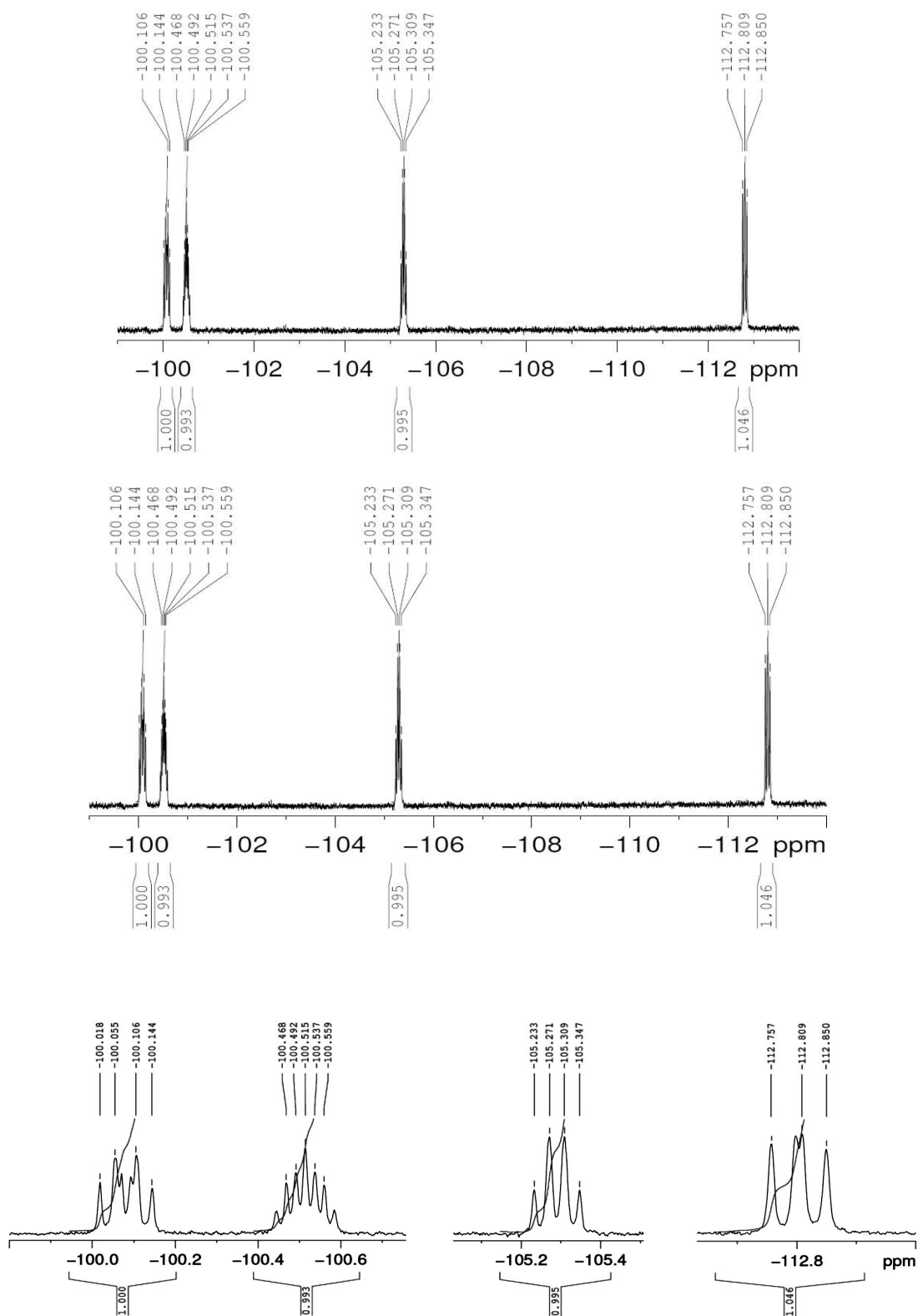
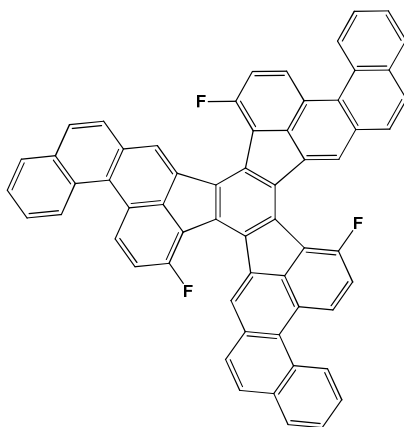


Figure 3.15. ^{19}F -NMR of 2-(2,3-dihydro-5,7-difluoro-1H-inden-1-ylidene)-2,3-dihydro-5,7-difluoro-1H-Inden-1-one (235 MHz, $\text{C}_2\text{Cl}_4\text{D}_2$, 120°C).

C₆₀H₂₇F₃ (35)

THF was refluxed over KOH and distilled over metallic sodium. THF was degassed using "freeze-thaw-pump" technique and additionally distilled under reduced pressure before use. All follow-up manipulations were carried out under argon atmosphere using Schlenk technique. 100 mg (0.25 mmol) of **32a** were suspended in 10 mL of THF. 0.5 mL of 1.6M *n*-BuLi in hexane (0.8 mmol) was slowly added to the mixture at -78 °C. After stirring for about 40 min, the mixture was slowly warmed to 0 °C. After 1 h the solution of 1-bromo-2-bromomethylnaphthalene 250 mg (0.83 mmol) in THF (15 mL) was drop-wise added to the red solution of truxene trianion. The resulting mixture was stirred for 2 h and diluted with EtOAc, washed with saturated aqueous NaCl solution, dried over Na₂SO₄ and concentrated. The product was precipitated through addition of hexane, filtered and dried, resulting in compound **34** which was used without additional purification (mixture of *syn/anti* isomers). White powder (162 mg, 61 %). ¹H-NMR aliphatic/aromatic proton ratio 1/3. R_{f1} = 0.21, R_{f2} = 0.30 (CCl₄ : hexane 1 : 1). The mixture of 150 mg of **34**, Pd(OAc)₂ (45 mg), trimethylbenzylammoniumbromide (70 mg), Cs₂CO₃ (500 mg) and 10 mL of dimethylacetamide was stirred at 140 °C for 72 h. The mixture was cooled and solid was filtered off, washed with DCM, acetone and water. The solid obtained was suspended in aqueous NaCN and stirred for 3 h, filtered off and washed with water, acetone and DCM to give **35** as yellow solid (83 mg, 67 %). LDI-TOF MS: m/z = 804.2

$[M]^+$ (Exact mass: 804.20648) (Figure 3.16). UV: λ_{\max} (1,2,4-trichlorobenyene)/[nm] 322, 371, 390, 408, 521. Mp > 300 °C.

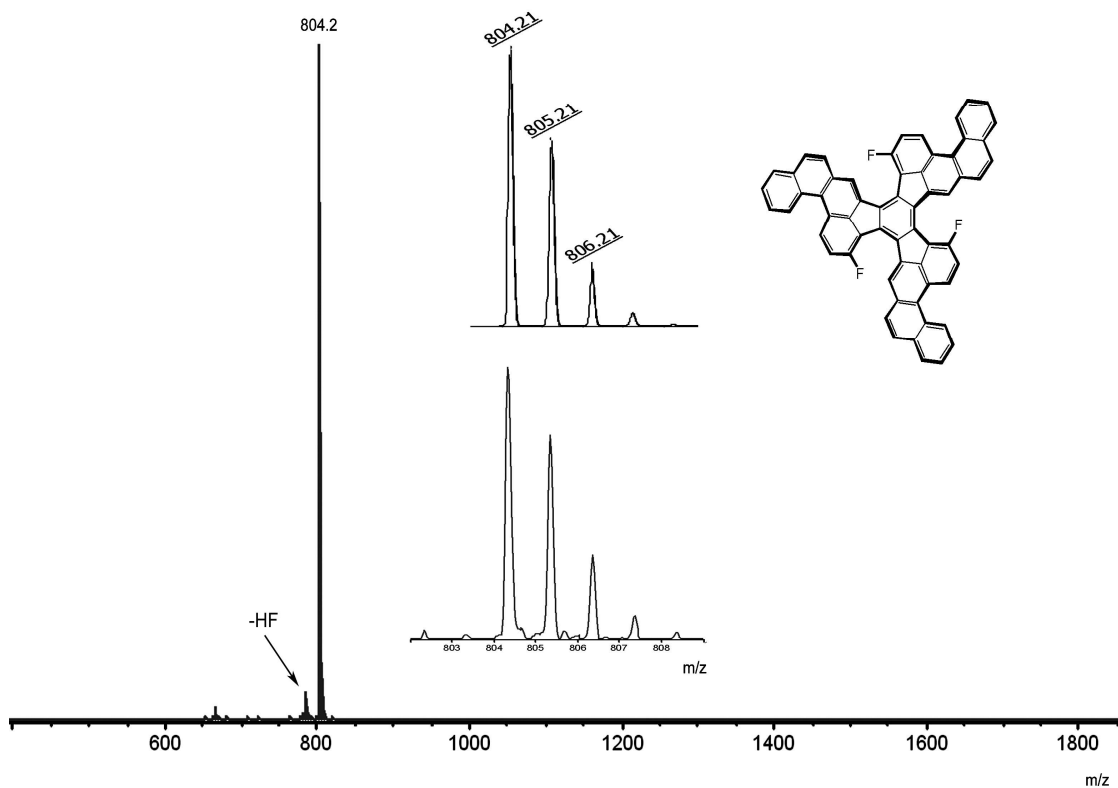
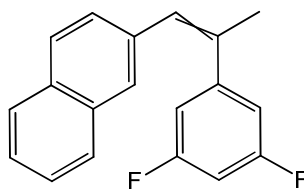


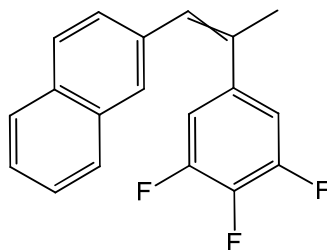
Figure 3.16. LDI mass spectrum of **35** ($C_{60}H_{27}F_3$) (positive mode).

(E/Z)-2-[2-(3,5-Difluorophenyl)-propen-1-yl]-naphthalene (37a)



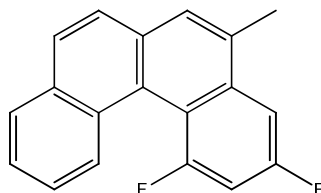
Compound **37a** was obtained from 3,5-difluoroacetophenone using general method **3.2.3**.

(E/Z)-2-[2-(3,4,5-Trifluorophenyl)-propen-1-yl]-naphthalene (37b)



Compound **37b** was obtained from 3,4,5-trifluoroacetophenone using general method **3.2.3**.

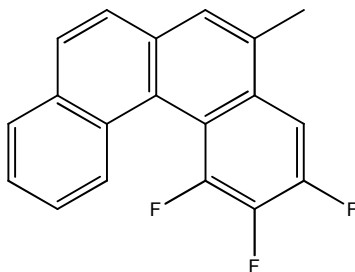
1,3-Difluoro-5-methylbenzo[c]phenanthrene (38a)



8.0 g (28.6 mmol) of **37a** as a mixture of *cis/trans* isomers were dissolved in 350 mL of cyclohexane. The resulting solution was placed in a 500 W water cooled quartz photochemical reactor and 8.0 g (31.4 mmol) of iodine were then added. Argon was bubbled through the stirred solution for 15 min before excess of propylene oxide (40 mL) was added. After irradiation for 20-30 h the color of iodine had disappeared. The mixture was washed with aqueous $\text{Na}_2\text{S}_2\text{O}_3$ to remove residual iodine traces, concentrated in vacuo, and then purified by flash chromatography on silica gel. The mixture of light petroleum and DCM 1:1 was used as an eluent. The targeted compound was obtained with 67 % yield as a white solid (5.2 g). $R_f = 0.17$ (Hexane). $^1\text{H-NMR}$ (CDCl_3 , 300 MHz) $\delta = 2.68$ (s, 2H), 7.08 - 7.2 (m, 1H), 7.48 - 7.7 (m, 5H), 7.82 - 7.95 (m, 2H), 8.08 - 8.22 (m, 1H). $^{13}\text{C-NMR}$ (CDCl_3 , 75 MHz) $\delta = 19.83$,

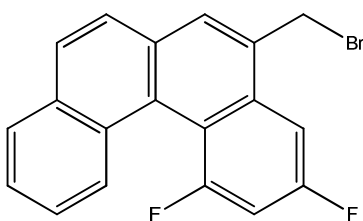
102.37 (t, $J = 28.2$), 104.89 (dd, $J_1 = 3.5$, $J_2 = 21$), 124.97 (d, $J = 2.86$), 125.44, 125.8, 127.48, 128.37, 128.96, 129.11, 129.34.

1,2,3-Trifluoro-5-methylbenzo[*c*]phenanthrene (**38b**)



38b was synthesized analogously to **38a** starting from 5.25 g (17.86 mmol) of **37b**. White solid 3.25 g (65 % yield). $R_f = 0.45$ (Hexane:DCM, 2:1). $^1\text{H-NMR}$ (CDCl_3 , 300 MHz) $\delta = 2.66$ (s, 3H), 7.48 - 7.72 (m, 5H), 7.86 - 7.94 (m, 2H), 8.07 - 8.2 (m, 1H). $^{13}\text{C-NMR}$ (CDCl_3 , 75 MHz) $\delta = 19.65$, 106.02 (dd, $J_1 = 3.7$, $J_2 = 17.3$), 125.29 (d, $J = 2.9$), 125.97, 127.56, 128.3 (broad), 128.66, 128.89, 128.93.

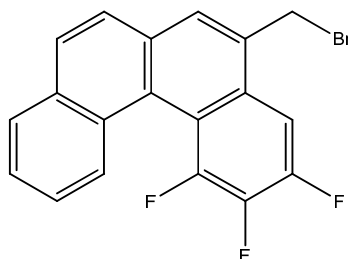
1,3-Difluoro-5-(bromomethyl)benzo[*c*]phenanthrene (**39a**)



4.65 g (16.7 mmol) of **38a** and 2.98 g (16.7 mmol) of NBS with catalytic amount of dibenzoyl peroxide (5 mg) were dissolved in 70 mL of CCl_4 . According to the general procedure **3.2.1**, a grayish solid (4.1 g, 68 % yield) was obtained. R_f (Hexane:DCM, 1:1) = 0.76. $^1\text{H-NMR}$ (CDCl_3 , 300 MHz) $\delta = 4.9$ (s, 2H), 7.1 - 7.22 (m, 1H), 7.48 - 7.6 (m, 2H), 7.63 - 7.74 (m, 2H), 7.82 - 7.95 (m, 3H), 8.08 - 8.22 (m, 1H). $^{13}\text{C-NMR}$ (CDCl_3 ,

75MHz) δ = 31.36, 103.14 (t, J = 27.8), 105 (dd, J_1 = 3.8, J_2 = 21.4), 125.31 (d, J = 3.02), 125.44, 126.63, 127.56, 128.84, 129.34, 129.59, 130.56, 133.28.

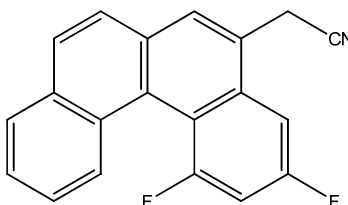
1,2,3-Trifluoro-5-(bromomethyl)benzo[*c*]phenanthrene (39b)



39b was synthesized analogously to **39a** starting from 3.2 g (11.0 mmol) of **38b**.

Yellowish solid (2.9 g, 72 % yield). R_f (Hexane:DCM, 2:1) = 0.40. $^1\text{H-NMR}$ (CDCl_3 , 300 MHz) δ = 4.87 (s, 2H), 7.49 - 7.6 (m, 2H), 7.68 (d, J = 8.5, 2H), 7.76 - 7.86 (m, 2H), 7.87 - 7.94 (m, 2H), 8.03 - 8.19 (m, 2H). $^{13}\text{C-NMR}$ (CDCl_3 , 75 MHz) δ = 30.99, 106.23 (dd, J_1 = 3.6, J_2 = 18) 125.43, 125.63 (d, J = 2.9), 126.8, 127.65 (d, J = 1.1), 128.91, 129.14, 129.40, 129.83, 130.9 (broad), 133.19.

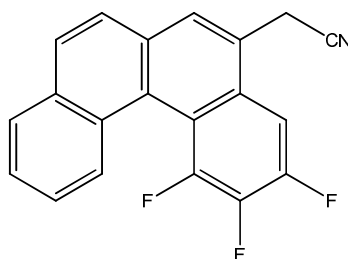
1,3-Difluorobenzo[*c*]phenanthrene-5-acetonitrile (40a)



3.85 g (11 mmol) of **39a** were dissolved in mixture of 200 mL of EtOH and 20 mL of H_2O . 600 mg (12 mmol) of NaCN were added and the solution was refluxed for 24 h, diluted with H_2O and extracted with DCM. The extract was washed with H_2O , dried over Na_2SO_4 and evaporated in vacuo resulting in an orange oil. The oil was purified by chromatography using a mixture of DCM and petroleum 1:1 as eluent. Yellow

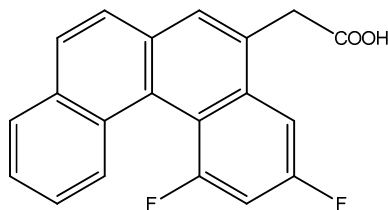
solid (2.5 g, 75 % yield) R_f (Hexane:DCM, 1:1) = 0.20; $^1\text{H-NMR}$ (DMSO- D_6 , 300 MHz) δ = 4.51 (s, 2H), 7.6 - 7.7 (m, 2H), 7.7 - 7.81 (m, 1H), 7.88 - 7.97 (m, 1H), 7.99 - 8.05 (m, 1H), 8.06 - 8.22 (m, 4H). $^{13}\text{C-NMR}$ (DMSO- D_6 , 75 MHz) δ = 21.17, 103.71 (t, J = 28.1), 105.30 (dd, J_1 = 3.7, J_2 = 22.1), 118.76, 125.64 (d, J = 2.88), 126.43 (dd, J_1 = 3.1, J_2 = 7.8), 126.77, 127.78, 128.81 (d, J = 3.2), 128.93, 129.11, 129.15, 129.26, 130.38, 132.82.

1,2,3-Trifluorobenzo[c]phenanthrene-5-acetonitrile (40b)



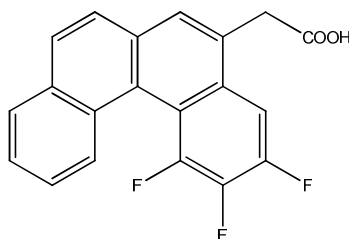
40b was synthesized analogously to **40a** starting from 2.7 g (7.2 mmol) of **39b**. White solid (1.95 g, 85 % yield) R_f = 0.16 (Hexane:DCM, 1:1). $^1\text{H-NMR}$ (CDCl_3 , 300 MHz) δ = 4.10 (s, 2H), 7.49 - 7.61 (m, 3H), 7.71 - 7.79 (m, 1H), 7.90 - 8.0 (m, 3H), 8.08 - 8.20 (m, 1H). $^{13}\text{C-NMR}$ (CDCl_3 , 75 MHz) δ = 22.07, 104.74 (d, J = 3.47), 104.88 (d, J = 3.84), 106.65, 116.70, 125.4, 125.71, 125.83, 126.85, 127.71, 128.8, 128.93, 129.02, 129.7, 130.87, 133.16.

1,3-Difluorobenzo[c]phenanthrene-5-acetic acid (41a)



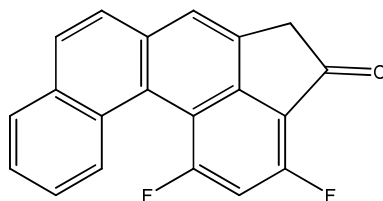
2.5 g (8 mmol) of **40a** were dissolved in mixture of acetic acid (60 mL), H₂SO₄ (40 mL) and water (40 mL). The mixture was heated under stirring at 120 °C for 24 h. After cooling down, 100 mL of H₂O were added and the product was filtrated, washed with H₂O and dried. Purification of the crude product was performed by dissolution in DCM, addition of active carbon followed by filtration. The product was precipitate by addition of hexane, filtered and dried. Grey solid (2.3 g, 90% yield). R_f = 0.36 (EtOAc:DCM, 1:2). ¹H-NMR (CDCl₃, 300 MHz) δ = 4.06 (s, 2H), 7.08 - 7.18 (m, 1H), 7.48 - 7.58 (m, 3H), 7.68 - 7.75 (m, 2H), 7.88 - 7.95 (m, 2H), 8.09 - 8.2 (m, 1H). ¹³C-NMR (CDCl₃, 75 MHz) δ = 38.71, 125.14, 125.18, 125.42, 126.32, 127.53, 128.70, 129.3, 129.52, 131.12.

1,2,3-Trifluorobenzo[*c*]phenanthrene-5-acetic acid (**41b**)



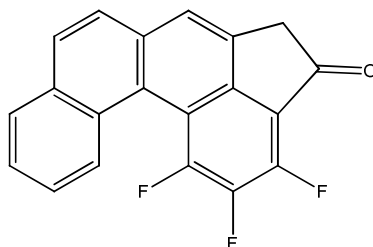
41b was synthesized analogously to **41a** starting from 1.95 g (6.07 mmol) **40b**. Grey solid (1.73 g, 84 % yield) R_f = 0.33 (EtOAc:DCM, 1:2). ¹H-NMR (DMSO-D₆, 300 MHz) δ = 3.38 (s, 2H), 6.78 - 6.89 (m, 2H), 7.1 - 7.19 (m, 2H), 7.2 - 7.48 (m, 4H). ¹³C-NMR (DMSO-D₆, 75 MHz) δ = 39.02, 107.91 (d, *J* = 18.3), 126.32, 127.16, 128.36, 129.13, 129.35, 129.94, 130.59, 131.15, 131.9, 133.11, 172.9.

1,3-Difluorobenz[*l*]acephenanthrylen-4(5H)-one (**42a**)



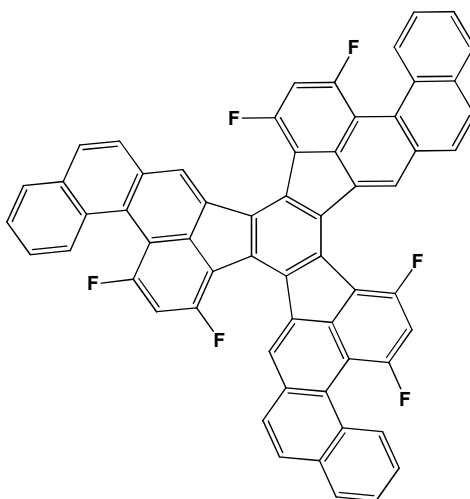
2.3 g (7.2 mmol) of **41a** were stirred with more than 10 times excess of SOCl₂ (10 mL) for 2 h at 65 °C. After cooling down SOCl₂ was evaporated and a yellow-brown oil was obtained. The oil was dissolved in DCM (20 mL) and 1.43 g of AlCl₃ (11 mmol) were added in small portions while stirring. A black solution obtained was stirred for 3 h and then poured into ice resulting in an orange mass. After extraction with DCM the solution was dried over Na₂SO₄ and evaporated. The crude product was purified by chromatography using DCM as eluent. White solid (0.66 g, yield 30 %). R_f (DCM) = 0.53. ¹H-NMR (CDCl₃, 300 MHz) δ = 3.88 (s, 2H), 7.21 - 7.29 (m, 1H), 7.57 - 7.68 (m, 2H), 7.78 - 7.84 (m, 2H), 7.91 - 8.02 (m, 2H), 8.25 - 8.4 (m, 1H). ¹³C-NMR (CDCl₃, 75 MHz) δ = 42.08, 124.75, 125.64 (d, J = 2.88), 126.62, 127.74, 128.89, 129.14, 129.2.

1,2,3-Trifluorobenz[*h*]acephenanthrylen-4(5H)-one (**42b**)



42b was synthesized analogously to **42a** starting from 1.38 g (3.85 mmol) of **41b**. Cream solid (0.3 g, 23 % yield). R_f (DCM) = 0.47. ¹H-NMR (CDCl₃, 300 MHz) δ = 3.87 (s, 1H), 7.58 - 7.67 (m, 2H), 7.72 - 7.82 (m, 2H), 7.91 - 8.2 (m, 2H), 8.22 - 8.39 (m, 2H). ¹³C-NMR (CDCl₃, 75 MHz) δ = 41.58, 124.08, 125.96, 126.63, 126.80, 127.86, 128.48, 129.78.

C₆₀H₂₇F₆ (43a)



20 mg of indanone **42a**, 1.5 mL of *o*-dichlorobenzene and 0.045 mL of TiCl₄ (6 molar equivalents) were transferred in a glass ampoule and sealed. The ampoule was heated at 180 °C for 20 h. After cooling down the glass ampoule was opened and the mixture was poured into 50 mL of acetone. The precipitate was filtered, washed with acetone, DCM and petroleum ether resulting in orange-brown solid (12 mg, 57 % yield.). LDI-TOF MS: $m/z = 858.2$ [M]⁺ (Exact mass: 858.1782) (Figure 3.17). UV: λ_{max} (1,2,4-trichlorobenzene)/[nm] 324, 373, 415. Mp > 300 °C.

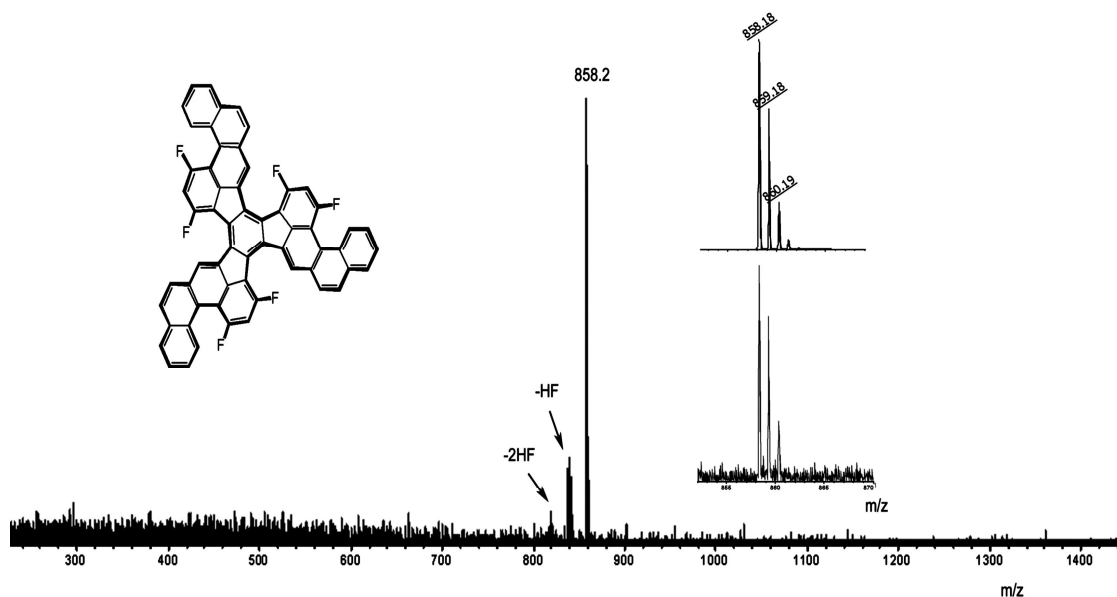
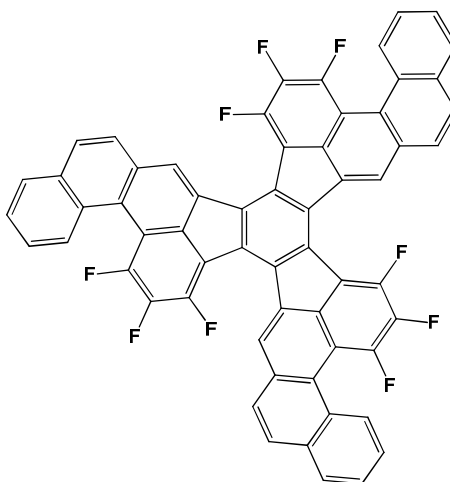


Figure 3.17. LDI mass spectrum of **43a** (C₆₀H₂₄F₆) (positive mode).

$C_{60}H_{21}F_9$ (**37b**)



43b was synthesized analogously to **43a** starting from 20 mg of **42b**. Orange solid (16 mg, 85 % yield.). LDI-TOF MS: $m/z = 912.2$ $[M]^+$ (Exact mass: 912.14995) (Figure 3.18). UV: λ_{max} (1,2,4-trichlorobenzene)/[nm] 322, 374, 410. Mp > 300 °C.

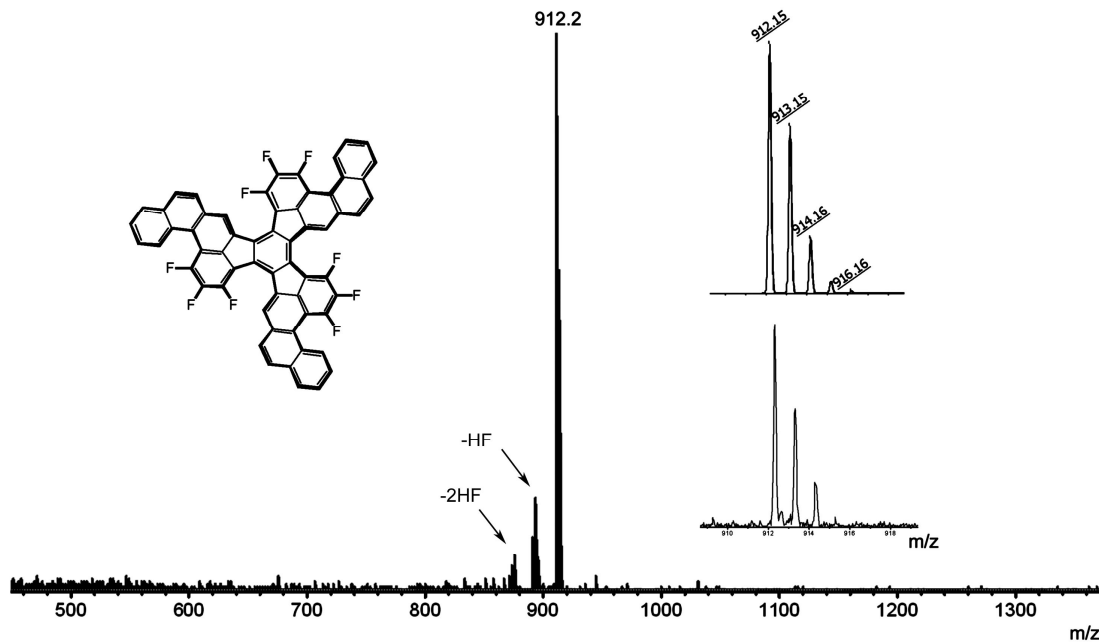
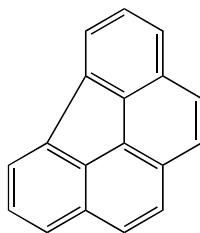


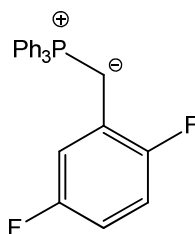
Figure 3.18. LDI mass spectrum of **43b** ($C_{60}H_{21}F_9$) (positive mode).

Benzo[ghi]fluoranthene (6)



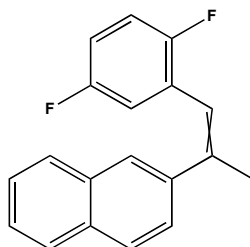
Compound **6** was synthesized from compound **5h** according the general procedure **3.2.6**. The NMR analysis is in agreement with reported data.^[4]

2,5-Difluorobenzyltriphenylphosphonium salt



Compound **44** was synthesized according the general procedure **3.2.2**. and was used for the next step without additional separation.

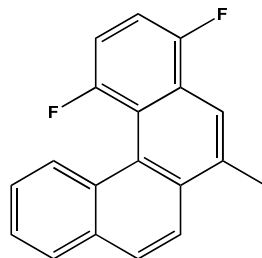
(E/Z)-2-[1-Methyl-2-(2,5-difluorophenyl)ethenyl]-naphthalene (45)



Compound **45** was synthesized according the general procedure **3.2.3**. 20 g (43.7 mmol) of (2,5-difluorobenzyl)triphenylphosphonium bromide, 4.9 g (43.7 mmol) of

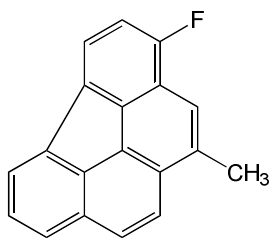
t-BuOK, 7.43 g (43.7 mmol) of 2-acetonaphthone and 400 mL of absolute ethanol were used. The product was obtained as a mixture of *cis/trans* isomers. White solid, 7.2 g (60 %). The mixture was used in the next step without additional purification.

1,4-Difluoro-6-methylbenzo[*c*]phenanthrene (46)



Compound **46** was obtained according the general procedure **3.2.4**. 7.2 g (25.7 mmol) of **45** and 400 mL of cyclohexane were used. Yellow Solid, 6.4 g (89 %). R_f (hexane:DCM 3:1) = 0.62. $^1\text{H-NMR}$ (300 MHz, CD_2Cl_2) δ 8.24 – 8.11 (m, 1H), 8.03 – 7.91 (m, 4H), 7.61 – 7.49 (m, 2H), 7.28 – 7.12 (m, 2H), 2.77 (s, 3H). $^{13}\text{C-NMR}$ (75 MHz, CD_2Cl_2) 155.40 (dd, $J = 248.7, 2.8$ Hz), 154.76 (dd, $J = 245.4, 2.6$ Hz), 134.77 (dd, $J = 2.0, 1.3$ Hz), 132.40 (d, $J = 42.3$ Hz), 130.02 (d, $J = 16.8$ Hz), 129.97 (d, $J = 3.0$ Hz), 128.92 (s), δ 127.35 (d, $J = 1.3$ Hz), 126.47 (d, $J = 0.9$ Hz), 125.20 (d, $J = 2.9$ Hz), 124.66 (dd, $J = 3.8, 2.2$ Hz), 124.07 (dd, $J = 17.0, 5.0$ Hz) 121.97 (s), 118.77 (d, $J = 4.2$ Hz), 111.55 – 110.54 (m), 20.34 (s). LDI-TOF MS: $m/z = 278.11$ $[\text{M}]^+$ (Exact mass: 278.0907).

3-Fluoro-1-methylbenzo[*ghi*]fluoranthene (47)



Compound **47** was synthesized from compound **46** according to the general procedure **3.2.6**. $^1\text{H-NMR}$ (300 MHz, CD_2Cl_2) δ 7.98 – 7.78 (m, 5H), 7.69 (q, $J = 1.2$ Hz, 1H), 7.58 (dd, $J = 8.1, 7.0$ Hz, 1H), 7.12 (dd, $J = 11.6, 7.6$ Hz, 1H), 2.73 (d, $J = 1.2$ Hz, 3H). $^{13}\text{C-NMR}$ (75 MHz, CD_2Cl_2) δ 159.13 (d, $J = 259.2$ Hz), 137.24, 135.36, 134.60 (d, $J = 8.3$ Hz), 133.66, 133.05, 132.10, 128.77, 128.01, 127.28, 126.00, 123.70 (d, $J = 7.9$ Hz), 123.31 (d, $J = 1.0$ Hz), 123.00 (d, $J = 3.7$ Hz), 119.03, 117.65 (d, $J = 18.6$ Hz), 112.78 (d, $J = 22.7$ Hz), 18.81. LDI-TOF MS: $m/z = 258.09$ $[\text{M}]^+$ (Exact mass: 258.0845). HPLC profile and UV spectra see in Figure 3.19.

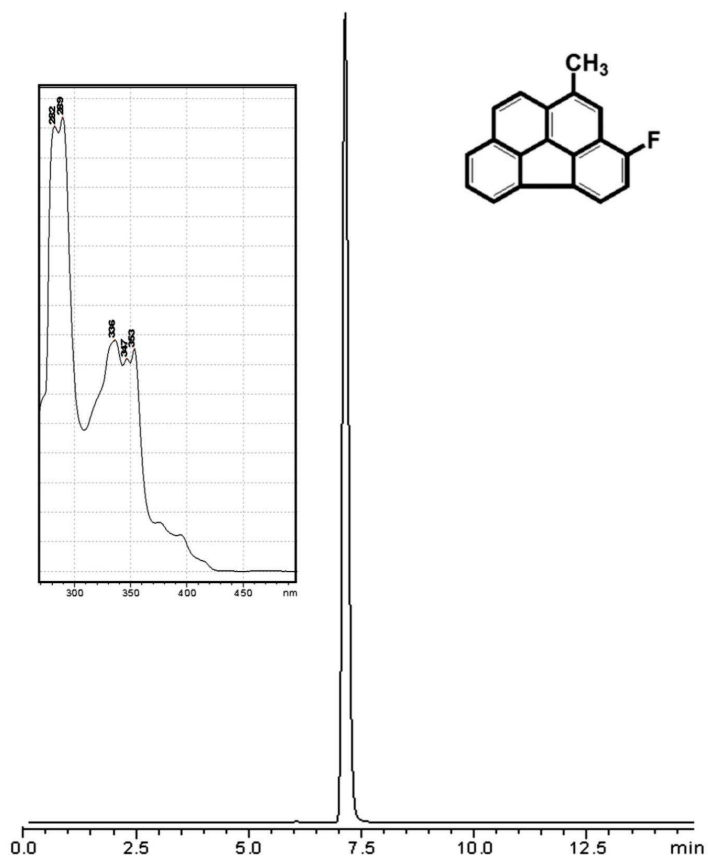
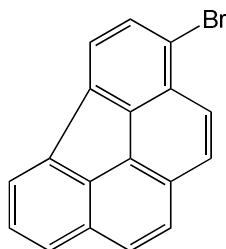


Figure 3.19. HPLC profile of the compound **47** as obtained after reaction (200 °C, 2 h). 5PYE column, toluene:MeOH 1:4 as eluent. (inset) UV-Vis spectrum of **47** (toluene/MeOH).

3-Bromobenzo[ghi]fluoranthene (**48**)



Compound **48** was synthesized from **5g** according to the general procedure **3.2.6**. $^1\text{H-NMR}$ (300 MHz, CD_2Cl_2) δ 8.06 (d, $J = 7.0$ Hz, 1H), 8.01 – 7.87 (m, 6H), 7.80 (d, $J = 7.4$ Hz, 1H), 7.68 – 7.61 (m, 1H). $^{13}\text{C-NMR}$ (75 MHz, CD_2Cl_2) δ 137.09, 136.80, 131.58, 131.43, 128.99, 128.14, 127.92, 127.60, 127.33, 127.00, 126.62, 125.68, 125.16, 124.79, 124.74, 124.03, 121.63, 106.75. LDI-TOF MS: $m/z = 304.04$ $[\text{M}]^+$ (Exact mass: 303.9888). HPLC profile and UV spectra see in Figure 3.20.

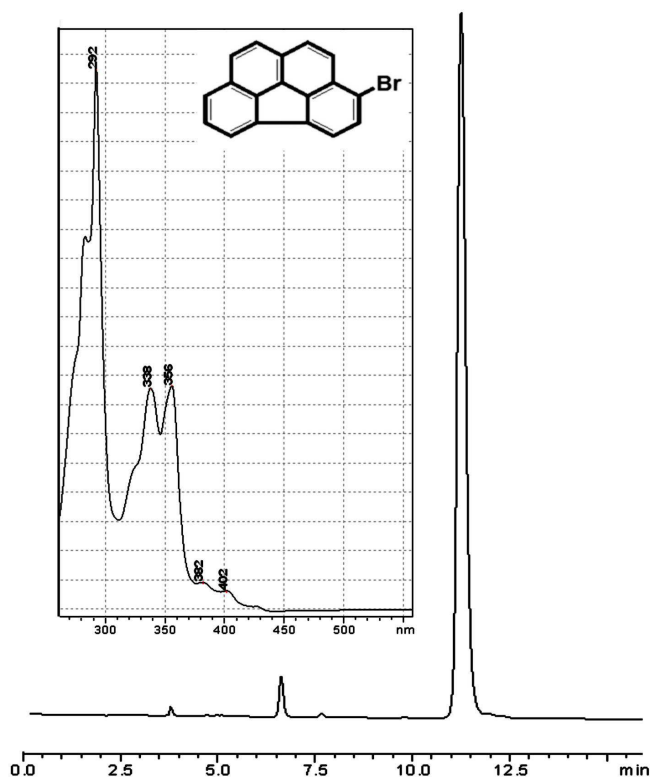
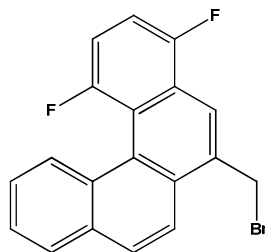


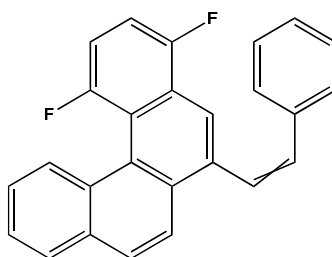
Figure 3.20. HPLC profile of the compound **48** as obtained after reaction (200 °C, 40 min). 5PYE column, toluene:MeOH 1:4 as eluent. (inset) UV-Vis spectrum of **48** (toluene/MeOH).

1,4-Difluoro-6-bromomethylbenzo[*c*]phenanthrene (49)



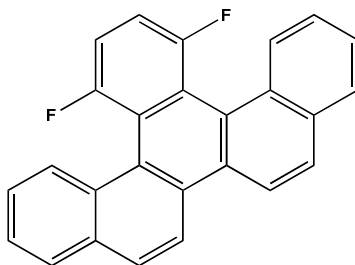
Compound **49** was synthesized from 6.4 g (23 mmol) of **46** according to the general procedure **3.2.1**. White solid, 8.0 g (97.4 %). R_f (hexane:DCM 3:1) = 0.5. $^1\text{H-NMR}$ (300 MHz, CD_2Cl_2) δ 8.23 – 7.85 (m, 5H), 7.62 – 7.48 (m, 2H), 7.31 – 7.12 (m, 2H), 4.99 (s, 2H). $^{13}\text{C-NMR}$ (75 MHz, CD_2Cl_2) δ 155.23 (dd, $J = 247.8, 10.4$ Hz), 133.66 (s), 132.84 (s), 130.07 (s), 129.98 (s), 129.85 (s), 127.46 (s), 126.96 (s), 125.64 (s), 125.47 (s), 120.79 (d, $J = 6.3$ Hz), 113.17 (dd, $J = 27.7, 9.0$ Hz), 111.45 (dd, $J = 23.2, 9.5$ Hz), 32.01 (s).

1,4-difluoro-6-(2-phenylethenyl)-benzo[*c*]phenanthrene (50)



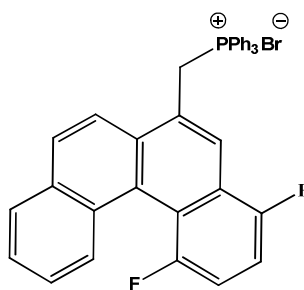
Compound **50** was synthesized according to the general procedure **3.2.3**. 11.3 g (18.3 mmol) of 1,4-difluoro-6-bromomethyl-benzo[*c*]phenanthrenyl triphenylphosphonium bromide, 2.05 g (18.3 mmol) of *t*-BuOK and 1.93 g (18.3 mmol) of benzaldehyde were used. The product was obtained as a mixture of *cis/trans* isomers 4.1 g (58 %) and was used in the next step without additional purification.

13,16-Difluorobenzo[s]picene (51)



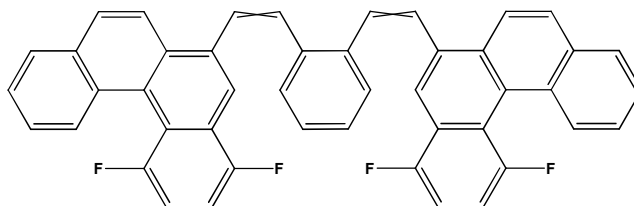
Compound **51** was synthesized according the general procedure **3.2.4**. 4 g (11 mmol) of **50** and 400 mL of cyclohexane were used. White solid, 3.34 g (89 %). R_f (hexane:DCM 3:1) = 0.45. $^1\text{H-NMR}$ (300 MHz, CD_2Cl_2) δ 8.50 (d, J = 8.9 Hz, 2H), 8.19 – 8.10 (m, 2H), 8.07 (d, J = 8.9 Hz, 2H), 7.92 (dd, J = 5.6, 3.8 Hz, 2H), 7.52 (dd, J = 6.2, 3.3 Hz, 4H), 7.33 (t, 2H). $^{13}\text{C-NMR}$ (75 MHz, CD_2Cl_2) δ 155.47 (d, J = 249.5 Hz), 132.59 (s), 130.29 (s), 129.91 (s), 129.81 (s), 129.71 (s), 129.56 (s), 127.33 (s), 126.39 (s), 125.48 (s), 123.51 (s), 120.04 (s), 114.58 (dd, J = 21.3, 16.6 Hz). LDI-TOF MS: m/z = 364.13 $[\text{M}]^+$ (Exact mass: 364.1064).

1,4-Difluoro-6-methylbenzo[c]phenatrenyltriphenylphosphonium salt (52)



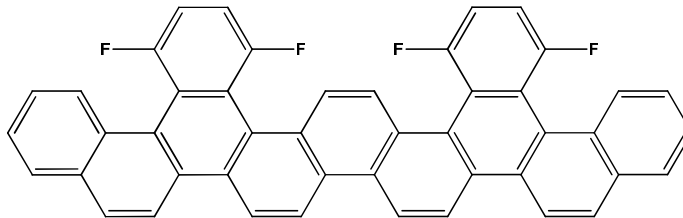
Compound **52** was synthesized from **49** according the general procedure II and was used for the next step without additional separations.

Compound 53



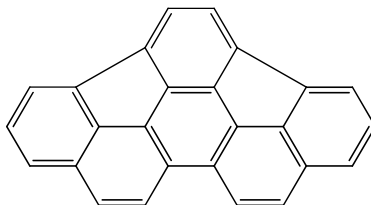
Compound **53** was obtained according the general procedure **3.2.3**. 2.4 g (4 mmol) of **52**, 0.45 g (4 mmol) of *t*-BuOK, 0.53 g (4 mmol) of 1,2-benzenedicarboxaldehyde and 100 mL of absolute ethanol were used. The product was obtained as a mixture of *cis/trans* isomers and was used in the next step without additional purification. White solid, 0.46 g (20 %).

Compound 54



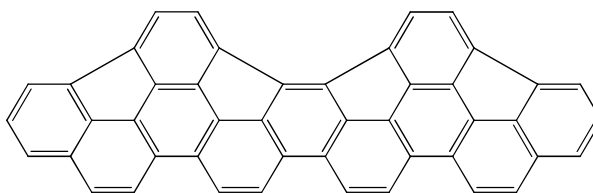
Compound **54** was synthesized according the general procedure **3.2.4**. 0.41 g (0.63 mmol) of **53** and 200 mL of cyclohexane were used. After irradiation for 30 h the color of iodine had disappeared. The yellow precipitate formed was filtrated, dissolved in 1:1 DCM:toluene mixture (1 L) and filtered through silica. After evaporation the product was obtained as a yellowish solid. 0.21 g (52 %). $^1\text{H-NMR}$ (300 MHz, $\text{C}_2\text{D}_2\text{Cl}_4$, 110 °C) δ 9.11 (d, $J = 9.2$ Hz, 2H), 8.76 (d, $J = 9.2$ Hz, 2H), 8.58 (d, $J = 9.0$ Hz, 2H), 8.26 – 8.04 (m, 6H), 7.99 – 7.88 (m, 2H), 7.62 – 7.31 (m, 8H). The compound is too insoluble for $^{13}\text{C-NMR}$ measurement. LDI-TOF MS: $m/z = 650.16$ $[\text{M}]^+$ (Exact mass: 650.1658).

Indaceno[3,2,1,8,7,6*qrstuv*]picene (**56**)



Compound **56** was synthesized from **51** according to the general procedure **3.2.6**. $^1\text{H-NMR}$ (300 MHz, CD_2Cl_2) δ 8.01 (d, $J = 8.8$ Hz, 1H), 7.70 (d, $J = 8.8$ Hz, 1H), 7.63 (d, $J = 7.0$ Hz, 1H), 7.31 (dd, $J = 8.2, 7.0$ Hz, 1H). $^{13}\text{C-NMR}$ (75 MHz, CD_2Cl_2) δ 139.48, 139.42, 138.87, 138.52, 137.27, 130.56, 129.69, 129.39, 127.44, 127.29, 126.13, 124.51, 124.06. LDI-TOF MS: $m/z = 324.10$ $[\text{M}]^+$ (Exact mass: 324.0939). UV (Toluene/MeOH) λ (nm): 316(s), 366, 384, 426, 450, 492 (s). mp 178-179 °C. Crystal Data: orthorhombic; space group $Pna2_1$; $a = 18.033$, $b = 21.834$, $c = 3.8291$ Å; $\beta = 91.147(2)$, $V = 1507.6$ Å³, $Z = 4$; $2\theta_{\text{max}} = 41.84^\circ$; $-18 < h < 18$, $-21 < k < 21$, $-3 < l < 3$; $\lambda = 0.71073$ Å; $T = 293(2)$ K; final R value 0.0649 ($R_w = 0.1624$). CCDC-860433.

Compound **57**



Compound **57** was synthesized from **54** according to the general procedure. $^1\text{H-NMR}$ (300 MHz, $\text{C}_2\text{D}_2\text{Cl}_4$, 110 °C) δ 8.29 – 8.16 (m, 2H), 8.14 (d, $J = 8.5$ Hz, 1H), 7.99 (d, $J = 7.6$ Hz, 1H), 7.85 – 7.73 (m, 2H), 7.67 (d, $J = 8.3$ Hz, 1H), 7.42 (t, $J = 7.8$ Hz, 1H), 5.21 (s, 1H). LDI-TOF MS: $m/z = 570.20$ $[\text{M}]^+$ (Exact mass: 570.1404). UV (Toluene) λ (nm): 331, 360, 379, 394. mp > 300 °C.

3.4. References

1. Bruker Suite, Version 2008/3, Bruker AXS Inc., Madison, USA, **2008**.
2. G.M. Sheldrick, SADABS - *Bruker AXS Area Detector Scaling and Absorption*, Version 2007/4, University of Göttingen, Germany, **2007**.
3. G.M. Sheldrick, A Short History of SHELX, *Acta Cryst., Sect. A* **2008**, 64:112.
4. Spectral Atlas of Polycyclic Aromatic Compounds, Ed. W. Karcher. D. Reidel Pub. Co, Dordrecht **1985**.

Zusammenfassung

Im Rahmen dieser Arbeit wurde Grundlagenforschung zur rationalen Synthese von Fullerenen durchgeführt. Das Hauptaugenmerk liegt auf der Direktsynthese von isomerenreinen höheren Fullerenen und Buckybowls, wobei die entwickelten Methoden jedoch auch auf eine Vielzahl weiterer Kohlenstoffnanostrukturen ausgeweitet werden können. Die allgemeine Strategie der Direktsynthese basiert auf der Synthese von Vorläufermolekülen – polyzyklischen aromatischen Kohlenwasserstoffen (PAKs) mit der für das Zielfulleren benötigten Kohlenstoffkonnektivität.

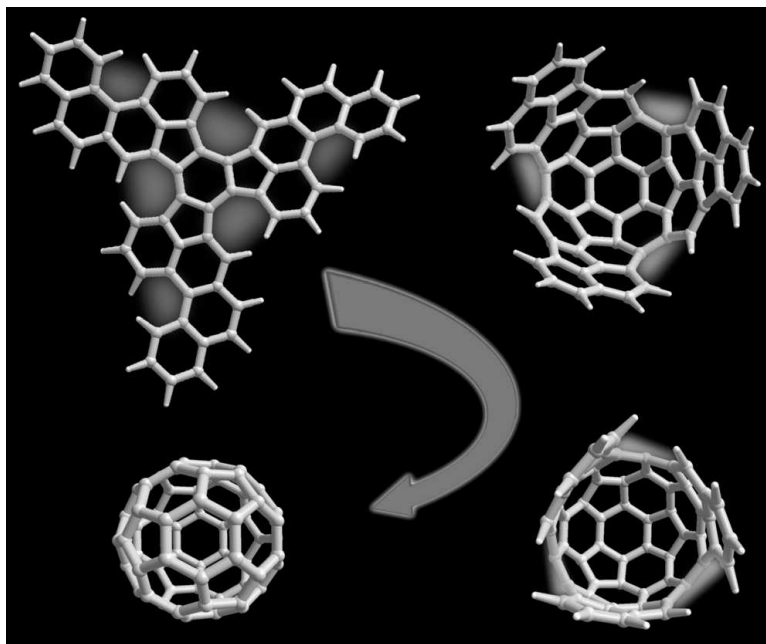


Abbildung 1. Strategie der Direktsynthese am Beispiel der I_h -C₆₀ Fullerenbildung ausgehend von einem C₆₀H₃₀-Vorläufermolekül durch intramolekulare Aryl-Aryl-Domino-Kupplung. Die Cove- und Fjord-Regionen, in welchen die direkte Aryl-Aryl-Kupplung stattfinden kann sind in Orange hervorgehoben. Jede konsekutive Kondensation führt zur Ausbildung neuer Cove-Regionen, so dass die Reaktion auf Domino-Art (Tandem-Kondensation) ablaufen kann, bis der gewünschte Käfig komplett ist.

Das Vorläufermolekül kann durch intramolekulare Aryl-Aryl-Domino-Kupplung zum entsprechenden Kohlenstoffkäfig aufgerollt werden. Dieses Konzept der Direktsynthese ist in Abbildung 1 am Beispiel von C₆₀ schematisch dargestellt.

Das charakteristische Merkmal des Ansatzes ist die Zyklisierung im letzten Syntheseschritt durch den Zipper-Mechanismus. Die Regiospezifität jedes Kondensationsschritts kann durch die speziell entworfene Präkursorstruktur festgelegt werden. Der Direktsyntheseansatz kann zur Synthese verschiedener Nanostrukturen, einschließlich Nanographenen, Nanoribbons, Buckybowls und Nanoröhren, mit bereits im Präkursormolekül programmierter Konnektivität, erweitert werden. Da die Fullerenbildung bei den konventionellen Hochtemperatursynthesemethoden thermodynamisch kontrolliert ist, gibt es keine Möglichkeit den Prozess auf die Bildung von weniger stabilen Fullerenenisomeren einzustellen. Daher erscheint der hier vorgestellte Ansatz der Direktsynthese als eine Möglichkeit, diese Fullerene in Bulkmenge zugänglich zu machen.

Der größte Anteil dieser Arbeit befasst sich mit der Direktsynthese. Mehrstufige organische Synthesen der Präkursormoleküle und ihre Umwandlung zu den entsprechenden Kohlenstoffnanostrukturen werden beschrieben. Das Hauptaugenmerk liegt auf dem letzten Schlüsselschritt – der Tandem-Kondensation zur Nanostruktur und der Entwicklung effektiver Aryl-Aryl-Kupplungs-Techniken zu deren Durchführung. Auf der Problematik hinsichtlich Präkursorlöslichkeit und Fullerenreaktivität liegt ein besonderer Schwerpunkt.

Obwohl die selektive und effektive Bildung höherer Fullerene durch oberflächenkatalysierte Zyklodehydrierung demonstriert wurde, bleibt die Direktsynthese von Fullerenen für makroskopische Mengen eine Herausforderung. Alternativ können die Vorläufermoleküle durch Flash Vakuum Pyrolyse (FVP) zum Fulleren umgesetzt werden. Die Effizienz der intramolekularen Aryl-Aryl-Kupplung ist in diesem Fall aufgrund fehlender effektiver Ringschluss-Promotoren oft sehr schlecht. Die Untersuchung einer Vielzahl verschiedener Ringschluss-Promotoren für FVP ergab, dass die Fluor-Funktionalisierung ein exzellenter Kandidat ist. Diese

Funktionalisierung zeigt eine unerwartet hohe Effizienz für intramolekularen Ringschluss durch HF-Eliminierung mit einer für Pyrolyseprozesse ungewöhnlich hohen Selektivität (mehr als 96%). Des Weiteren stellt Fluor aufgrund seiner geringen Größe, seines geringen Gewichts und seiner hohen Thermostabilität einen perfekten Aktivator für die rationale Fulleren synthese durch die FVP dar. Weitere Untersuchungen ergaben, dass die HF-Eliminierung ein synchroner Prozess ist, welcher ohne Bildung von Zwischenprodukten direkt zum Zielmolekül führt und daher durch die Vermeidung von Nebenprodukten eine hohe Selektivität aufweist.

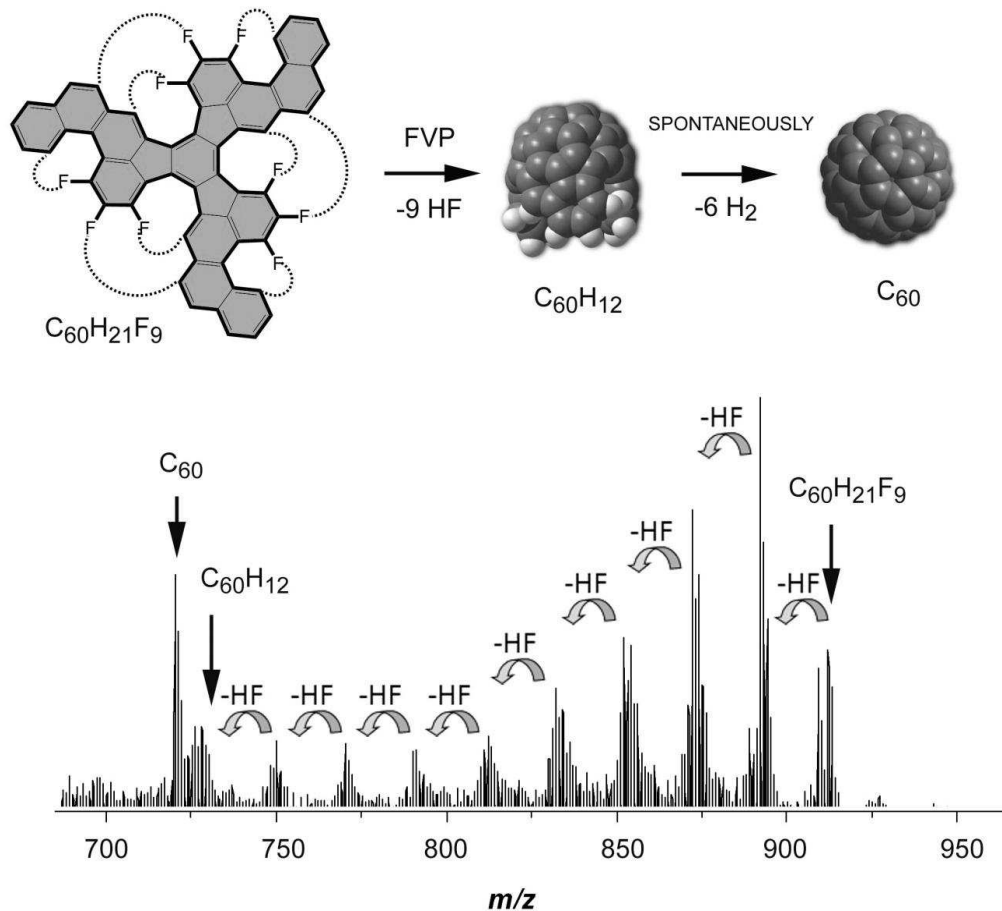


Abbildung 2. Tandem-HF-Eliminierung im C₆₀H₂₁F₉-Präkursor und spontaner Kollaps zum C₆₀-Fulleren unter LDI-MS-Bedingungen.

Mehrere C₆₀-Fullerenpräkursoren mit unterschiedlicher Anzahl von Fluoratomen in Schlüsselpositionen wurden synthetisiert und als C₆₀-Präkursoren untersucht. Die synthetisierten Vorläufermoleküle zeigen bereits unter LDI-MS-Bedingungen eine effiziente, regiospezifische, intramolekulare Kondensation via HF-Eliminierung und die Bildung des entsprechenden Fullerenkäfigs (Abbildung 2).

FVP des Präkursors zeigt ebenfalls eine hoch selektive C₆₀-Fulleren-Bildung mit ca. 1% Ausbeute. Ausgehend von der Bildung von 15 neuen Bindungen während des FVP Prozesses kann die Ausbeute für eine einzelne Zyklisierung auf 70% abgeschätzt werden. Weitere Optimierung führte zur Entdeckung einer alternativen hoch effektiven Festkörper-Strategie zur intramolekularen Aryl-Aryl-Kupplung via HF-Eliminierung. Die Effizienz des Ansatzes wurde durch quantitative Umsetzung der Vorläufermoleküle zu den entsprechenden PAK- und Buckybowlstrukturen demonstriert (Abbildung 3).

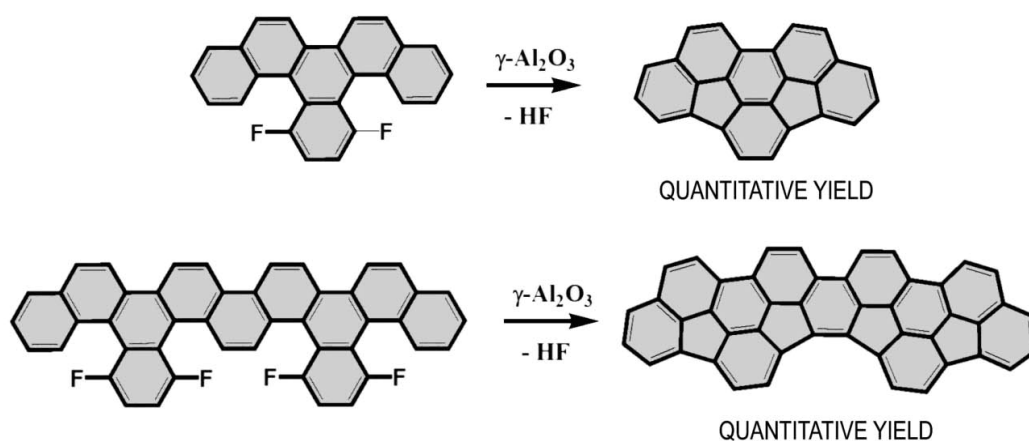


Abbildung 3. Aryl-Aryl-Kupplung durch Al₂O₃ vermittelte HF-Eliminierung.

Fluor kann den gewünschten Ringschluss nur dann fördern, wenn Wasserstoff in einer räumlich benachbarten Position in der Präkursorstruktur vorhanden ist. Die vollständige Kontrolle des Prozesses und die Durchführung der Kondensation auf

Domino-Art erscheinen daher möglich. Die quantitative Umsetzung des C_{46} -Buckybowls, welche mehr als 75% der C_{60} -Fullerenkonnektivität darstellt, demonstriert das große Potential der Technik für die Konstruktion von ausgedehnten nicht-planaren Kohlenstoffnanostrukturen, einschließlich höherer Fullerene, großer Buckybowls und Nanoröhren. Die hohe Toleranz zu Chlor- und Bromfunktionalisierungen macht den Ansatz zu einem sehr guten synthetischen Werkzeug zur Synthese von funktionalisierten Buckybowls, welche nützliche Bausteine für die Konstruktion von komplexen kohlenstoffbasierten Nanostrukturen darstellen.

Zusammenfassend zeigen die erzielten Resultate einen Weg zur Herstellung von Fullerenen sowie anderen Kohlenstoffnanostrukturen, wie einwandiger Kohlenstoffnanoröhren und Nanoribbons, auf kontrollierte Art und Weise auf. Die Produktion dieser einzigartigen Materialien in Bulk-Mengen scheint nicht länger unerreichbar und es besteht die vielversprechende Aussicht, dass diese Verbindungen in naher Zukunft in makroskopischen Mengen zugänglich werden.

Abbreviations

HPLC	High performance liquid chromatography
FVP	Flash-Vakuum-Pyrolyse
MS	Massenspektrometrie
LDI	Laser-Desorption/Ionisation
NMR	nuclear magnetic resonance
UV-Vis-NIR	Ultra violet – visible – near infrared
MALDI	Matrix assisted laser desorption ionization (Matrix-unterstützte Laser-Desorption/Ionisation)

Publications and poster contributions

1. K. Y. Amsharov; M. A. Kabdulov; M. Jansen, Highly Efficient Fluorine-Promoted Intramolecular Condensation of Benzo[c]phenanthrene: A New Prospective on Direct Fullerene Synthesis, *Eur. J. Org. Chem.* **2009**, 6328 – 6335.
2. K. Y. Amsharov; M. A. Kabdulov; M. Jansen, Homo-elimination of HF-An Efficient Approach for Intramolecular Aryl-Aryl Coupling, *Chem. Eur. J.* **2010**, 16, 5868 – 5871.
3. M. Kabdulov; K. Y. Amsharov; M. Jansen, A step toward direct fullerene synthesis: C-60 fullerene precursors with fluorine in key positions, *Tetrahedron* **2010**, 66, 8587 – 8593.
4. K. Y. Amsharov; M. A. Kabdulov; M. Jansen, Facile Bucky-Bowl Synthesis by Regiospecific Cove-Region Closure by HF Elimination, *Angew. Chem. Int. Ed.* **2012**, 51, 4594-4597.
5. K.Yu. Amsharov, M.Kabdulov, M. Jansen “Direct synthesis of fullerenes”, *3rd EuCheMS Chemistry Congress*, Nürnberg, Germany, **2010**.
6. M. Kabdulov; A. Mueller; K. Amsharov and M. Jansen, Direct Synthesis of Carbon Nanostructures, *International winterschool on Electronic Properties of Novel Materials*, Austria, **2011**.
7. K. Amsharov, M. Kabdulov and M. Jansen “Direct Fullerene Synthesis”, *Joint International Conference Advanced Carbon Nanostructures*, St.Petersburg, Russia, **2011**.

Acknowledgements

First and foremost I would like to express sincere gratitude to my supervisor **Prof. Dr. Dr. h. c. M. Jansen** for giving me opportunity of working in his group, freedom during setting of tasks, advices and his constant interests in my research.

Prof. Dr. F. Effenberger and **Prof. Dr. B. Plietker** for accepting being my examiners, reading thoroughly the thesis and giving valuable comments and remarks.

Particularly I would like to thank my PhD advisor **Dr. Konstantin Amsharov** for his continuous support during these 4 years, for his patience and readiness to help at any time. I am also very grateful to him for sharing his extensive knowledge and experience with me. He was my primary source for getting my questions answered.

I am very thankful to my friend **Dr. Vyacheslav Saltykov** for the support, friendship and creating a nice environment.

Also I would like to thank:

Dr. Thomas Bräuniger and **Dr. Dejan Zagorac** for help and fruitful discussions.

Mr. N. Schumacher and **Mr. P. Merz** for assistance with syntheses.

My labour colleges **Dr. Andreas Müller**, **Mr. Evangelos Krokos**, **Nina Kozhemyakina**, and **Karolin Ziegler** for the good working atmosphere, help and support during the promotion period.

All my colleagues who contributed to this project.

Eidesstattliche Erklärung

Hiermit erkläre ich an Eides statt, dass ich die vorliegende Arbeit selbstständig angefertigt und keine anderen Hilfsmittel als die angegebenen verwendet habe. Diejenigen Stellen der Arbeit, die anderen Werken direkt oder indirekt entnommen wurden, sind in jedem einzelnen Fall unter Angabe der Quelle kenntlich gemacht.

Ein früherer Promotionsversuch an einer deutschen Hochschule hat nicht stattgefunden.

Stuttgart, den

Mikhail Kabdulov